Antiscarp initiation and evolution

A thesis submitted in partial fulfilment

of the requirements for the degree of

Doctor of Philosophy in Engineering Geology

at the

University of Canterbury

by

Verne Harlan Pere

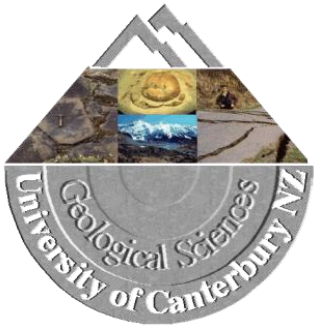

University of Canterbury 2009

Abstract

Antiscarps are defined here as any uphill facing scarp that may be observed on slopes, regardless of size or scale. They are not present on all slopes, but where they have been observed, they typically occur sub-parallel to the valley axis near the ridge crests in mountainous regions. Antiscarps are generally, but not exclusively, found in glaciated regions, where loading and unloading of the rock mass has effected changes to the in situ stress fields through cycles of compression and elastoplastic rebound and has also removed large volumes of material by the formation of cirques. Non-glacial antiscarps are commonly associated with tectonic activity.

An extensive review of current literature has been used to assist in the identification of key parameters associated with antiscarps and to provide a basis for clearly defining the terminology used to address antiscarp related processes and features. All of the reviewed material has been collated into a chart where the factors that have been extracted from the articles are grouped and compared. The chart has been instrumental in selecting the nomenclature to be used when addressing different types of antiscarp and also in constraining the extent to which the term can be reasonably used.

A flowchart has been developed to assist in the identification of the primary antiscarp forming process. The flowchart was successfully used to identify the primary processes associated with antiscarps observed in field studies in both the South Island of New Zealand and in the Scottish Highlands.

Physical base friction models and numerical finite element modelling, using Plaxis v6.1 and FLAC 2D v3.40, both indicate that antiscarps can form solely under a gravitational load. Base friction models used individual elements of various geometries. Antiscarps formed in most of the models and were best identified in models that had a clearly defined discontinuity surface. The numerical models also indicate that shear along existing discontinuities is the dominant mode for the formation of antiscarps under a gravitational load in homogeneous massifs.

Table of Contents

Appendices

List of Figures

List of Tables

Acknowledgements

I would firstly like to thank my family for their perseverance and constant encouragement as I undertook this course of study, especially my partner Eva. Thanks for sticking by me through thick and thin, I have really appreciated all your awhi and aroha.

Thanks to my Supervisors Tim Davies and Jarg Pettinga for their input and for encouraging me through to the end. Cheers to Dave Bell for his fine conversation, assistance on some of the sticky bits, and general all round encouragement. Thanks also to all the other staff within the University of Canterbury Geology Department for all their input over the past few years.

Thanks to Otago University for generously allowing me access to some of their software and computing facilities, and to Phaedra Upton for her guidance with FLAC 2D.

I would also like to acknowledge the support and funding provided for this Doctorate by the Foundation for Research Science and Technology in the form of the Tuapapa Putaiao Maori Fellowship (Contract UOCX0309) and Ngā Pae O Te Māramatanga for the Doctoral stipend. Thanks also to the University of Canterbury for Te tohu whai hiranga - The Maori meritorious award and also to the Mason trust for support with fieldwork.

Thank you very much to David Jarman for his assistance in pointing me in the right direction in Scotland and for introducing me to haggis, your support was invaluable. Cheers to Rob Langridge for bringing the Lewis Tops to my attention and for spending the day with me up there.

Thanks to Mai ki Otautahi for all the good times and for all the awhi that was provided within our group. Tu meke!

Thanks also to the doctors, physiotherapists, and other health professionals who helped me through the mid thesis broken back and also to the University of Canterbury for allowing me an extension. Sometimes you don't know what you have got until its gone.

Last and by no means least a special thanks to Dr Florian Buech for his packhorse-like capabilities in hauling equipment up mountains, his support in midwinter forays into the alps to assess rock mass response to snow loading and also for his invaluable assistance in helping me to get my thesis through the printing and final processes due to my being overseas.

1 Antiscarp initiation and evolution

1.1 Motivation

Antiscarp is an umbrella term for any uphill facing scarp. Antiscarps are a feature within many mountainous areas and appear as linear features on slopes. There are many different ideas on how antiscarps may form and many proposed processes associated with these ideas.

The majority of antiscarps are features that have endured in the landscape for thousands of years and generally little is known about the exact timing of their formation. The lack of timing constraints adds further complication when trying to understand antiscarps as there is also no control on the rate of formation, which can be anywhere on a scale from creep to episodic movement through to a single event displacement. Some studies have been able to determine rates of movement that are akin to creep but it appears that this is only related to processes that by their nature deform a massif at slow rates. The concept of different antiscarp forming processes having subtly different attributes is an important distinction to make because it assists in being able to identify what the key process may be.

Antiscarps are not a case of singularity, which is where one particular process can be considered as the causal mechanism, but are considered to form under different conditions and therefore driven by different processes. Throughout published literature antiscarps are referred to by a plethora of different terms which are often aligned to different processes. Many of the terms currently in use are increasingly being used to represent more than was originally intended and run the risk of losing their explanatory power. Tighter constraints on the definitions and use of antiscarp-related nomenclature will assist in clearer communication between practitioners when presenting antiscarp related material.

Some antiscarps are related to seismic events. Determining the role of seismicity in antiscarp formation and evolution will assist in understanding how antiscarps may be used as a geomorphological feature to assess paleoseismicity. Again the notion of singularity is an important aspect as it is incorrect to assume that all antiscarps require a seismic input based on observations that some do.

The role of gravity is important because it is a component of many of the processes that are associated with antiscarp formation. Assessing the role of gravity will help to understand some of the base conditions required for antiscarps to form.

1.2 Objectives

There are two main objectives that this research project aims to achieve.

The first is to provide a systematic approach to identifying and communicating antiscarp features and the related processes. As the body of knowledge surrounding antiscarps continues to grow so must the way in which we communicate this knowledge. Clear and concise definitions are provided for antiscarp-related nomenclature to facilitate better communication and a flowchart is constructed to assist in the identification of primary antiscarp process.

The second objective is to assess the role of gravity in antiscarp formation. In particular there will be a focus on establishing whether antiscarp formation can occur solely under gravity or whether there is a need to have a secondary trigger or process to initiate formation.

1.3 Methodology

Several different avenues of study were undertaken to contribute to achieving the objectives outlined in the previous section and involved an in-depth review of available antiscarp literature, field observations, and modelling of antiscarps.

1.3.1 Literature review

Numerous journal articles and books were reviewed with a focus on extracting information factors that are essential to antiscarp occurrences and processes. These factors were then collated within a chart so that the information could then be interrogated to try and identify and significant trends.

The literature review also provided the background to understanding how the different nomenclature has been used, and how this use has changed over time as older terms are used to represent newer features that are not necessarily encompassed by the definition of the older term. As an example, “sackung" (Zischinsky 1966) has evolved from representing a slope deformation that requires plastic deformation in a less competent underlying unit to being applied to seismically-related antiscarps.

Terminology that was identified in the reviewed literature was sorted into expressions that represented aspects of antiscarp morphology and those that related to antiscarp formational processes. Clear definitions for the identified terms and how they relate to antiscarps have been provided. These definitions are integral to the production of an antiscarp formative process flowchart and are also used throughout this thesis.

The key term defined within this thesis is antiscarp, which is thought to be a contraction of antislope scarps although its etymology is uncertain. Antiscarp is a morphological term used to describe any uphill-facing scarp on a slope and its use has no dependence on the process by which it may have formed. A morphological approach to addressing uphill facing scarps is considered necessary as the primary approach because it does not appeal to any process and therefore does not infer any particular process, which is the role of the process based terminology.

1.3.2 Compilation of an antiscarp processes flowchart

The approach of using morphological properties to determine a process is akin to the use of antiscarp as the umbrella term for all uphill facing scarps, in that process-based terms cannot be used to establish the most likely process without there being confusion. The antiscarp-related information that has been teased out as part of the literature review is presented as a glossary in Chapter 3 to support the production of a system for assessing the most likely process for any observed antiscarp.

A flow chart has been compiled that can be used to input morphological antiscarp properties while following a series of prompts to identify the probable antiscarp formative process, and uses the definitions as presented in the glossary.

1.3.3 Field studies

Five areas were investigated or visited to gain insights and observations on antiscarps in the field. The sites were selected based on the types of antiscarp features that have been observed in the past and also on the likelihood that these localities would provide some insights that could be applied to physical and numerical models.

Two of the localities were chosen for more detailed study than the other three, these being the Kelly Range in the South Island of New Zealand and Beinn Fhada in the Scottish Highlands.

The Kelly Range was chosen because of the work presented by Beck (1968) on gravity faulting as a means of topographic adjustment. The discontinuity sets that are exposed above the Kelly saddle allow a view of a natural cross section through the upper section of a massif with antiscarps. The proximity of the massif to known active faults provided an opportunity to compare these antiscarp structures with others that have formed within a seismically quiet area.

Beinn Fhada has been studied by several authors (Holmes and Jarvis 1985; Holmes and Jarvis 1986; Whiteside 1986; Fenton and Ringrose 1992; Fenton 1992a; Jarman and Ballantyne 2002; Jarman 2003a; Jarman 2003c; Jarman 2006) and has extensive antiscarp development on the southern slope with cirque development on the northern slope. Like the Kelly Range there has been extensive glacial activity in the past with the last glacial maximum appearing to coincide with the onset of antiscarp formation. A key difference between Beinn Fhada and the Kelly Range is the level of seismicity, with Scotland not being exposed to either the same magnitude or frequency of seismic events, thus providing a good basis for comparison.

The other locations visited included the Lewis Tops and Stag Hill in the South Island of New Zealand, and Ben Each in the Trossachs region of Scotland. These trips involved a day of field work where the focus was more on observing the features in the field in order to better understand the subtle differences and similarities across different localities.

Key information taken from the field localities was the physical appearance and geometry of the antiscarps, spatial distribution, other associated slope features, field estimated rock mass properties, and a general overview of the geological setting of the with a focus on identifying glacial and/or tectonic features.

1.3.4 Modelling

Both physical and numerical models were used to examine and assess the role of gravity in antiscarp formation, with the numerical models also used to assess the response of a massif to the removal of large volumes of material to simulate cirque development. All models were two dimensional.

Base friction models were used for the physical modelling and utilised individual elements that were fabricated together to form a two dimensional massif. The models were then slid over a static surface to generate friction along the base of the model, with the direction of

sliding representing the simulated gravitational load. Varieties of materials were used to form the models and gave massifs that ranged from a uniformly fractured material with pervasive discontinuities, through to models that represented what could essentially be considered to be a granular massif.

Antiscarps were generated in several of the base friction models and a dependence upon structural attitude was observed.

The numerical modelling utilised finite element models to numerically simulate the massifs. Initially Plaxis v6.1 which had a limitation of only 50 elements so was only able to deliver relatively coarse resolution on the models developed. Outputs from Plaxis were deformed grids and displacement vectors. Basic grid deformations indicated that antiscarps could form solely under a gravitational load, and also under conditions where the massif deformed in response to the removal of a large volume of material representative of a cirque.

FLAC 2D v3.4 was used because it was able to generate grids with greater detail thereby allowing more complex massif geometries to be tested. FLAC models provided outputs that showed stress redistributions conducive to antiscarp formation.

1.4 Thesis organisation

The initial portion of this thesis reviews the available literature and presents key antiscarp terminology which is used throughout the thesis. A chart accompanies this chapter and presents key data extracted from the reviewed literature in a tabulated format. A flowchart has been developed that utilises many of the definitions derived from the literature review with the specific aim of enabling a simple approach to identifying the probable process for the formation of antiscarps is presented next.

Data and observations from the fieldwork are covered and set the scene for a section on physical and numerical modelling. The closing section of the thesis is a synopsis and recap on all of the aspects covered and provides details on where the insights developed here can be applied and possible directions for future work.

2 Antiscarp terminology, properties and geological setting

The term “antiscarp” is a relatively recent addition to the geological vocabulary and one of the key aims of this study is to provide a detailed definition for these features, where none has been made before. To adequately define an antiscarp requires insights into associated terminology and how these have been applied in order to understand how the term has developed. “Antiscarp” is an umbrella term for all uphill facing scarps and utilises a morphological approach in the initial assessment, where previously this was undertaken using a wide variety of terms that are generally aligned with processes. To unify the broad range of reviewed material, and to identify commonalities or trends between diverse types of antiscarps, a review table has been produced with accompanying definitions of the associated terminology currently in use.

Properties intrinsic to antiscarps are explored with a view to providing constraints on how they contribute to antiscarp formation and evolution. The geometry, slope aspect, frequency, spatial distribution, and chronology are factors that facilitate key definitions of antiscarps for use in comparative studies.

How a rock mass is able to respond to perturbations is a function of the interaction between the rock material and the discontinuities throughout the rock mass. Discontinuities within the rock mass play an integral part in antiscarp formation by providing interfaces with lower shear and/or tensional strength than the intact rock material that can be exploited where shearing or dilation occur. Principles of engineering rock mechanics, predominantly derived from tunnelling within hard rock, provide a suitable platform for addressing rock mass response to stress field changes.

The geological setting and other factors that shape and affect the massif present controls on the conditions conducive to antiscarp initiation and evolution.

2.1 Review table

Numerous articles on antiscarps have been read to develop ideas and understanding of the approaches taken by various authors, with each author bringing a particular perspective to what they consider key factors for antiscarp formation. A table was constructed (Chart 1) to aid in the comparison of information extracted from a wide selection of articles and to address factors prominent across the examined literature.

2.1.1 Factor selection

Seventeen factors were identified within the reviewed literature as relevant to antiscarp formation and representative of typical antiscarp morphologies; these are used to produce Chart 1. The three mechanisms considered (gravity, slope loading/unloading, and seismicity) are central to antiscarp formation and are the primary factors addressed in Chart 1. Fundamental data such as author, date, locality, geology, etc., are presented alongside information on the glacial and seismic history of the region. The remaining factors are all specific to the antiscarps themselves and are related to measurements and the relationship of the antiscarps to the massifs upon which they are found.

2.1.2 Data limitations

The majority of the data are sourced from article text and tables with the remainder inferred from maps, diagrams and photographs. While every attempt has been made to outline where such inferences are made there are some instances where inferred data are not differentiated. No margins of error are presented for numerical values and no differentiation is made between data extracted from maps and diagrams and those presented in text. Inferred numerical data are considered to be a robust representation of the original authors' work.

While values for most of the factors could be extracted from the reviewed articles there are some that either could not be determined or were not referred to in the reviewed text. Question marks are used to indicate either no reference to the specific factor within the article or an inability to satisfactorily extract the information from diagrams or text. Where an author alludes to a factor, but does not substantiate it elsewhere within the article, then it is typically noted as inferred. No attempt is made to infer anything that cannot be directly taken from the article, for example, Japan is a seismically active region yet there is no reference to seismicity in an article from a Japanese field site, so a question mark is inserted in the relevant cell on Chart 1.

For an article to be incorporated into Chart 1 it needed to have either a focus, in whole or part, on antiscarp features, or on one of the primary driving mechanisms. Article accessibility also controls inclusion in Chart 1 and in some cases the lack of availability may have led to the exclusion of potentially key articles.

2.1.3 Data presentation

Data presented in Chart 1 are initially ordered based upon the most common mode for the primary mechanism, in this case gravity, then chronologically, and subsequently by the author's name. Phrases or terms used by authors are presented in the table where possible to try and preserve the essence of their ideas and reduce the possibility of misrepresentation within this study.

2.2 Currently used terminology

There is much variability in the terms used to describe antiscarp features. As the body of literature referring to antiscarps in all their different guises has grown, so too have the ways in which the terminology has been applied. This seems especially prevalent for terms that are based upon a mechanistic approach, such as "sackung", which has evolved beyond its original scope into use as a morphological term.

The following is a selection of terms used by the authors reviewed in Chart 1 with a brief description of the key aspects of that term. Where different terms have the same meaning they are grouped together under what is considered to be the most dominant or suitable term.

Terms that have a morphological background are listed first and are followed by terms that are deemed to be process- or mechanism-based, as the morphological features are often an integral aspect of specific processes.

2.2.1 Morphology based terminology

2.2.1.1 Antiscarp

Other names: antislope scarps, obsequent scarplets, uphill facing scarps, counterscarps, upslope-facing scarps, trenches.

Antiscarp is a morphological term for a scarp that faces up the slope towards the ridge (Figure 2.1) (Ballantyne 2002; Jarman 2002; Jarman 2003a; Kinakin and Stead 2005; Wilson 2005; Jarman 2006; Wilson and Smith 2006). While it is difficult to tease out the origin of the term antiscarp, it is considered that it is a contraction of the term antislope scarp. The earliest published use of the term antiscarp found by this author is Ballantyne (2002) where it is used within the article and also appears erroneously in the references as "Tephrochronology of antiscarp slopes…" when referring to Beget's 1985 paper "Tephrochronology of antislope scarps…".

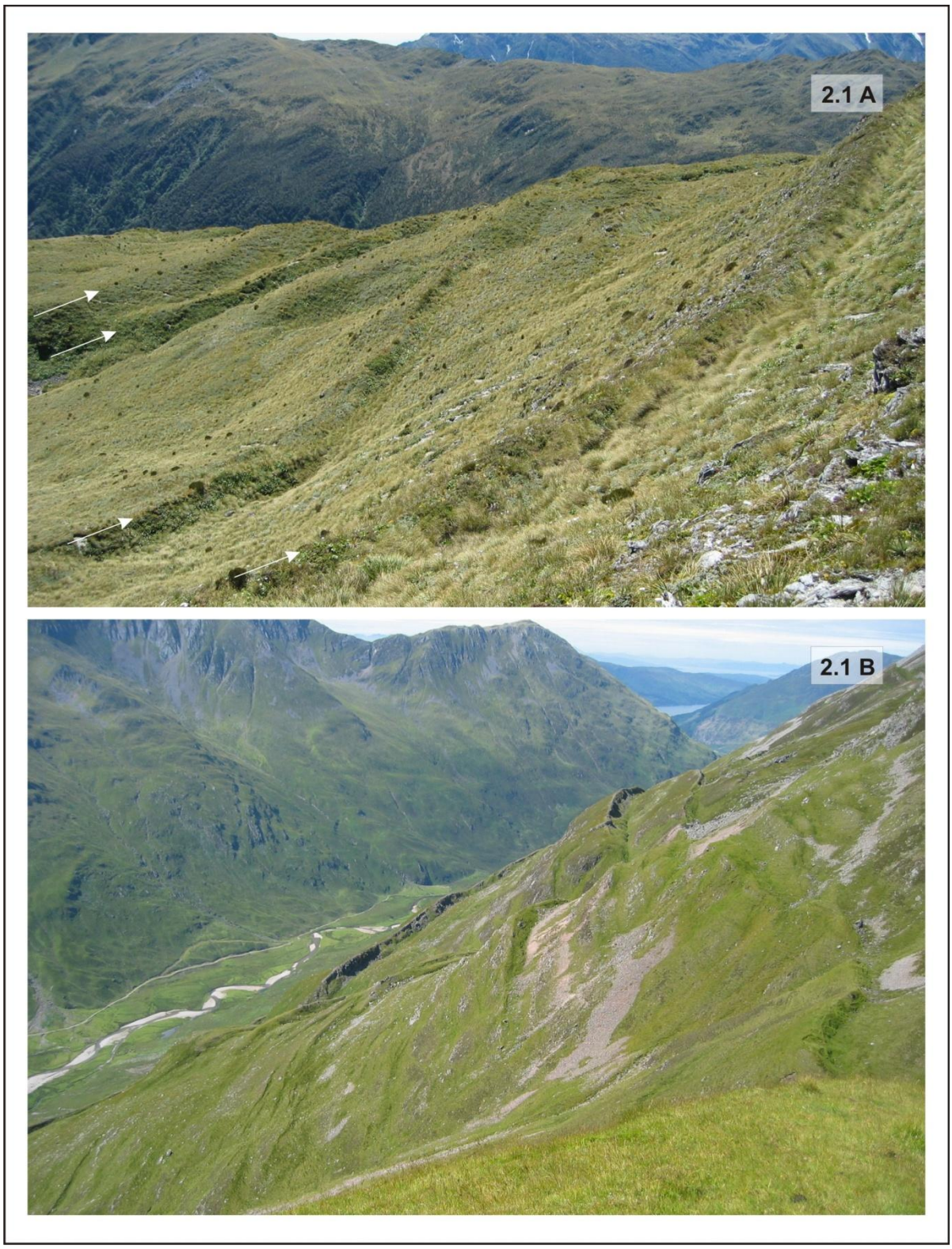

Figure 2.1: Antiscarps on the Kelly Range, Otira, New Zealand, are highlighted by white arrows in Figure 2.1A. Multiple antiscarps on Beinn Fhada (Ben Attow), Kintail region, Scotland, in Figure 2.1B show a wide variance in the degree of displacement.

Antiscarps are most often found in the upper reaches of slopes near ridges and tend to run sub-parallel to the slope contour. They may appear singly or in multiples and often have a preferred alignment to the structural fabric of their respective massifs. Antiscarps are typically more prolific in areas of tension upon the slope as evidenced by typical associated dilation.

As a morphological term there is no association of antiscarps with a particular mechanism, rather they are a product of a variety of mechanisms and processes.

2.2.1.2 Oblique antiscarps

Other names: crossing trenches (Parise et al. 1997; Di Luzio et al. 2004).

Oblique antiscarps are angled relative to the contour of the slope and in many instances intersect contour parallel antiscarps to form complex interference patterns (Figure 2.2).

While no references are made to oblique antiscarps they are considered to be the equivalent of crossing trenches as referred to by Di Luzio et al. (2004) and Parise et al. (1997). Examples of this phenomenon appear in Bovis and Evans (1996), Mokudai and Chigira (1999), Sorriso-Valvo et al. (1999), Agliardi et al. (2001), Jarman (2003b, 2003d) and Di Luzio et al. (2004).

As with antiscarps, oblique antiscarps are generally found in the upper sections of slopes and tend to follow major structural trends.

2.2.1.3 Lineations

Other names: linears, lineaments

Lineations is a collective term used to describe features that have a linear expression on a slope, such as antiscarps, tension cracks, graben, or other structural discontinuities (Figure 2.3) (Fenton 1992b; Bovis and Evans 1996). Lineations may be active fault traces, structural fabric, or tensional features related to zones of specific stress regimes or seismic rupture and may be located anywhere on a massif.

Figure 2.2: The small white arrows are used to highlight slope parallel antiscarps, with the red arrows defining an oblique antiscarp, on the Lewis Tops, Lewis Pass, New Zealand. The large white arrow in Figure 2.2A shows the direction of view for Figure 2.2B. The person in the central part of the photograph gives a scale of around 1.8m.

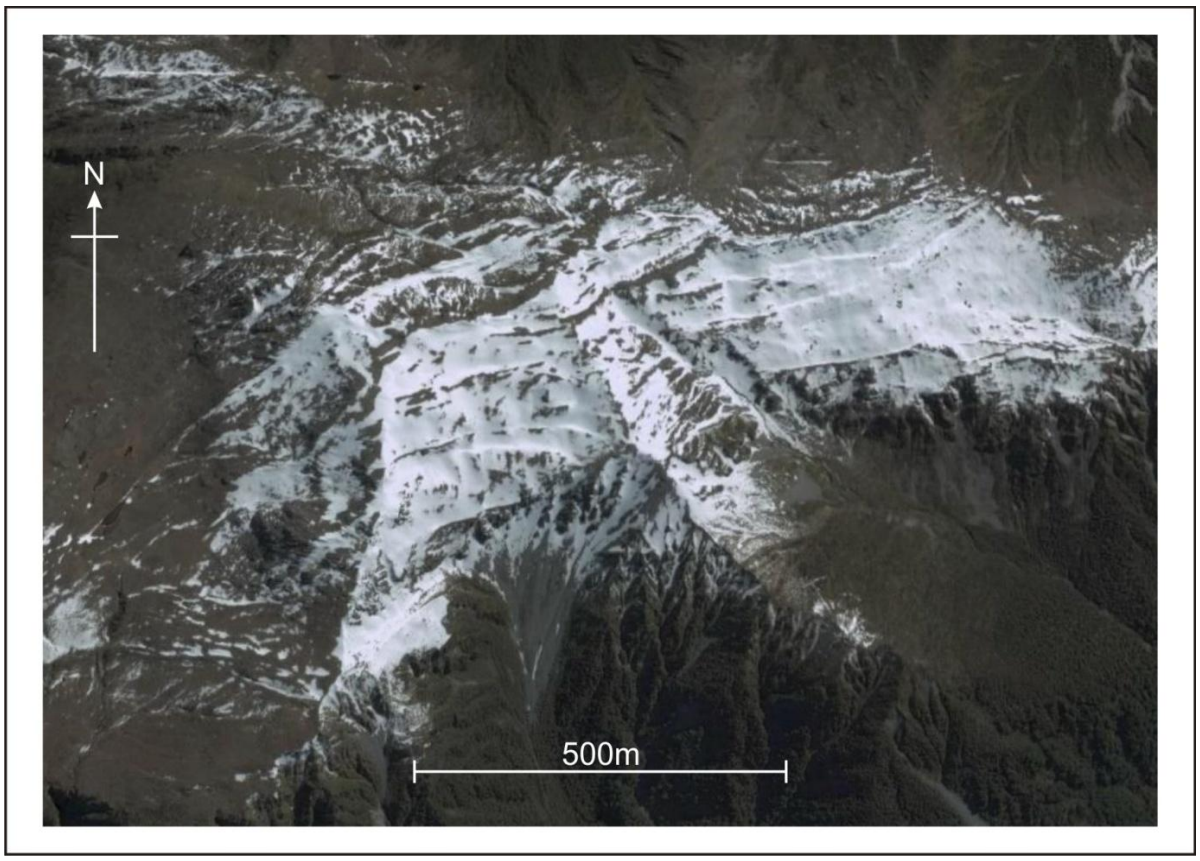

Figure 2.3: Antiscarp features are accentuated by snow on Kelly Hill, Otira, New Zealand, and form lineations, running across the picture, when viewed from above (Image sourced from Google Earth).

2.2.1.4 Tension cracks

Other names: fissures.

Tension cracks form when the tensile strength of the rock material has been exceeded and results in the splitting of, or dilation within, the rock mass.

Tension cracks are often observed in the upper reaches of slopes and are commonly regarded as a precursor for rapid failures. Some tension cracks are considered to be antiscarps under certain scenarios where there is an element of toppling (refer2.2.2.5) (Jahn 1964; Hippolyte et al. 2006).

Tension cracks are typically arcuate although they can be linear depending upon the setting and type of deformation process that they are associated with (Figure 2.4). Tension cracks do not necessarily have a significant component of vertical separation and may appear as short

discontinuous features a few metres in length or as laterally extensive features whose length can be measured in tens to hundreds of metres.

Tensional failure occurs where a slope or massif has been exposed to a static gravitational load for an extended period of time or when a surcharge is added to the existing load. Such surcharges may be long term tectonic loads, seasonal water/snow/ice loading, or short term seismic accelerations. Most gravity driven processes related to antiscarp formation involve massifs under tension, with accompanying tension cracks, and suggest a relationship between tensional environments and antiscarps.

Figure 2.4: A tension crack on the Kelly Range (approximately 500m south of Figure 2.1A) is highlighted by the red arrows with the yellow arrows and lines showing the amount of dilation expressed at the surface. The person in the picture stands to the west of the tension crack and provides a scale of 2m.

2.2.1.5 Release joints

Other names: sheeting.

Release joints are slope- or valley floor-parallel jointing resulting from stress redistribution and relaxation following the removal of material from a slope or valley (Figure 2.5) (Slivovský 1977).

Stress relief occurs during the transition from a three dimensional stress distribution at depth to a two dimensional stress distribution at the surface, where there is an absence of stresses normal to an unloaded surface (Terzaghi and Richart Jr. 1952; Jaeger 1972; Hoek and Brown 1980; Hoek 2000). This type of stress relief rarely occurs at depths greater than 15m (Jaeger 1972) and is typically observed in the lower sections of valleys.

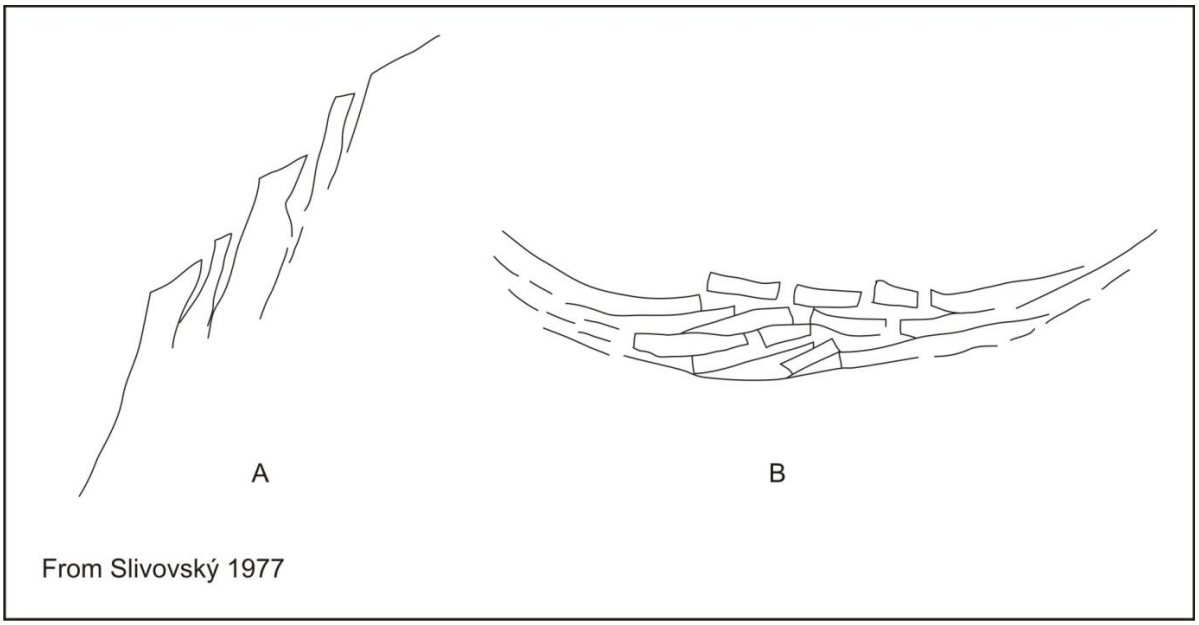

Figure 2.5: Release joints as presented by Slivovský (1970) showing the release of sheets of rock following unloading of the rock mass in A) slopes and B) valley floors.

2.2.1.6 Graben

Graben are downthrown blocks bordered by parallel faults and are indicative of a tensional environment. The term graben is of German origins and is used for both the singular and the plural forms.

Graben are observed at all elevations on slopes, from the crest to the toe, with downthrown blocks ranging from several metres to several hundred metres in width and 20m to 1000m+ in length (Figures 2.6 to 2.8)(Beck 1968; Beget 1985; Varnes et al. 1989).

2.2.1.7 Doppelgrat

Other names: ridge top depressions, double crested ridges, ridge top linear depressions, double crests, double crest lines, doubled ridges, trenches.

The term *doppelgrat* is a literal translation of double ridge in German and is the singular form. In many English texts the plural form *doppelgrate* is often used to represent both the singular and plural forms. The German convention of doppelgrat for the singular form and doppelgrate for the plural form is adopted here.

Doppelgrate are linear troughs or depressions upon ridges that give the appearance of two ridge lines. Depths range from a few to 10 metres, for the ridge top depressions of Tabor (1971), and up to 60m for an example by Radbruch-Hall (1976) related to ridge splitting processes. Linear extents are typically 1000m+.

The formation of doppelgrate can be the result of extension within the massif, in particular the ridge splitting process (refer 2.2.2.2; Fig. 2.10), or particular geometries related to translational failures (Figure 2.6; Jahn 1964).

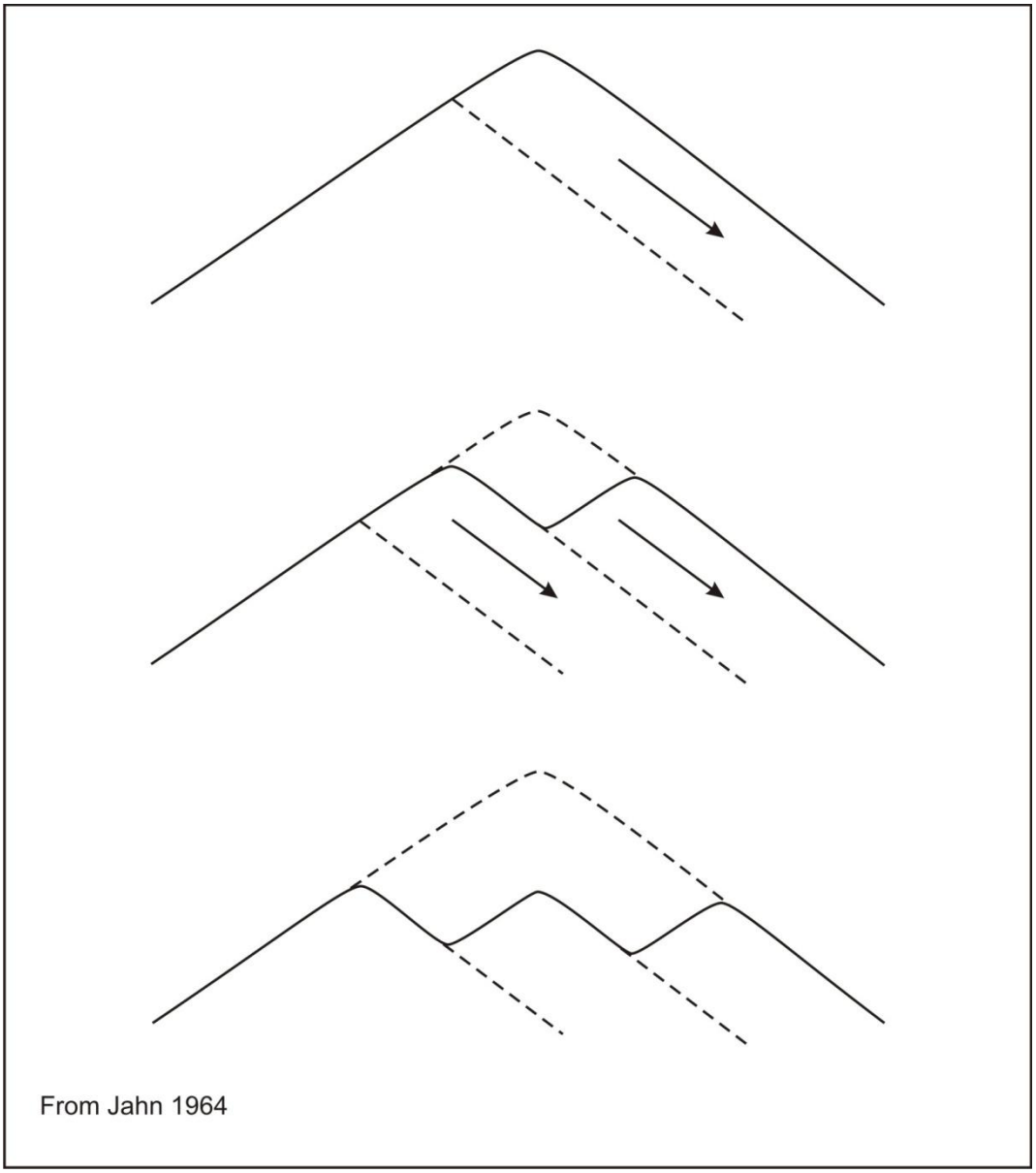

Figure 2.6: Formation of doppelgrate through bedding or joint controlled translational failures (Jahn 1964).

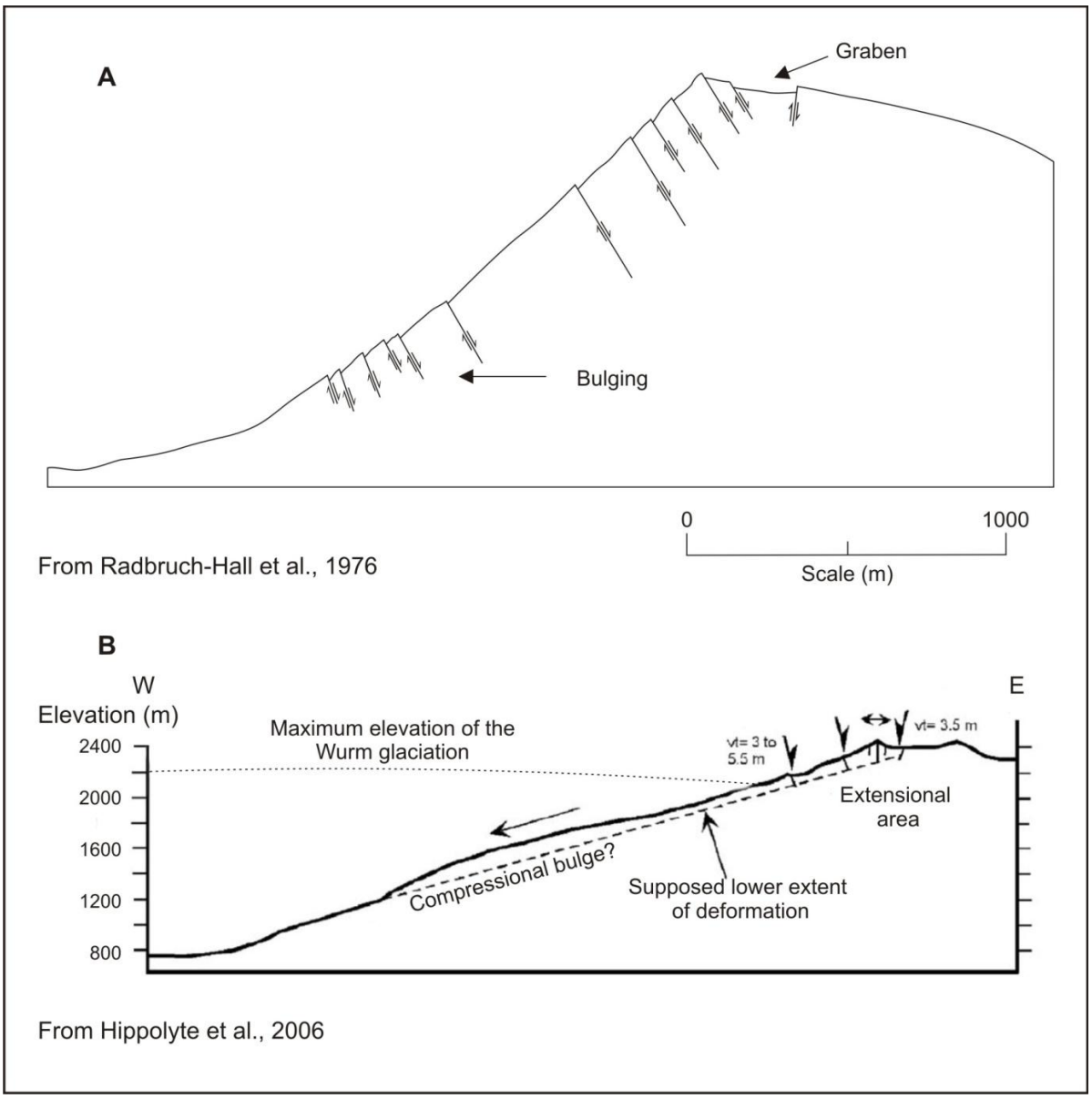

Figure 2.7: Bulging in the toe of a slope can form under both tensional and compressional conditions. Lateral extension within Figure 2.7A is considered to form crestal graben along with suites of antiscarps, clustered on the upper slope and in the bulging lower slope. In Figure 2.7B antiscarps are associated with extension in the upper slope while the lower slope bulging is related to compression.

Figure 2.8: Exposed face to the northeast of the Kelly Saddle, Otira, New Zealand, looking down the axis of the ridge. The models proposed by Beck (1968) (refer Figure 2.9) are indicative of what can be observed at this outcrop. Intersecting joint sets define the margins for graben style collapse with two joint sets identified by the red and yellow arrows.

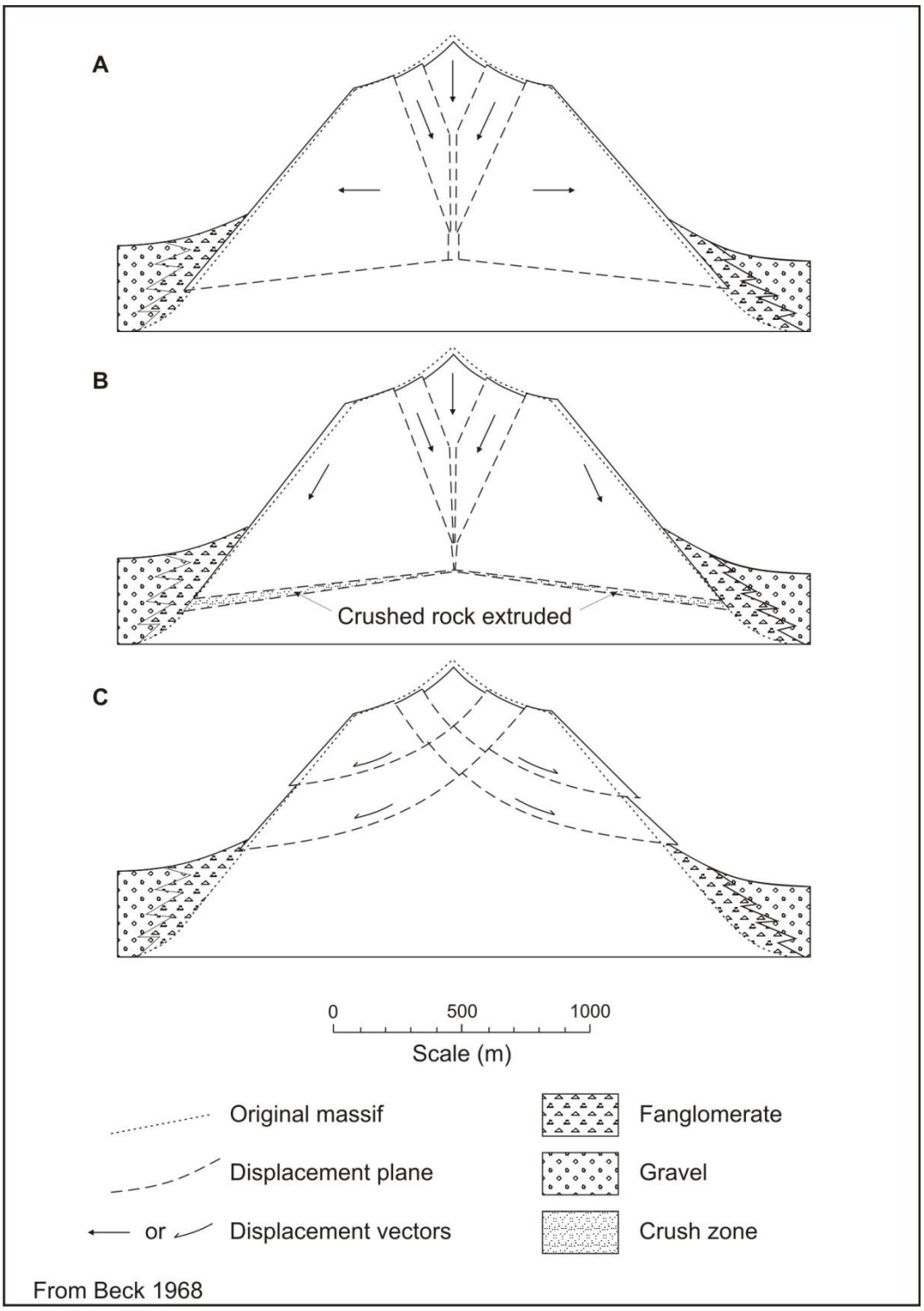

Figure 2.9: Alternative mechanisms for the formation of antiscarps related to gravity faulting (Beck 1968). Topographic lowering is associated with graben style collapse in response to lateral movement within the massif. All models infer lateral movement in the lower sections of the massif, in some instances below the valley infill, whether through the extrusion of crushed rock or by displacing material in the valley. Oversteepening as a result of lateral movement is only

seen to occur in Figure 2.9B, with both of the other scenarios effectively shallowing the slope angle relative to its pre-deformation position.

2.2.1.8 Ridge rent

Ridge rent is a colloquial term used primarily in New Zealand used to describe ridge-parallel lineations that often incorporate a component of vertical displacement to form antiscarps (Lensen 1976; McLean 1986; Wood et al. 1990; Chamberlain 1996; McCalpin 1996; Paterson 1996; Cook 2001).

The term ridge rent has been used as a descriptor for antiscarps related to gravitational spreading (Lensen 1976), surficial collapse (McLean 1986), and to seismic activity (Wood et al. 1990; McCalpin 1996). McLean (1986) notes that ridge rents are especially prominent on steep slopes where bedding, schistosity, or jointing parallel the slope contours. Ridge renting has been predominantly used to describe antiscarp features that occur in the upper third of a massif, hence the qualifying term 'ridge', although it is now sometimes used to describe features in the lower slope as well.

In some instances ridge rents are interpreted as precursory phenomena for accelerated, or possibly catastrophic, failure (Korup 2005a) in much the same way tension cracks are.

There are many similarities between tension cracks and ridge rents in that they are both extensional phenomena that exhibit dilation. A major difference is that ridge rents may have a component of vertical displacement ranging from centimetres to decametres, whereas any vertical displacement on a tension crack is typically measured in the range of several centimetres.

2.2.1.9 Bulging

Bulging relates to slope morphologies that have a distinctive protuberance in the lower section of the slope.

Radbruch-Hall et al. (1976) suggest the formation of antiscarps and graben on a massif is coincident with bulging in the lower slope and that the bulging is an expression of tension within the massif (Figure 2.7A). Tensional bulging is the dominant perspective throughout antiscarp related literature and suggests a strong relationship between tensional stresses within a massif and antiscarp formation (Zischinsky 1966; Nemčok 1972; Radbruch-Hall et al. 1976; Savage and Varnes 1987; Varnes et al. 1989; Chigira 1992; Bovis and Evans 1996;

Sorriso-Valvo et al. 1999; Agliardi et al. 2001; Jarman and Ballantyne 2002; Schwab and Kirk 2002; Di Luzio et al. 2004).

Hippolyte (2006) provides a contrasting condition where slope bulging is attributed to compressional processes occurring in the toe of a translational landslide deposit (Figure 2.7B).

While the slope morphology between the cross-sections of Radbruch-Hall and Hippolyte are similar, the distribution of antiscarps is markedly different. Under tensional conditions antiscarp distribution is clustered in the upper slope and consequent to the slope bulge, while in compressional tensional conditions antiscarps are only observed near the extensional zone adjacent to the ridge.

Consideration must be given to correct identification of bulging in the field. Landslide deposits, talus, or glacial deposits on the lower slope morphologically can appear to be bulges in the slope but are only a surficial deposit (Figure 2.10).

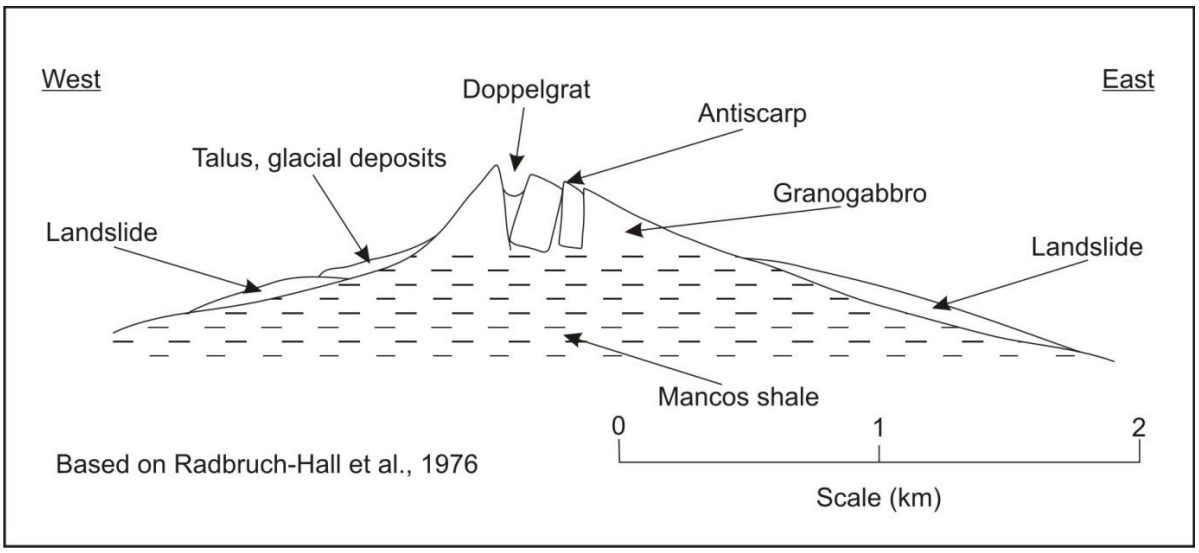

Figure 2.10: Lateral movement of the granogabbro is driven by slow plastic deformation in the lower strength shale via the process of ridge splitting to form antiscarps and a doppelgrat. Surficial deposits on the lower flanks of the slope may give the appearance of bulging.

2.2.2 Process-based terminology

2.2.2.1 Gravity faulting

Large scale deep-seated failure surfaces through a massif are considered to accommodate movement driven by gravity acting upon the massif (Figures 2.8 and 2.9; Beck 1968). Gravity faulting is typified by graben style collapse of the ridge into the massif, having a primary sense of motion vertically downward, and is accompanied by a component of lateral movement in the rock mass. Extensive jointing through the rock mass is deemed to accommodate the movement

Beck (1968) is the only author to utilise the term gravity faults.

2.2.2.2 Ridge splitting

Spreading or lateral displacement in a lower weak unit drives deformation in the strong upper unit to form a linear trough, or doppelgrat (refer 2.2.1.7), adjacent to the ridge (Figure 2.10) (Radbruch-Hall et al. 1976). Movement is accommodated along disconnected planes or by slow plastic deformation as the result of tectonic uplift, seismic activity, rapid incision, or debuttressing (Tabor 1971; Radbruch-Hall et al. 1976; Varnes et al. 1989; Mokudai and Chigira 1999; McCalpin and Hart 2000; Di Luzio et al. 2004).

Jahn (1964) outlines another scenario for ridge splitting where the infilling of tension cracks with debris derived from the local slopes accompanies progressive dilation of the massif (Figure 2.11). The resulting morphology gives a doppelgrat and accompanying antiscarps.

Some of the features associated with ridge splitting are antiscarps, doppelgrat, and bulging.

2.2.2.3 Sackung

Sackung translates from German as “sagging” with the plural form being sackungen. Deformation of competent material in the upper slope is induced by plastic deformation within underlying weak units and is considered to be driven by gravity loading on the slope. The response within the surface morphology is the formation of antiscarps, hummocky terrain, trenches, rockslides and rock avalanches (Zischinsky 1966). There is no requirement for a throughgoing basal failure surface.

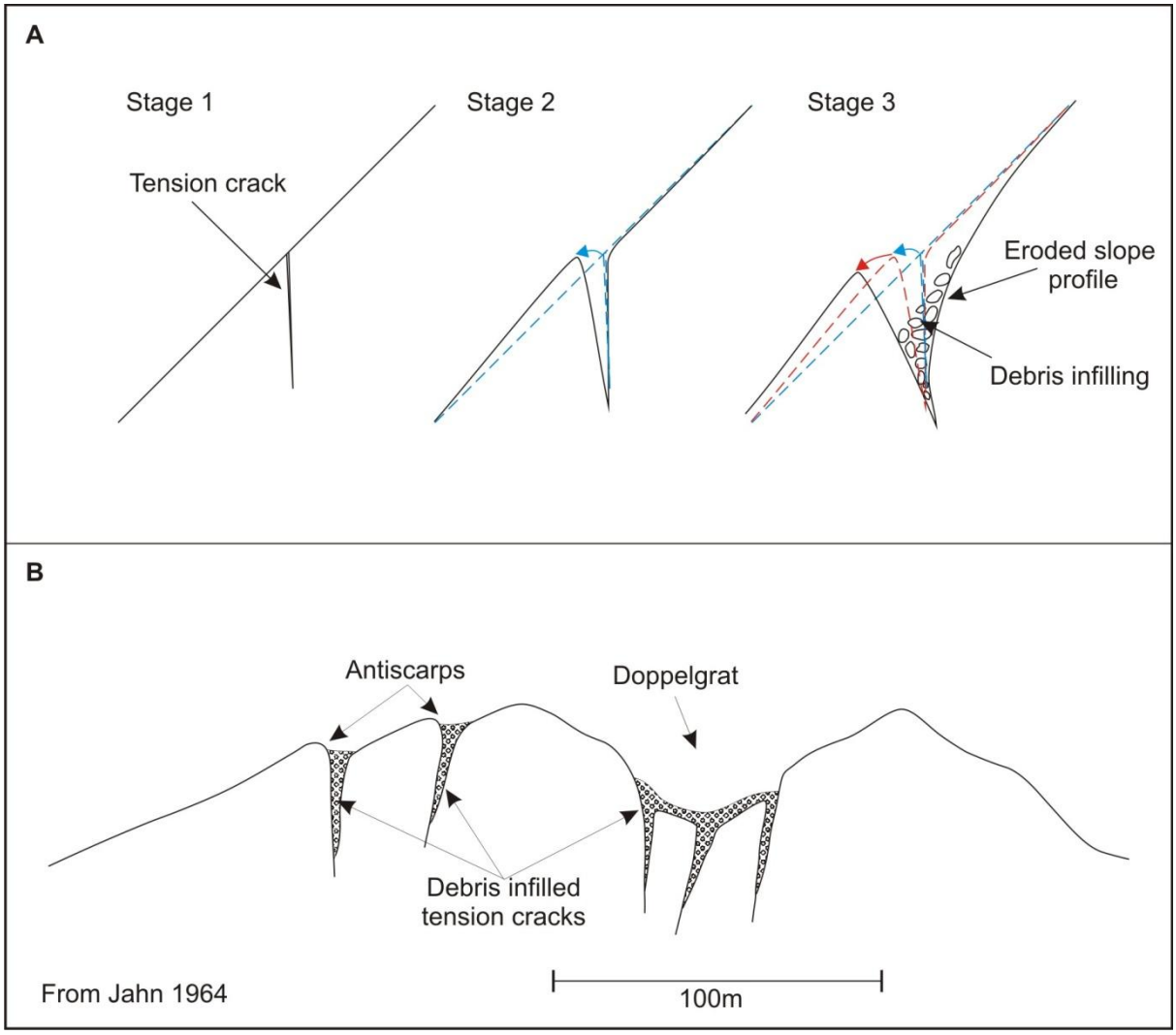

Figure 2.11: Widening of the tension crack through the stages outlined in part A occurs in response to gravitational displacement of the lower slope section and accompanying scarp degradation above the crack. The displaced lower section is consequently undergoing tilting out of the slope, or more correctly toppling, during this process. When placed in the broader context of the massif, as seen in part B, Jahn argues for accommodation of slope debris within the tension cracks which highlights the appearance of antiscarps and doppelgrat in the slope profile (Jahn 1964).

The term sackung has evolved and has been used to describe flow type of movement within rock (Radbruch-Hall et al. 1976), gravitational spreading of steep sided ridges to form antiscarps and linear fissures (Savage and Varnes 1987), landform features associated with mass rock creep (refer 2.2.2.4; Chigira 1992), shallow gravitational mass movements 100m to10km long occurring over periods of 1 – 10 000 years (Shroder and Bishop 1998), some

tectonic fault scarps (McCalpin 1999), and deep-seated gravitational slope deformation (Dramis and Sorriso-Valvo 1994; Ambrosi and Crosta 2006).

By definition sackung infers slow rates of movement, akin to creep. McCalpin (1999) notes that the term sackung is increasingly being applied to landform phenomena based on morphological expression, and as such, landforms related to rapid or episodic events are being referred to by a term that denotes slow movement. McCalpin utilises the plural form sackungen as a descriptive term for landforms such as antiscarps, ridge-crest troughs, and closed depressions while acknowledging that formation may have been rapid or slow.

Field studies undertaken in the phyllites, paragneisses, and mica-schists of mountains in the Austrian Alps were used to develop Zischinsky's (1966) ideas on sackung. Observed strain was used to construct differential velocity profile vectors for the upper sections of some mountains and showed reducing displacement with depth (Figure 2.12). Zischinsky further proposes that a sackung, devoid of a basal failure surface, is a transition to a gleitung, which is where through- going rupture occurs to create a failure plane.

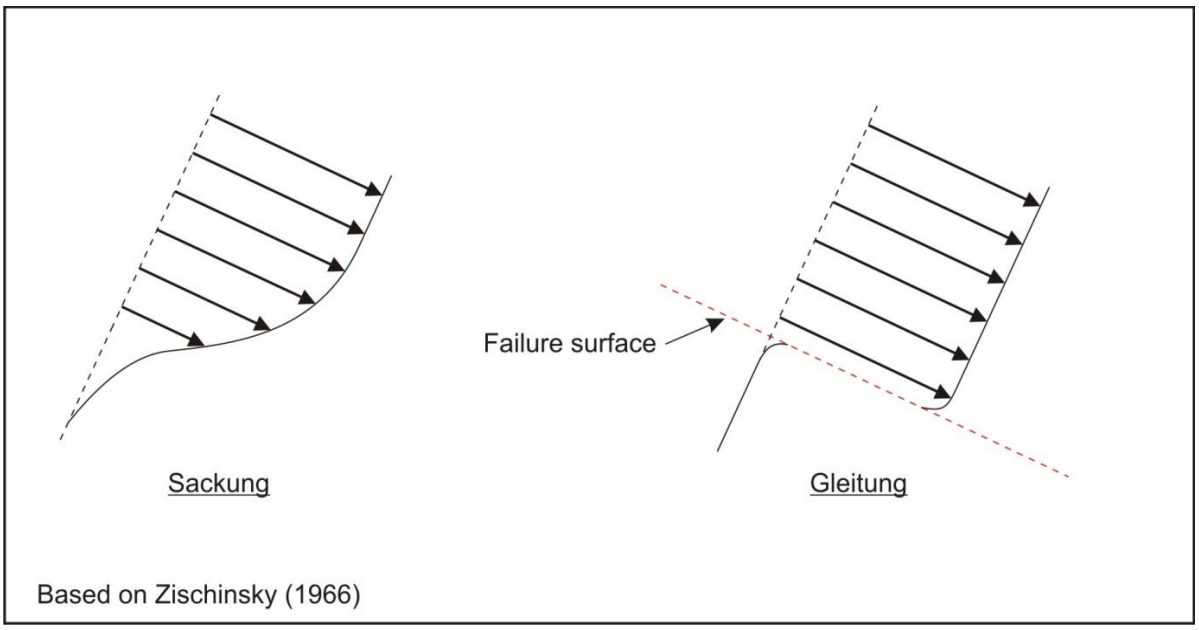

Figure 2.12: Velocity profiles developed by Zischinsky (1966) reflect observed strain within a massif under conditions of plastic deformation, for the sackung, and after a throughgoing failure surface has developed, in the case of the gleitung.

2.2.2.4 Mass rock creep

Other names: creep.

Radbruch-Hall (1978) defines mass rock creep (MRC) as an encompassing term for very slow downward and outward movement of material adjoining a slope. As with sackung there is no need for a through going rupture surface. MRC typically deforms plastically, with strain being non-recoverable, and is in response to gravitational loading. MRC is generally ascribed to occur within homogeneous material and may be influenced by discontinuities and variations in material properties within the rock mass (Radbruch-Hall 1978).

Deformation is assumed to be continuous (Chigira 1992), although closely spaced episodic events can also appear as ongoing movement, and may be driven by seasonal variability (Radbruch-Hall 1978) (Figure 2.13). In some instances MRC may be punctuated by episodic movement (Beck 1968; Nemčok 1972; Mahr 1977; Mahr and Nemčok 1977; Bovis 1982; Beget 1985; Chigira 1992; Bovis and Evans 1996; Kellogg 2001; Schwab and Kirk 2002; Di Luzio et al. 2004).

Localised bulging, faulting, folding, and toppling, can occur within the deforming rock mass in response to MRC (Chigira 1992).

2.2.2.5 Toppling

Toppling involves the forward rotation of a block or mass of material out of the slope about an axis lower than the centre of gravity of the displaced mass (Jaeger 1972; Goodman and Bray 1976; Hoek and Bray 1981; Turner and Schuster 1996). Several modes of toppling are identified by various researchers and in many instances are related to antiscarp formation.

Goodman and Bray (1976) describe one type of topple as flexural toppling where dipping foliated or layered masses are likened to cantilever beams which break as they bend forward under flexure (Figure 2.14A). Flexural toppling is accompanied by deep, wide tension cracks in the upper section of the slope, which propagate up the slope, with flexural slip accommodating movement at depth. Flexural toppling is typically initiated by the undermining or removal of lateral or toe.

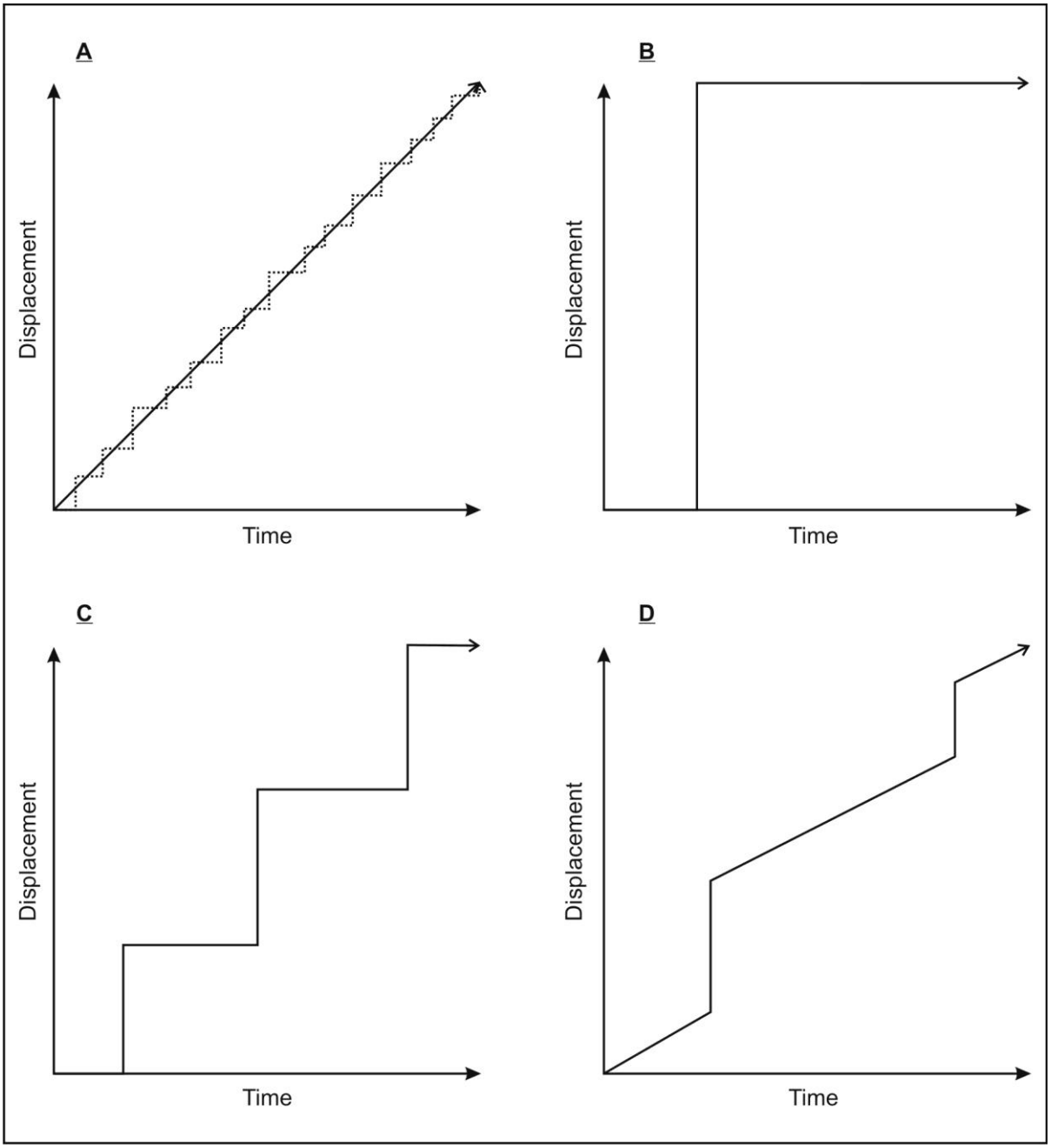

Figure 2.13: Rates at which creep may operate to give the same total displacement. A) constant strain rate with the dotted line showing the relationship with multiple small displacements; B) single event displacement; C) multiple displacement events; and D) multiple displacement events with an accompanying constant strain rate.

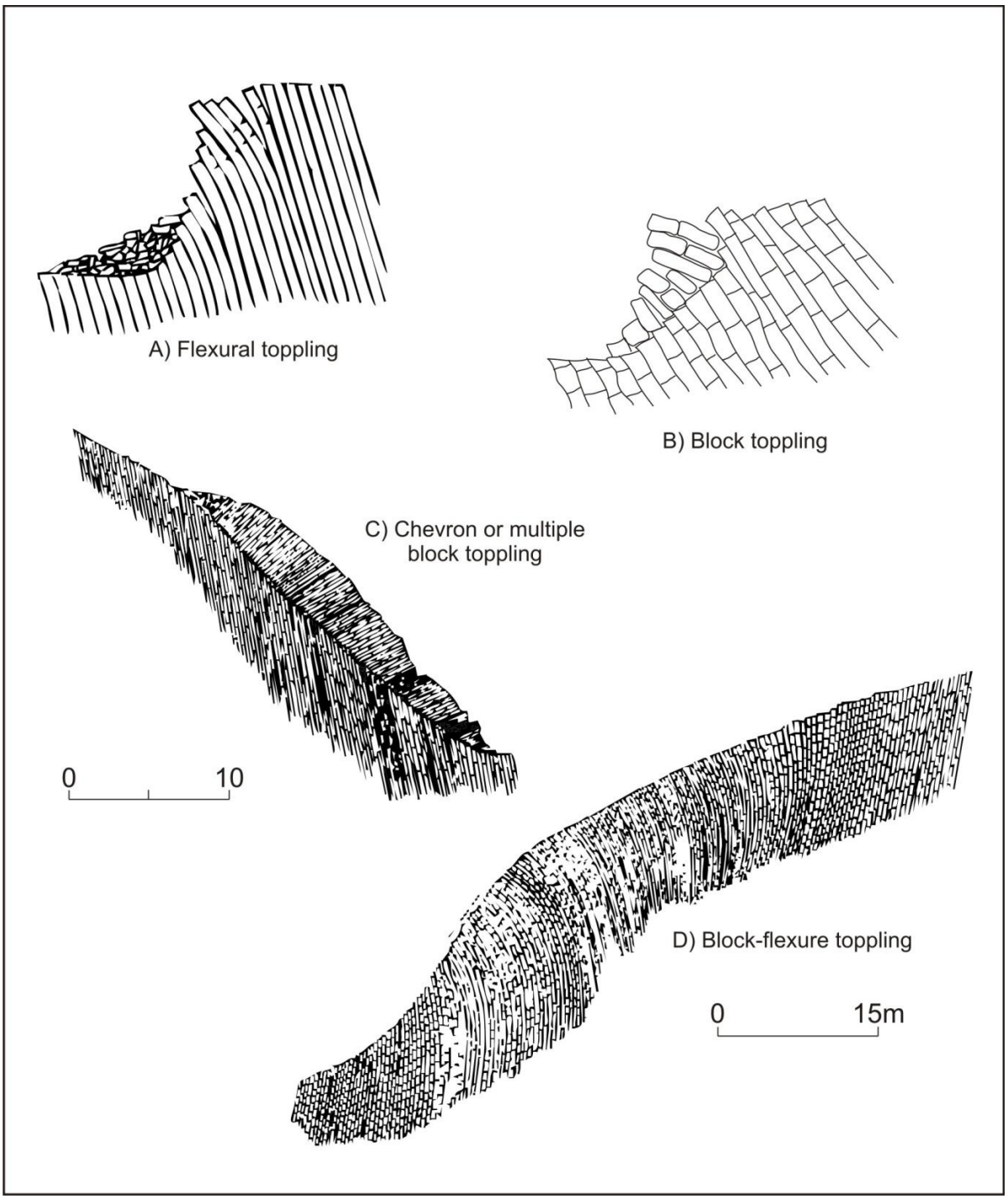

Figure 2.14: Modes of toppling (Figures A, C, and D from Turner and Schuster 1996)

Block toppling occurs within hard rock masses with widely spaced orthogonal joints where columns of rock rotate out of the slope (Figure 2.14B; Hoek and Bray 1981). Shorter columns at the slope edge, or toe, are loaded by the often longer overturning columns up-slope, which typically have a point of rotation getting progressively higher.

Chevron topples occur on slopes with steeply dipping foliation or layers and are typified by the regular dip of the toppled beds. The abrupt change in dip is concentrated at the rupture surface and gives the appearance of a chevron fold, hence the name chevron topple (Figure 2.14C; Cruden et al. 1993; Turner and Schuster 1996).

Block-flexure toppling occurs where the continuous flexure of rock columns is accommodated by existing orthogonal joints as opposed to new breaks through the column (Figure 2.14D; Turner and Schuster 1996; Jarman 2006).

Other forms of toppling include slide toppling (Figure 2.15), where deformation within the substrate induces toppling of blocks or columns, also known as slide-spreads (refer 2.2.2.7), and slump related toppling, where internal rotation occurs at the head of or within a landslide mass as it is transferred down slope (Kamenov et al. 1977; Bovis 1982; Bovis and Evans 1996). The sense of rotation must be out of the slope for the scarp to be uphill facing.

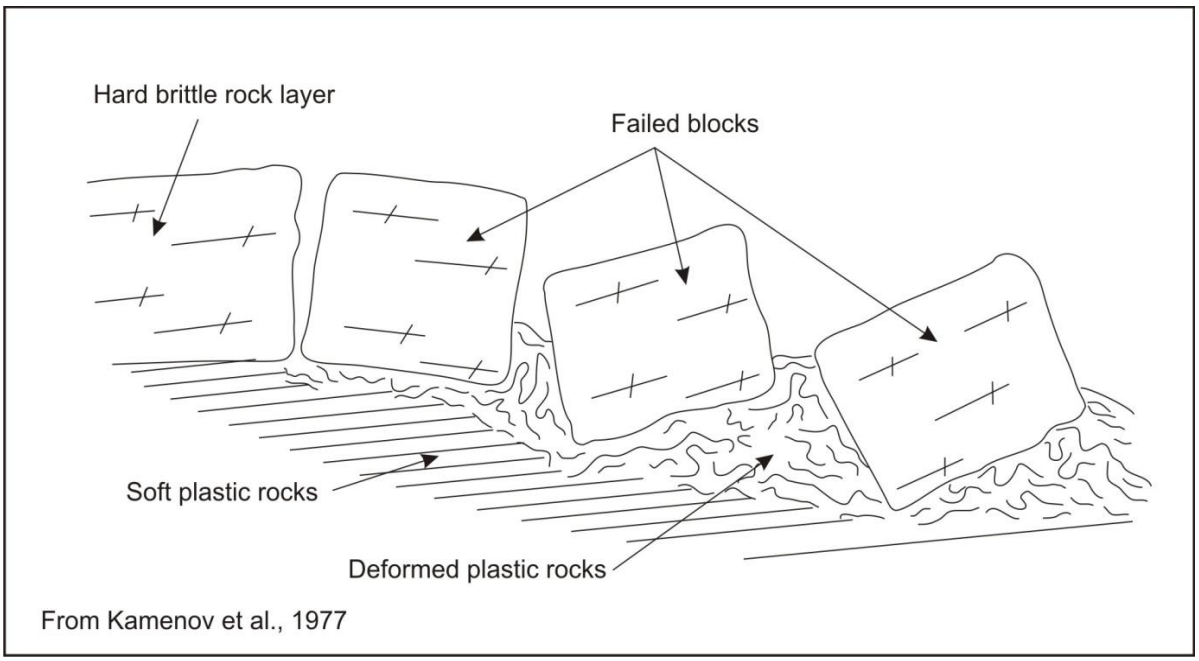

Figure 2.15: A slide topple where blocks of brittle material are rotated during down slope transportation driven by plastic deformation in the underlying rock (Kamenov et al. 1977).

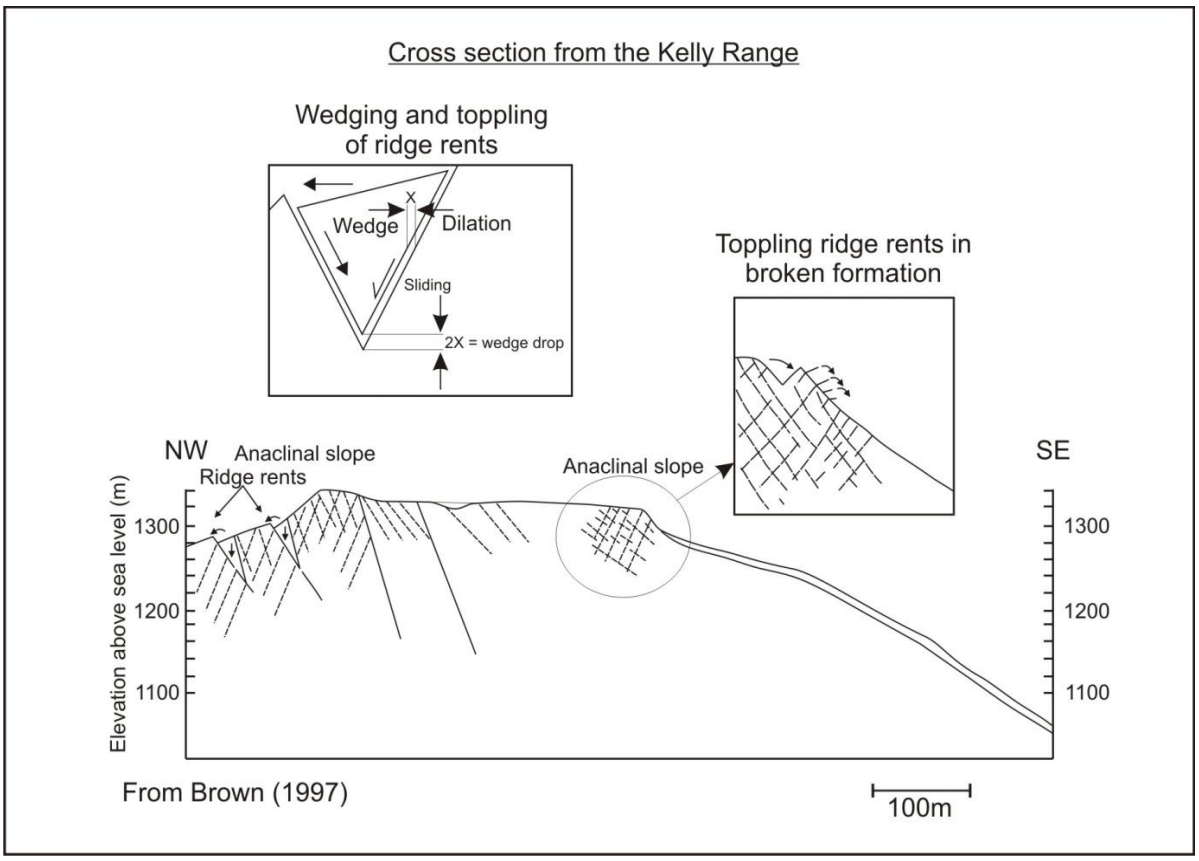

Figure 2.16: Wedging failures as proposed by Brown (1997).

2.2.2.6 Wedging

Brown (1997) uses the subsidence of intact rock wedges into joint controlled dilational voids as one method for the formation of antiscarps, essentially forming what could be considered small scale graben (Figure 2.16). Wedging requires a tensional setting to drive dilation within the joints.

2.2.2.7 Spreading

Spreading movement is characterised by lateral extension, accommodated by shear or tensile fractures (Varnes 1978) and can move at rates akin to creep through to discrete high velocity events (Turner and Schuster 1996).

Varnes (1978) divides spreads into two types; the first is where movement distributed throughout the spread gives an overall sense of extension without a controlling basal shear surface or zone of plastic flow being defined; the second type is where extensional deformation of a coherent material is driven by plastic flow or liquefaction in underlying material. Deformation may occur as subsidence, translation, rotation, or disintegration of the

coherent material and may involve one or many of the processes outlined in section 2.2.2. Spreads often occur on gently dipping slopes.

Features attributed to spreading are typically non-unique and can form by many of the processes covered in section 2.2.2. While spreading is referred to by some authors it is not considered within this thesis to provide a distinct process that could be integrated into a classification system, and is only presented here to provide clarification for where it occurs in Chart 1.

2.2.2.8 Deep-seated gravitational slope deformation

Other names: rock slope deformation, deep-seated creep, DGSD or DSGSD.

Deep-seated gravitational slope deformations (DSGSD) are defined by Dramis and Sorriso-Valvo (1994) and are portrayed as a group of mass-movement phenomena characterised by the following four factors:

1. A continuous failure surface may or may not be present; however the continuity of such a surface may be relevant to explanations for surface deformation.
2. Mass volumes are typically in excess of ~0.2 x $10^6 m^3$ with thicknesses greater than ~20m.
3. The mechanical properties of the rock are subject to scale factors which will consequently influence deformation mechanisms.
4. Displacement is small compared to the magnitude of the deformed mass.

Three processes are considered to be indicative of DSGSD; 1) sackung style deformation; 2) lateral spreading of ridges; and 3) spreading of thrust fronts (Sorriso-Valvo et al. 1999).

DSGSD encompasses many of the processes discussed in section 0 in a similar fashion to spreading, and is more a catch-all term for all features associated with gravity deformation rather than a specific term for antiscarps. The use of DSGSD as a term provides an avenue for classifying identified deformations where there is insufficient data, or interpretation, to adequately assign them to more clearly defined processes.

2.2.2.9 Unloading

Unloading is a term introduced here to represent a process where rebound of the rock mass occurs in response to the removal of a surcharge, buttress, or large volumes of material such

as a cirque. While this process does not feature in any of the reviewed material is has been included here as it is referred to in later parts of this study.

2.3 Antiscarp properties

Antiscarps are morphologically simple structures that can be readily defined by their geometry relative to the slope and their relationship with the geological characteristics of the host massif. The regularity and location of antiscarps upon a slope further aid in correlations with massif geology and formative mechanisms.

The lack of definitive data on formation times for most antiscarps, with the notable exception of some fault related antiscarps, leaves a large gap in the knowledge base and gives scope for much conjecture regarding rates of movement. Poor constraints on time also make it difficult to determine the lifespan of antiscarps.

2.3.1 Geometric attributes

Antiscarps can be represented by two basic dimensions; these being the amount of lateral displacement and the height, or vertical separation of the antiscarp crest from the slope (Figure 2.17).

Vertical displacements between several centimetres, in the case of tension cracks and some ridge rents, through to over 30m, for doppelgrat, are identified in Chart 1. The majority of recorded antiscarps are between 3m and 10m in height with a typical height of approximately 6m (Figure 2.18).

Antiscarp lengths have a wide degree of variation ranging from 20m to over 9000m, although a distinct cluster of antiscarp lengths is apparent around 1000m for antiscarps that have a single continuous expression. Discontinuous antiscarps, or those that are composed of numerous short sections over a long distance, have a widespread distribution with no correlation to a specific length.

2.3.2 Aspect to the slope

The majority of antiscarps are slope or ridge parallel features and therefore are congruent to the slope but some antiscarps, such as oblique antiscarps, do occur at an angle to the ridge.

Existing ridge-parallel discontinuities are considered by many to accommodate movement associated with antiscarps (Beck 1968; Nemčok 1972; Slivovský 1977; Bovis 1982; Holmes

and Jarvis 1985; Varnes et al. 1989; Ferrucci et al. 2000; Agliardi et al. 2001; Hippolyte et al. 2006).

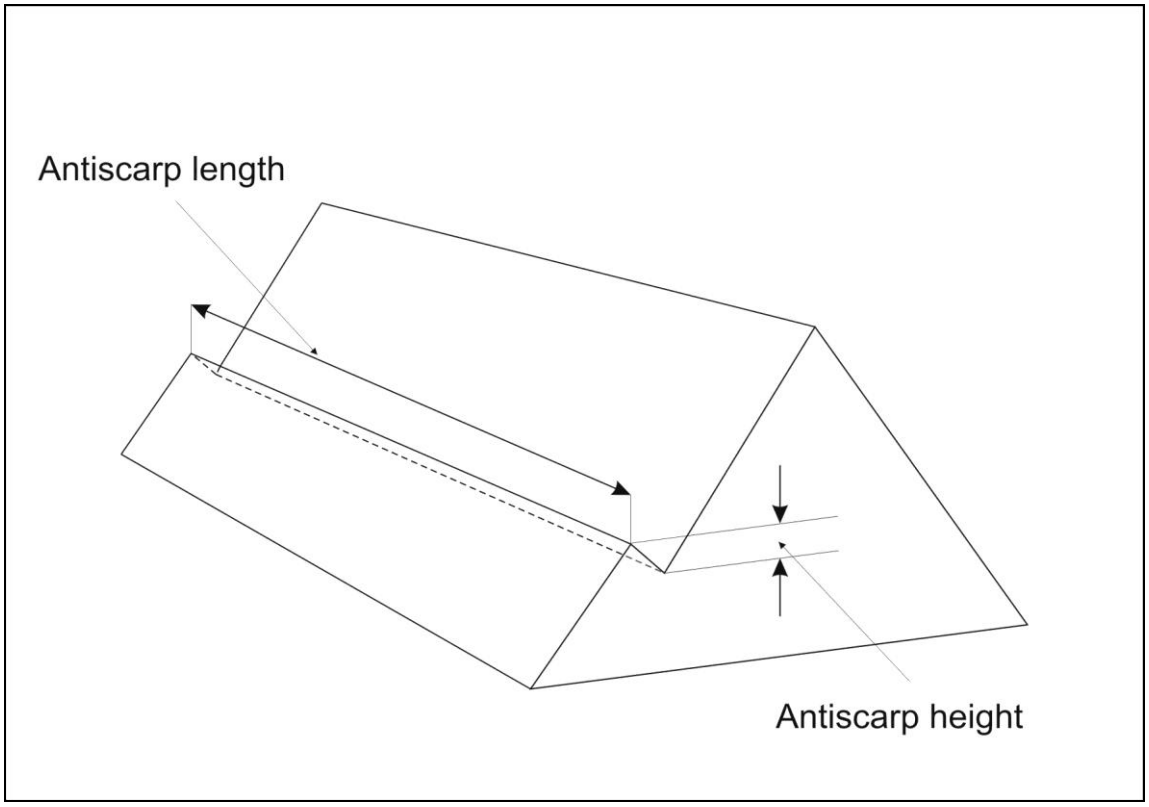

Figure 2.17: An idealised massif showing the measurement parameters for antiscarps.

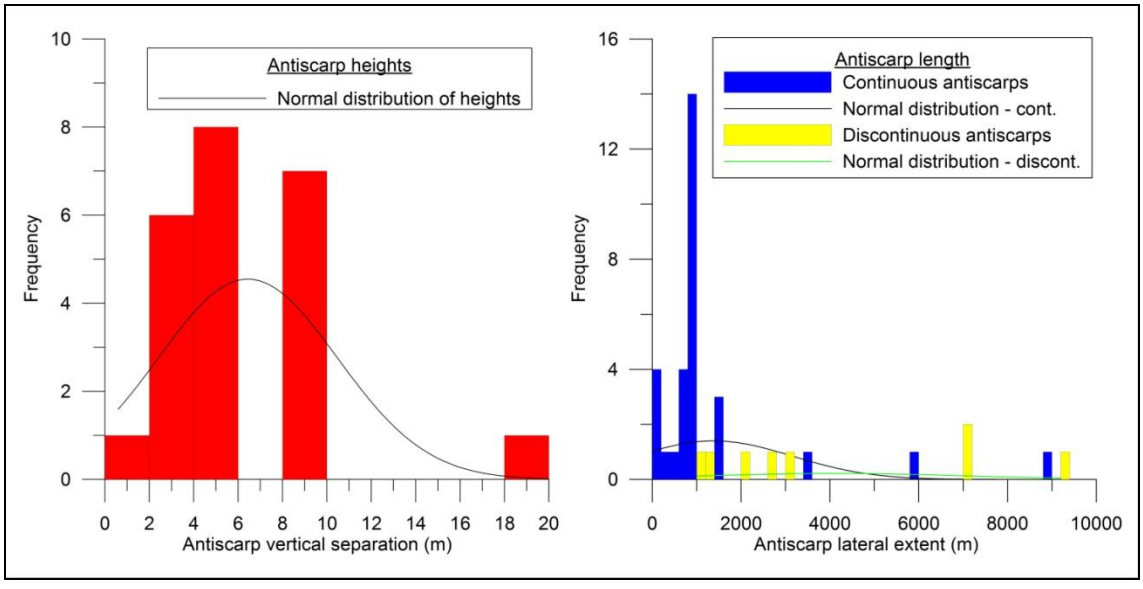

Figure 2.18: Distribution of values for antiscarp measurements determined from Chart 1.

Release joints are a phenomenon driven by stress redistribution parallel to the slope and are indicative of the load removed from different elevations on the slope (refer 2.2.1.5). Because greater loading occurs on the valley floor and lower slopes there will be greater stress redistribution in these zones. Parallelism of antiscarps to slopes is related to the dependence on gravity (Tabor 1971) because stresses will be the same at any given elevation on a uniform slope.

Beck (1968) suggests there is no correlation of regional tectonic fault patterns to ridge-parallel antiscarps, based on observations of antiscarps parallel to many differently oriented ridges within a tectonically faulted region.

2.3.3 Frequency and distribution

The number of antiscarps upon a slope, their spacing, and the distribution of multiple antiscarps or antiscarp sets, give insights into the structural and stress history of a massif.

Singular antiscarps upon massifs, for example Gillett Pass in Alaska (Figure 2.19), are commonly associated with fault surface rupture and are typically found on the lower to mid-slope (McCalpin 1996; Jibson et al. 2006). Antiscarps related to ridge splitting processes, such as doppelgrat, are an exception to seismically related antiscarps when they appear singularly (Jahn 1964; Radbruch-Hall et al. 1976).

Most observed antiscarps occur in multiples on the ridges and upper slope, although they may also appear in sets on the mid or lower slope. Combinations of upper and lower slope sets, with no antiscarps on the mid slope, are not uncommon, and are often associated with bulging in the lower slope (Nemčok 1972; Radbruch-Hall et al. 1976; Savage and Varnes 1987). Total slope coverage is also observed in some areas (Holmes and Jarvis 1985; Ferrucci et al. 2000; Jarman and Ballantyne 2002; Rizzo and Leggeri 2004). Spacing between individual antiscarps within sets varies from massif to massif but is typically regular within any particular set.

Antiscarps and oblique antiscarps that occupy the same slope can create complex interference patterns (Figure 2.2; Bovis and Evans 1996; Mokudai and Chigira 1999; Sorriso-Valvo et al. 1999; Agliardi et al. 2001; Jarman 2003b; Jarman 2003d).

Most recorded antiscarps have been observed on only one side of a ridge although it is not uncommon to find them on both slopes bounding the ridge. Antiscarps on both sides of a

ridge are considered to be controlled by suitably oriented discontinuity sets within the massif (Beck 1968) or reactivated conjugate faults (Hippolyte et al. 2006).

The absence of antiscarps from a slope, or section of a slope, may relate to a lack of preservation due to surface processes acting upon the slope, such as erosion, glaciation, or debris deposition, rather than a lack of formation.

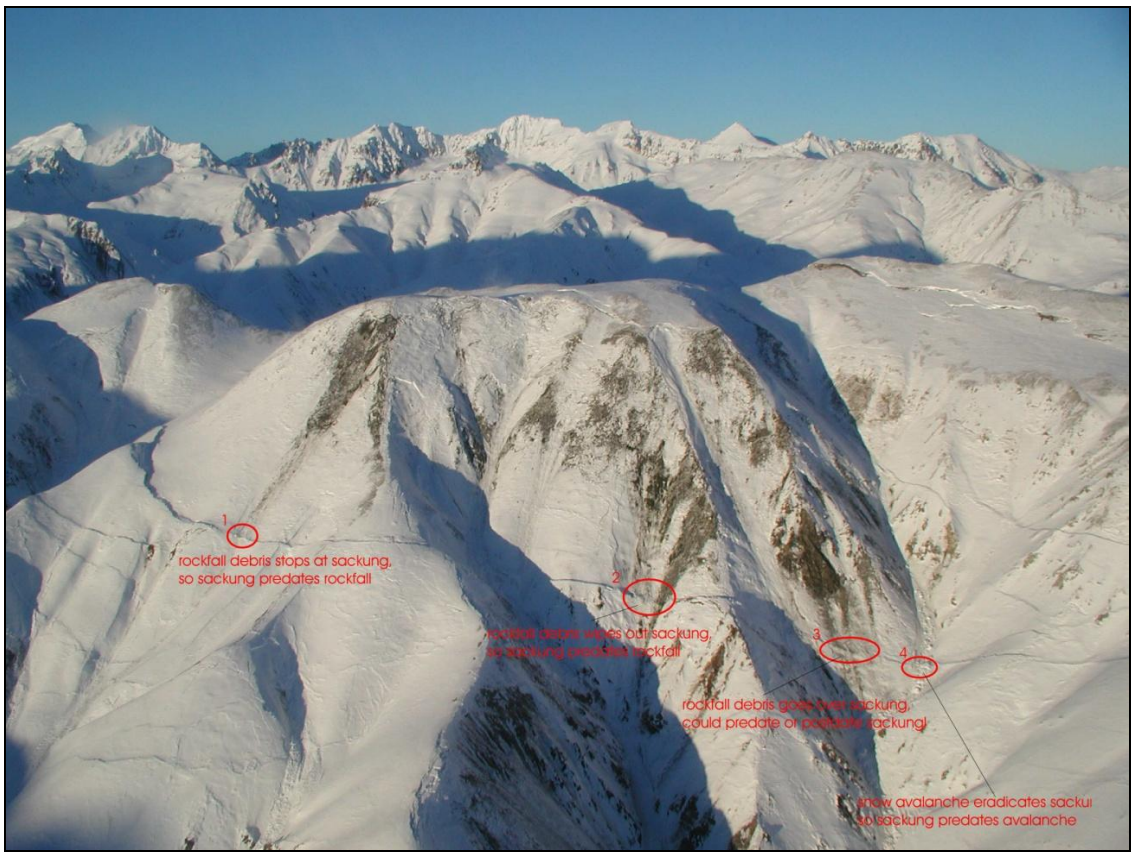

Figure 2.19: A single large antiscarp referred, to as a sackung in this picture, cuts across the massif in Gillett Pass, Alaska, and is considered to have been reactivated during the M7.9 Denali earthquake in 2002 (from McCalpin, http://www.geohaz.com/GravSpread4.htm)

2.3.4 Timing constraints

Few chronologic markers are identified to constrain either antiscarp initiation or rates of movement. Generally the constraints on timing result from correlations with glacial advances, since it can be assumed that glaciation resets the landscape and provides a benchmark surface that displacement and/or deformation can be measured against.

Coseismic antiscarp formation and antiscarps formed by internal deformation of a landslide mass are the few cases where the development of an antiscarp may be observed in modern

times (Wood et al. 1990; McCalpin 1996; Jibson et al. 2004; Saroli et al. 2005; Stramondo et al. 2005; Gutiérrez et al. 2008). Beget 1985 outlines timing for the prehistoric formation and episodic creep associated with antiscarps in Washington, U.S.A., based on tephra sequences, and correlates antiscarp formation with Holocene glacial advances.

Cosmogenic ^{10}Be dating has been employed to determine the age of rock glacier events considered to be contemporaneous with the Arcs sackung (Hippolyte et al., 2009). Six ^{10}Be ages indicate that movement on the sackung and associated antiscarp formation occurred over a few thousand years and stopped about 8462±432 ^{10}Be yr. The sackung deformation is considered to have initiated in the Younger Dryas, approximately 12 800 kya – 11 500 kya, as indicated by bedrock exposure ages. The study undertaken by Hippolyte et al. (2009) infers no seismic input and attributes all deformation to flexural toppling that propagated upslope in response to sackung type deformation.

Radiocarbon dating of peat trapped within antiscarps has been used to constrain the initiation of movement on a DSGSD that had gravitationally driven sliding occur on a ~500m deep shear zone (Agliardi et al., 2009). Movement commenced shortly after deglaciation with peat deposition in some areas indicating that no significant movement occurred during the Holocene.

A key issue with establishing timing is the inability to identify where in any possible continuum antiscarp formation lies with regard to massif evolution. Where there is no firm grasp on either the initial or final conditions of antiscarp formation there is great difficulty in establishing any correlation of the present expression of an antiscarp with massif evolution. For the purposes of this project the antiscarp is considered to be the end member, with an undeformed slope considered to be the initial condition.

2.3.5 Deformation rates

With few data available to constrain the timing of antiscarp formation events there is little scope to develop robust controls on deformation rates over long periods of time, or even whether displacement is ongoing or episodic. Deformation rates can be broken down into four types, these being creep, episodic displacement, creep with episodic displacement and single event displacement. Rates of movement or deformation are typically represented as mm/yr with the absolute displacement able to be represented as a vector (refer 2.2.2.4; Figure 2.13).

Creep is the easiest type of deformation rate to quantify as it is based on a known amount of displacement being evenly distributed over a fixed amount of time. Monitoring of ridge-spreading movements was undertaken by Varnes et al. (2000) in 1997 and 1999 using GPS to reoccupy survey marks used in an earlier survey undertaken during 1975-1989 using electronic distance measuring (EDM) methods. Rates of up to 4mm/yr were determined over a twenty year period with a sense of motion matching the gravitational spreading of the massif.

Gutiérrez et al. (2008) undertook trenching on a 1.3m high antiscarp in the central Spanish Pyrenees and inferred three displacement events based on colluvial wedge stratigraphy and fault truncation. Displacements are proposed as being related to seismic shaking from the nearby North Maladeta Fault. A vertical slip rate of 0.19mm/yr is calculated for the trenched antiscarp with an episodic displacement recurrence interval of 5.6 kyr.

Interferometric satellite Aperture Radar (InSAR) has been used by researchers in Italy to monitor ground movement between 1992 and 2000 and has detected movements ranging from 1 – 5mm (Saroli et al. 2005).

Bovis (1982) used lichenometry to deduce 1m of offset to have initiated and developed over a 110 year period, indicating rates of ~9 mm/yr.

Deformation rates associated with creep assume that movement is at a steady rate or that an average rate is a reliable representation of total displacement over time. By comparison, episodic movement and single event displacements are more difficult to quantify where there is no control on the progression of movement over time. Examination of the different scenarios presented in Figure 2.13 indicates the variability of possible rates depending on when within any of the given timelines the initial and ongoing displacement measurements are made.

2.3.6 Longevity and preservation

A lack of time constraints for the initiation of most antiscarp phenomena consequently gives problems when trying to establish how long they have been in existence.

Preservation of antiscarps is related to the strength of the rock within which they are found, slope surface processes, glacial history, and slope undercutting.

The proliferation of antiscarps within strong to very strong rock correlates well with the assertion that preservation in weak rock is less likely because weak rock is more readily eroded and modified by surface processes

Glacial advances, especially within valley systems, aid in the removal of antiscarps when the glaciers scour the slope surface.

Dense or high vegetation and inundation by rockfall or rill slopes can obscure or mask antiscarps on a slope.

2.4 Rock mass properties

Rock mass properties are an indicative measure of the strength and deformation characteristics of a rock mass (Hoek 2000). Rock mass properties can be defined by the properties of the intact rock material and of the associated discontinuities.

The strength of a rock mass can be expressed as a function of the strength of the rock material, the shear strength of the discontinuities, and discontinuity density.

2.4.1 Rock strength

Rock strength is the measure of the applied stresses at which a rock may fail, and provides constraints on the properties of a rock material, with regard to its tensile, compressive, and shear strength values (Goodman 1976; Hoek and Brown 1980; Bieniawski 1989; Hudson and Harrison 1997).

The rate at which a stress is applied to a rock mass is an important factor to consider. Similar scale rock failures or deformations can be produced by either large instantaneously applied stresses or by lesser stresses operating over longer periods of time.

Analysis of the ‘massif rock type’ column in Chart 1 indicates that antiscarps are found in strong rock, ranging from volcanic intrusives to well indurated sandstones, and through to foliated metamorphic rocks. All rocks are inferred to have uniaxial compressive strengths above 50 MPa based on typical values of UCS as presented in Table 2.1, but are more likely to be in excess of 100MPa, with the exception of underlying weak units related to sackung and some spreads.

Table 2.1: Some typical strength values for rocks (Hoek 2000).

Term	Class	Uniaxial Compressive Strength (MPa)	Point Load Index (MPa)	Field Estimate of strength	Examples
Extremely strong	R6	>250	>10	Specimen can only be chipped with a geological hammer	Fresh basalt, chert, diabase, gneiss, granite, quartzite
Very strong	R5	100 – 250	4 – 10	Specimen requires many blows of a geological hammer to fracture it	Amphibolite, basalt, sandstone, gabbro, gneiss, limestone, granodiorite, tuff, marble, rhyolite
Strong	R4	50 – 100	2 – 4	Specimen requires more than one blow of a geological hammer to fracture it	Limestone, marble, phyllite, sandstone, schist, shale
Medium strong	R3	25 – 50	1 – 2	Cannot be scraped or peeled with a pocket knife, specimen can be fractured with a single blow from a geological hammer	Claystone, coal, concrete, schist, shale, siltstone
Weak	R2	5 – 25	*	Can be peeled with a pocket knife with difficulty, shallow indentation made by firm blow with the point of a geological hammer	Chalk, rocksalt, potash
Very weak	R1	1 – 5	*	Crumbles under firm blows with point of a geological hammer, can be peeled by a pocket knife	Highly weathered or altered rock
Extremely weak	R0	0.25 – 1	*	Indented by thumbnail	Stiff fault gouge

2.4.2 Discontinuities

Discontinuities are pervasive surfaces such as joints, foliation and bedding through some massifs across which there is a lack of continuity of the material properties. Discontinuities provide zones of weakness within the rock mass and play an integral part in antiscarp

formation by providing both low shear strength or tensional strength interfaces, or planes, where shearing or dilation can take place.

Generally the properties of discontinuities have a greater bearing on the stability of a jointed rock mass than the properties of the rock material (Bieniawski 1989). While the rock material defines the maximum possible strength of the rock mass it is the properties and spatial arrangement of the discontinuities that determine the effective rock mass strength. Widely spaced discontinuities or weak rock material are instances where the rock material properties are the dominant factor.

Discontinuities are present in all of the rock types presented in Chart 1 with the majority of articles indicating a direct correlation between the presence of antiscarps and massifs that have prominent sets of joints or discontinuities. Varnes et al. (1989) go further to note that antiscarps have not been observed in unjointed rock. By inference the reduced shear strength associated with discontinuities is likely to be exploited during antiscarp formation.

Joints, foliation, and bedding are observed dipping at a variety of angles between horizontal and vertical. The degree of dip displayed by a discontinuity set will influence the types of mass movement process that that will predominate. Steeply dipping structures will be more prone to toppling and flat-lying discontinuities more able to accommodate lateral displacements.

Elevated pore pressures are not uncommon at discontinuity interfaces and can contribute to instability along these planes. An increase in water pressure reduces the effective normal stress and gives a correlating reduction in the shear strength of the discontinuity (Hoek and Bray 1981). The frictional and cohesive properties of discontinuities are dependent upon any infill material or cement. Clays, shales, mudstones and similar materials can change significantly when water is present whereas hard rock does not typically undergo any extensive alteration (Hoek and Bray 1981).

Complex arrangements of structural features and antiscarps are found in regions where multiple discontinuity sets are present.

2.4.2.1 Joints

Jointing can give a blocky appearance to a rock mass where there are parallel regularly spaced fractures, although joints are more commonly less regular or systematic. Jointing is

normally observed in hard rock masses that have a history of stress changes and can be produced by either compressional, tensional, or shear stresses. Compressional stresses that cause jointing are often related to a regional tectonic influence or to the geometry of the host massif itself where recognisable joint sets are observed (Park 1997). Joint penetration can vary from shallow surficial features through to those that penetrate the whole massif.

2.4.2.2 Foliation

Foliation is a set of planar surfaces within rock as a result of deformation and in part is a descriptor for the penetrative planar fabric in rocks such as phyllites, schists, and gneisses. Foliation forms perpendicular to the principal stress acting upon a massif with the rotation of minerals and alignment of new mineral growth controlled by the plane of the foliation. Platy minerals, such as micas, are common within foliated rock and allow the rock to cleave more easily along the plane of the foliation.

2.4.2.3 Bedding

Bedding interfaces often juxtapose rocks of varying rock mass properties along planar surfaces. Numerous mass movements on slopes are attributed to bedding-controlled failures (Bromhead 2004).

2.4.2.4 Discontinuity strength

Discontinuities have no tensile strength in open joints and low tensile strength in bedding or foliation where there is cementation. Compressive strength is related to the angle of the discontinuity relative to the load with maximum strength with the load normal to the discontinuity (Figure 2.20). Where the principal stress is oblique to the orientation of the discontinuity it is the shear strength that determines the rock mass strength.

Joint roughness, infilling, and aperture contribute to the overall shear strength of a discontinuity by defining the degree that opposing sides of the discontinuity may be able to interlock. Infilling however may exhibit its own shear strength and should be assessed in its own right (Bieniawski 1989). Continuity or persistence of discontinuities influences the extent that the rock material may contribute to the overall strength. Weathering of a discontinuity affects the rock material properties at the interface with decreasing strength relative to increasing weathering.

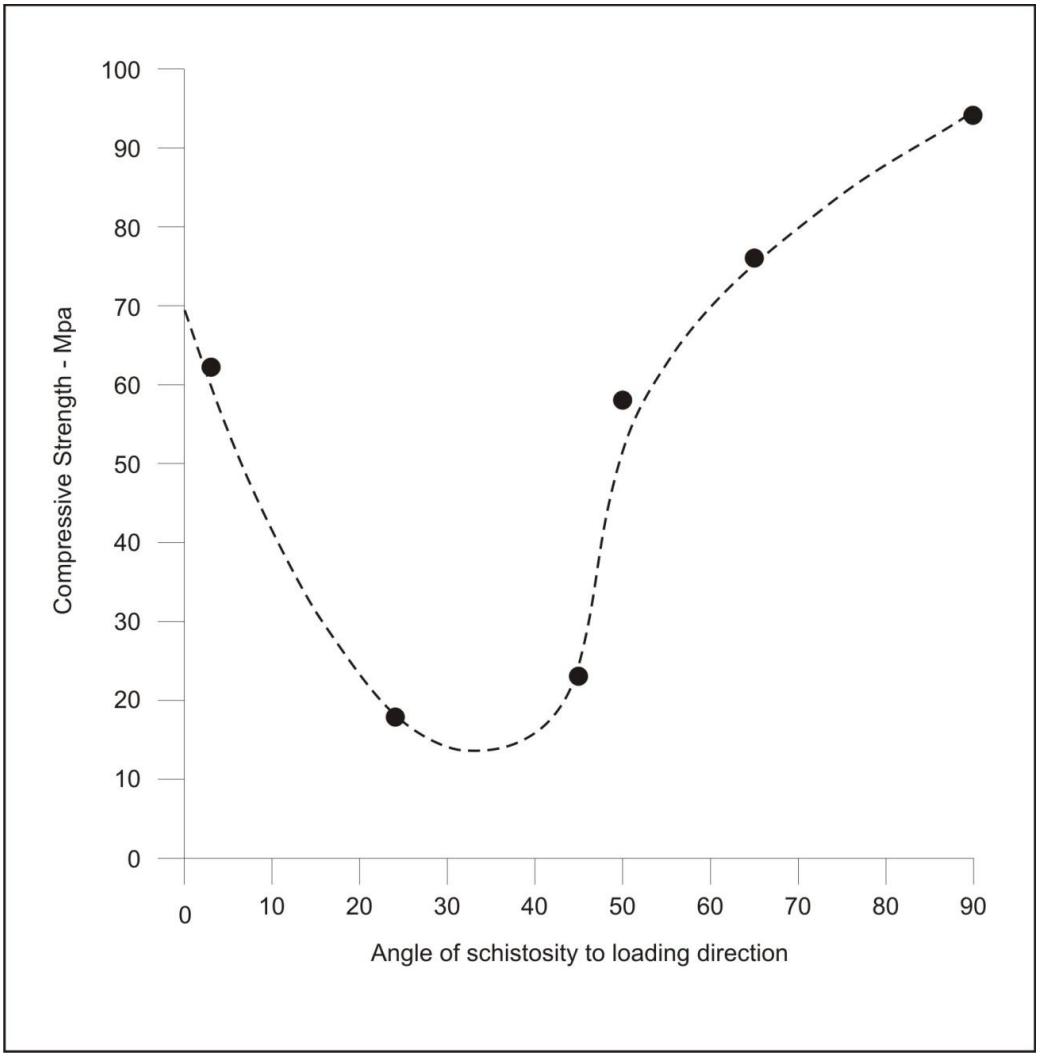

Figure 2.20: UCS of phyllites under varying angles of the schistosity to the applied load (modified from Jaegar 1972).

2.4.3 Rock types and lithology

Approximately 35% of the rock types presented in Chart 1 are foliated metamorphic rocks, 30% are related to unconformable units, 25% are within homogeneous jointed rock, and the remaining 10% are within bedded units. Some broad correlations can be drawn between the different antiscarp formational processes and the rock type of the massif within which they are found. For example, strongly foliated rocks such as phyllites and schists are more conducive to toppling than a paragneiss sitting on a weak shale, which would be more prone to ridge splitting or sackung type antiscarp formation.

Unconformable units ranged from carbonates overlying other marine sediments through to tuffs overlain by andesite, with the stronger more competent unit overlying the weaker unit.

The homogeneity of the rock within a massif influences the process most likely to drive antiscarp formation. As such a division can be made between antiscarps found on massifs composed of either heterogeneous rock or homogenous rock.

2.4.4 Heterogeneous massifs

Heterogeneous massifs are any massif primarily composed of two or more rock units that have distinctly different rock mass properties. Antiscarp forming processes that predominate in heterogeneous rocks are generally related to plastic deformation within a weak underlying material driving surface deformation in competent rock, through processes such as sackung formation and ridge splitting.

Foliated metamorphic rocks may be classified within the heterogeneous massif category when there are distinct differences in the mechanical properties between different parts of the massif. Where deformation is directly related to the properties of the foliation then these rocks can be treated as part of a homogenous massif that is controlled by jointing or foliation.

2.4.5 Homogeneous massifs

Where there is one distinct type of rock with relatively similar rock mass properties throughout the massif it is deemed to be a homogeneous massif. Antiscarp formation in homogeneous rock is primarily associated with movement occurring on discontinuities.

Typical related antiscarp features are ridge rents, tension cracks and gravity faults, all of which may be accompanied by bulging.

2.5 Geological setting

Identifying the geological conditions of areas where antiscarps occur will aid in constraining modes of formation. The geological properties considered here are the rock material, discontinuities within the rock, the geological setting of the massifs, and aspects of massif morphology.

Some broad correlations can be drawn between the styles of formation associated with a particular antiscarp and the geological conditions of the massif within which it is found. For example, toppling requires strong foliated rocks or sackung occur where there is variation of the rock mass properties between adjacent rock units at particular orientations.

The most basic component of all massifs is the rock of which it is composed, and this can be expressed by defining the properties intrinsic to the rock mass.

2.5.1 Glaciation

The majority of the case studies reviewed are found in glaciated regions, with the remainder also highly likely to have a glacial history given their mountainous localities. As antiscarps by definition are only found on slopes, they will typically be found in regions with relief such as mountain ranges.

Glacial events are considered to impact upon massifs in several ways; direct loading by the glacier on its surroundings; stress relief during post-glacial unloading; and valley incision with associated oversteepening.

Antiscarp initiation is often associated with glacial events, with most antiscarps proposed to have formed since the last glacial maximum (Beget 1985). Assignment of antiscarp formation as occurring after the last glacial maximum is based on the premise that glacial advances erase or obscure any antiscarps that may be present, effectively resetting the slope.

2.5.1.1 Glacial loading/unloading

Glacial loading of slopes can occur in two ways; as a surcharge load that is placed upon a slope, and as a lithospheric load.

The load, σ, placed by a glacier on a slope can be treated as a surcharge and can be calculated using ρgh, where ρ is the mass density, g is gravity, and h is the thickness of the surcharge. With $\rho_{ice} = 917 kg/m^3$ and $g = 9.81\ m/s^2$, a 1km thick glacier would equate to $\sigma = 9$ MPa acting vertically assuming the full load is transferred to the bedrock. The glacial load is relatively minor compared to the >50MPa strength of the rocks within which many antiscarps are found (Table 2.1) but it must be remembered that low stresses over long time frames can initiate strain (refer 2.4.1).

Lithospheric loads are temporally and spatially variable loads such as an ice mass that deform the Earth's surface. Such loads are generally related to sheet glaciers but large valley glaciers can also exert a significant load.

Glacial loads compress the bedrock or drive flexure in the lithosphere. Where the bedrock or lithosphere has elastic properties some of the strain within the rock may be recovered when

deglaciation occurs, while any plastic component will be observed as permanent strain. Such a process where strain is recovered is referred to as post-glacial rebound.

2.5.1.2 Post-glacial debuttressing

Glaciers can provide a buttressing effect for the bounding valley slopes during the period of time that they are in place. During glacial retreat the support provided for the slope by the glacier is removed allowing redistribution of stresses within the massif. Debuttressing of the slope can result in slope bulging, mass movements, and antiscarp formation (Radbruch-Hall et al. 1976; Beget 1985; Brown 1997; Agliardi et al. 2001; Jarman and Ballantyne 2002; Hippolyte et al. 2006).

A glacial buttress supports the slope rather than placing a load upon it, indicating that any subsequent failure of the rock mass was being kept in check for the period that the glacier was in place. There is a fine line between debuttressing and unloading and it would be negligent to assume that glacial buttresses only apply a load equivalent to that required to maintain the slope. Expected variations in glacier mass during its lifetime would suggest that there would be a corresponding variation in the load from the glacier on the slope; at times the load will be greater than that required to buttress the slope and at other times will be insufficient.

2.5.1.3 Glacial oversteepening

A glacially oversteepened slope is formed when glacial erosion of part or all of a slope removes material predominantly from the lower section of the slope leaving it steeper than the typical angle of repose for the host rock. Any part of the massif that is above the projected angle of repose, as extrapolated upwards from the toe of the slope, will effectively act as a surcharge on the slope. This provides an unstable condition where mass movements or slope deformations may occur.

While there are similarities between glacial oversteepening and post-glacial debuttressing, in that they are both related to glacial retreat, it must be kept in mind that not all debuttressed slopes are necessarily oversteepened and vice versa.

2.5.1.4 Water table

Elevated water tables within glacier bounding slopes are not uncommon and contribute to the pore pressures found internally and also those associated with the basal contact of the glacier.

Elevated water pressures at the interface with the glacier give a component of uplift that reduces the effective stress applied by the glacier upon the substrate.

The response of the massif to fluctuations in the water table is dependent upon the rapidity of water level change and the transmissivity of the rock mass. Pore pressure change during the drawdown or lowering of a water table occurs firstly when the surcharge of water drains from the slope and secondly via transient flows as the phreatic surface is lowered (Figure 2.21).

2.5.2 Fluvial incision

Downcutting by drainage systems deepens valleys and can oversteepen the bounding slopes when surface processes on the slope are unable to maintain grade in line with the rate of incision. Fluvial oversteepening has a similar impact upon a slope as glacial oversteepening where the massif is prone to mass movements and slope deformations.

Fluvial downcutting can also destabilise slopes by removing toe support from the slope, daylighting discontinuities, or both.

2.5.3 Tectonic setting

Antiscarps are often found in areas that have experienced tectonic activity, either currently or in the past, during mountain building events. Compressive tectonic stresses experienced during orogenic processes aid in the development of discontinuities and foliation, pervasively fracture the rock mass (Kellogg 2001), and provide a preconditioned rock mass that is susceptible to antiscarp development, especially for processes that exploit discontinuities.

Uplift associated with tectonic loading also elevates drainage systems above grade and consequently drives fluvial incision as the drainage downcuts to reach a state of equilibrium.

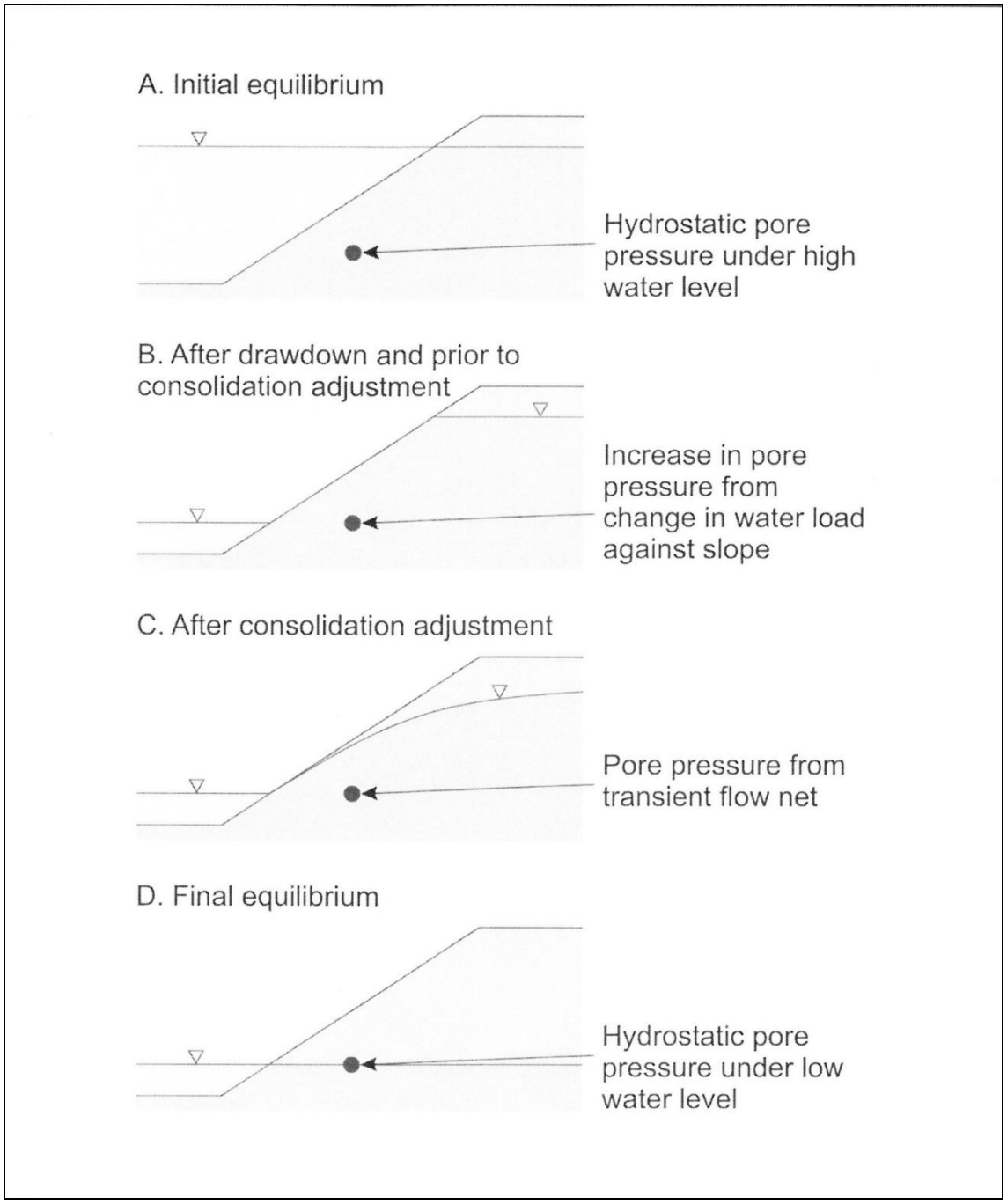

Figure 2.21: Response of a slope to rapid drawdown (Turner and Schuster 1996)

2.5.4 Seismicity

Antiscarps have been identified in both seismically active and seismically quiet regions. Ground rupture, spreading and offset along faults have all been attributed to seismic events with the formation of tension cracks, ridge rents and ridge splitting (Wood et al. 1990; McCalpin 1996; McCalpin 1999; McCalpin and Hart 2000; Jibson et al. 2004).

Less than 10% of the antiscarps recorded on Chart 1 have been attributed to seismic activity and indicates that earthquakes are not the primary mechanism for antiscarp formation.

2.5.5 Massif symmetry

Massifs included in this review are primarily asymmetrical. A possible relationship may be drawn between massif symmetry and the predominance of antiscarps to be found on only one of the bounding ridge slopes.

Kinakin and Stead (2005) analysed a variety of asymmetric land form shapes using finite element modelling, from which it may be inferred that the stress conditions in asymmetric slopes are conducive to antiscarp formation on the steeper of the two slopes (Figure 2.22).

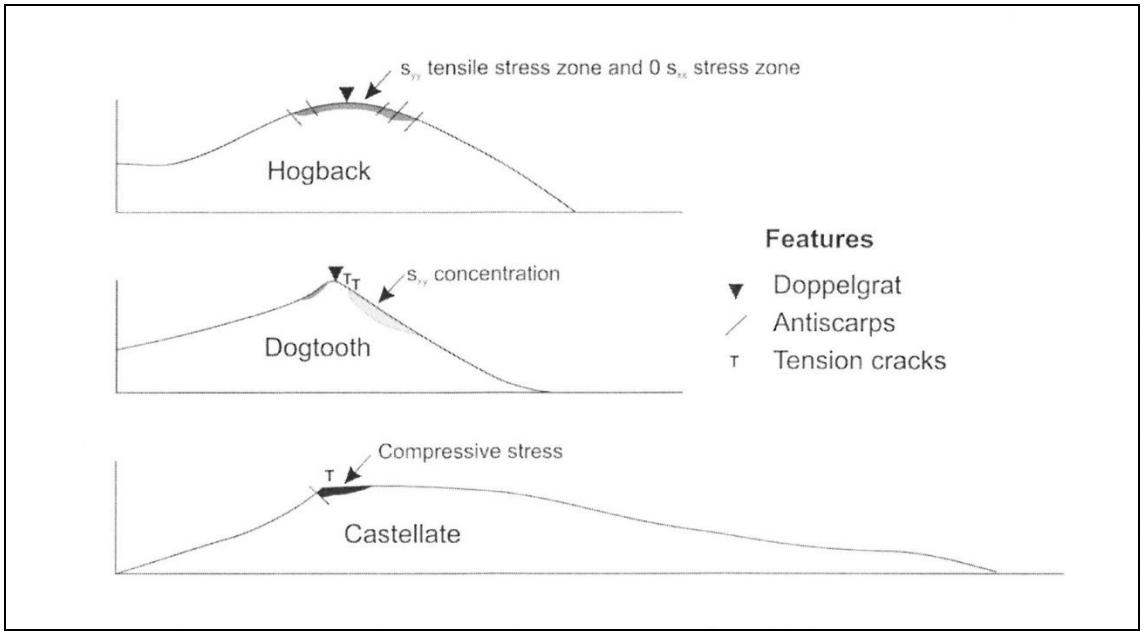

Figure 2.22: Stress distributions in a variety of asymmetric landforms (Kinakin and Stead 2005)

2.6 Applications of antiscarp terminology and properties

This chapter has been an overview on the existing state of knowledge on antiscarps and the factors that contribute to their formation and evolution. This information will be referred to throughout the thesis to clarify the terms already in use, to structure an approach to the classification of antiscarps, and to focus the approach in developing methods for testing suitable mechanisms.

3 Antiscarp classification

The introduction of the term antiscarp is a recent development and the way that terminology associated with antiscarps is used and defined has evolved as the corresponding body of knowledge has grown. The descriptors for some antiscarp related formative processes are sometimes used as a morphological term for the features they generate (e.g. sackung). If these terms are subsequently used to describe antiscarps related to a formative process then some confusion may arise and the explanatory power of the associated term is reduced. An example of this is the use of the term sackung, which was originally introduced by Zischinsky (1966) to define a slope deformation process driven by plastic deformation , and has subsequently been used to describe antiscarps related to a wide variety of processes such as those relating to movement on joints (Varnes et al. 1989; Varnes et al. 2000; Agliardi et al. 2001), debuttressing (Agliardi et al. 2001; Kellogg 2001), toppling (Schwab and Kirk 2002; Hippolyte et al. 2006), and normal faulting (Jibson et al. 2004). The expansion and evolution of terms is common when new concepts and approaches are integrated into established ideas, and it is considered that by clearly defining the scope of some antiscarp related terms, ambiguity in communicating concepts will be reduced.

The plethora of terms used to define antiscarps is considered by the writer to have reached a point where the state of knowledge is such that a framework, and firming of the definitions, needs to be introduced to ensure effective ongoing communication of ideas. No attempt is made here to introduce new terms, but merely to encourage the select use of well defined existing terms more specifically, and to use qualifiers to add more information. The terminology and reviewed material presented in Section 2.2 are used here as a basis for establishing clear definitions that will be used within this thesis, and a proposed classification scheme.

In the past antiscarps have often been used as an indicative feature of a particular process, although they are related to many processes. The classification scheme provided here follows an approach whereby related processes may be determined from basic observations of antiscarps and associated morphological features, and will assist in the selection of suitable investigative techniques for a variety of practitioners.

This is an initial approach to classification of uphill facing scarps, beyond the umbrella term of antiscarps and it is done in two parts. Primarily the emphasis is upon clarifying the

terminology to be used and what it covers; and secondly, a flowchart has been constructed to emphasise an approach to process-based terminology.

3.1 Antiscarp definitions

3.1.1 Motivation

The existing use of antiscarp related terminology has evolved to the point where there is much interchangeability between terms and this may result in some uncertainty where terms are no longer clearly defined. The establishment of an antiscarp classification scheme assists in constraining the definitions of associated terminology and provides a methodological approach to determining probable antiscarp formative processes.

3.1.2 Scope and presentation of the definitions

Concise definitions are provided for the primary terms that will be used as part of the classification scheme, and throughout the rest of this thesis. The definitions are presented alphabetically and no attempt is made to categorise or group them using any other parameters.

A qualifier is an expression or word that is appended before an item to give it greater definition and explanatory power, for example, in “oblique antiscarp” oblique is the qualifier and antiscarp is the term. The qualifying terms presented here are only those that have been utilised within this study, and it is envisaged that over time more qualifiers will be adopted. Qualifiers presented in the following section are indented and bulleted beneath the applicable term they relate to, along with a brief accompanying description.

There is an emphasis on preserving terminology that is currently in use, and also on maintaining the integrity and perceived intent of earlier definitions and uses of these terms.

3.1.3 Thesis glossary

Antiscarp – A descriptive term for an uphill facing scarp which is sub-parallel to the slope contour.

- Discontinuous antiscarps – numerous short antiscarps that appear to be related to a single linear structure.
- Oblique antiscarp – an antiscarp that is at an angle relative to the slope contour.

Antiscarp sets – denotes multiple antiscarps of a similar orientation on a slope. More than one antiscarp set can occupy a slope.

Bulging – protrusion of a section of the massif out of the slope. Bulging is often assumed to be associated with unloading or debuttressing of a slope.

Creep – very slow rate of movement of material, typically during downslope transfer. Is often assumed to be a continuous rate and is generally measured in mm/yr.

Debuttressing – Removal of lateral support from a slope. The buttress, lateral support, must have been providing an element of support to the slope in order for its removal to qualify as debuttressing.

Discontinuities – laterally persistent surfaces through a massif such as joints, foliation and bedding, which represent zones or planes of weakness through the rock mass.

Doppelgrat – (plural is doppelgrate) a split ridge, ridge top depression, or trough along the ridge that gives the appearance of twin ridges.

Fault – A planar fracture through rock that has a component of shear. Faults are typically regional phenomena driven by tectonic activity. Antiscarp related faults have a normal sense of displacement or require a thrust with the fault plane steeper than the slope.

Gravity fault – large scale surfaces that accommodate gravity driven movement conducive to antiscarp formation within a massif. Gravity faults differ from normal faults in that they are massif specific phenomena and may not necessarily be seen on a regional scale, or related to regional tectonics.

Incision – the process of downcutting in a valley by fluvial or glacial activity.

Lineation – a linear feature upon a slope.

Ridge rent – renting, generally related to seismic activity, which is often observed as ridge-parallel lineations but does not necessarily have a component of vertical displacement.

Ridge splitting – a process where lateral displacement in the massif forms a doppelgrat.

Sackung – (plural is sackungen, but sackung is used here as both singular and plural) deformation of competent upper units due to plastic deformation in weaker lower units. Features other than antiscarps that are associated with sackung are hummocky terrain, tension cracks, rockslides, rock avalanches, and bulging.

Topple – rotation of a rock mass out of the slope about an axis lower than its centre of gravity.

- Block topples – rotation of blocks out of the slope.
- Block-flexure topples – foliated or layered columns of rock that bend out of the slope and break along existing joints. Continuous flexure is accommodated by the existing joints.
- Chevron topples – regular steeply dipping foliated or layered rocks that have an abrupt change in dip concentrated at a rupture surface.
- Flexural topple - foliated or layered columns of rock that bend out of the slope and break under flexure.
- Slide topples – rotation of a rigid block within a slope as it is transferred downslope by plastic deformation in the underlying mass.

Unloading – rebound of the rock mass upwards in response to the removal of a surcharge, buttress, or large volumes of material, or the act of removing the material.

3.2 Antiscarp classification

Adopting a morphological approach for the first order classification of antiscarps allows unbiased inferences to be made based on associated slope features, geology, and observed processes. There is adequate scope for ongoing sub-division from this initial class with subsequent categorisation possible based on formative process, driving mechanism, and associated features.

Some terms, while related to antiscarps, do not explain antiscarp formative and evolutionary processes. An example of this is “deep-seated gravitational slope deformations” (DGSGD) which embraces a group of phenomena, within which antiscarps may be included, but does not represent any particular process.

3.2.1 Limitations of the classification scheme

The classification scheme provided here is designed to provide a framework for assessing antiscarp features and makes no attempt to define all aspects of any associated processes. The aim is to identify the primary mechanism associated with a particular antiscarp or antiscarp set/s and as such there is no accounting for the input of secondary mechanisms. For example; gravity faulting in the Lewis Tops occurs on a massif that has large scale mass movements on both flanks of the ridge and has been subject to incision on both sides (refer section 4.1). Effectively this indicates that these antiscarps are driven by gravity faulting with an input from both unloading and incision.

3.2.2 Antiscarp classification scheme

Figure 3.1 presents a flow chart based approach to the classification. The initial starting point is in the top left corner where the user is required to answer the posed question and then follow the arrow corresponding to the “Yes” or “No” response.

For example an initial assessment of the antiscarp in Fig 2.19 using the flow chart would give the following

- Multiple antiscarps or antiscarp sets? No
- Fault related Yes
- The antiscarp is probably the result of a normal fault, or a thrust with the fault plane steeper than the slope.

A second example are the antiscarps in Fig 2.1A and also appearing in Fig 2.8.

- Multiple antiscarps or antiscarp sets? Yes
- Homogeneous host massif? Yes
- Controlled by discontinuities? Yes
- Rotation out of the slope about the base? No
- Graben style collapse? Yes
- The antiscarp is probably the result of gravity faulting

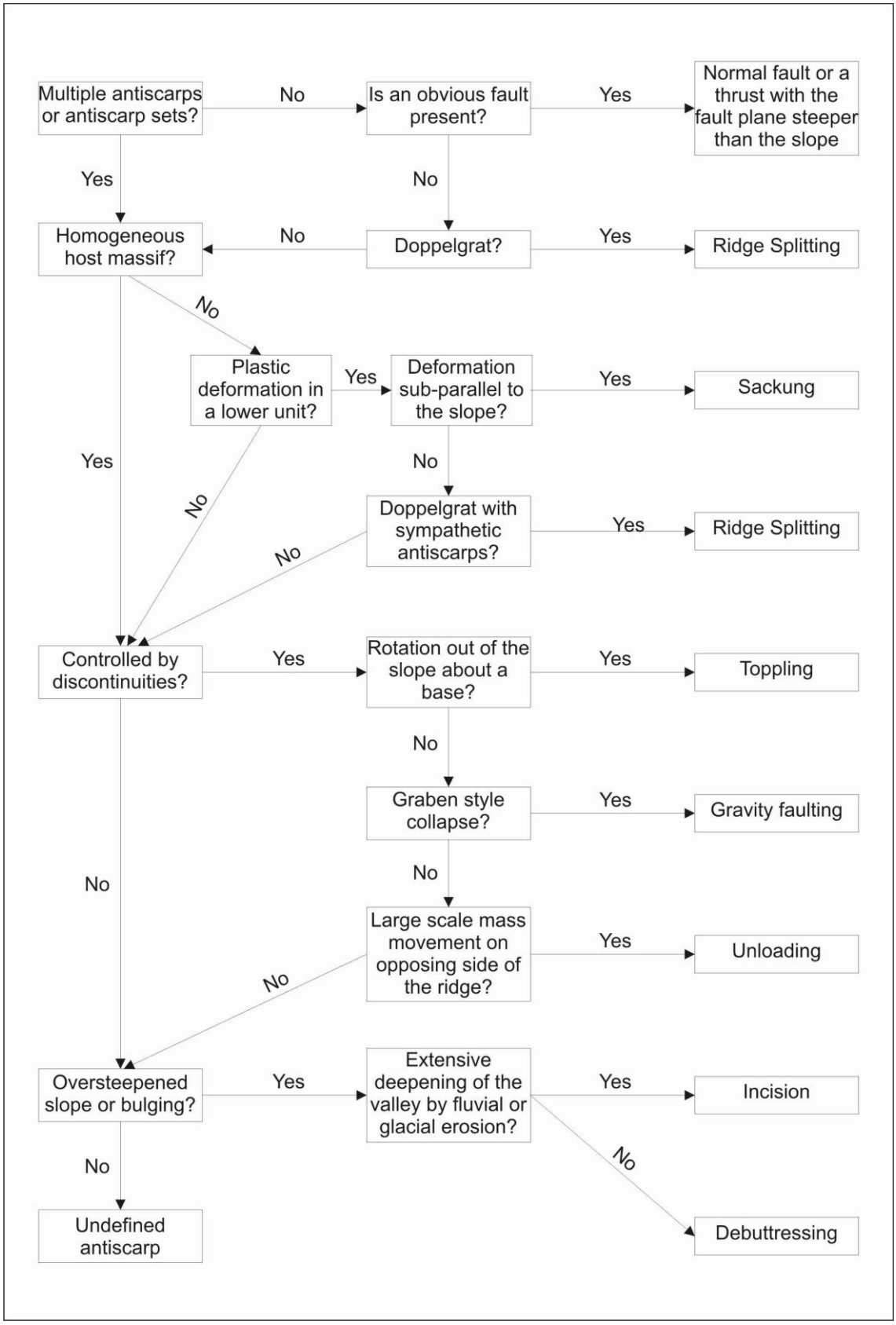

Figure 3.1: Flow chart classification scheme for assessing antiscarps from initial observations through to a probable mechanism.

3.3 Applications for the classification scheme

There are numerous opportunities for the use and application of this classification scheme. It has been constructed as a flow chart to enable it to be easily used by a wide variety of practitioners and to provide a checklist type guide to help in targeting an approach to field investigations.

Possible uses include land use planning, hazard analysis, and foundation condition investigations. Classification of antiscarps will also aid in studies that address massif stress histories, rock mass response to loading or unloading, and some glaciological investigations

4 Field studies

Field studies were undertaken to gain first hand observations and measurements of antiscarps in their natural state. Many sites were visited but only five field areas are presented here; these being the Kelly Range, Lewis tops, and Stag Hill from the South Island of New Zealand and Beinn Fhada and Ben Each in the Highlands of Scotland.

The details that are collected from the literature and used in the construction of Chart 1 are also targeted here during the field work where possible. This includes descriptions such as the rock mass properties, glacial and tectonic setting, massif geometries, associated slope features, and antiscarp properties.

Comparative studies were made between antiscarps observed in Scotland and those formed in New Zealand with a focus on seismicity. Scotland was chosen because it is seismically quiet and comparisons would provide the opportunity to isolate the seismic component in NZ antiscarps. Both countries have had a similar glacial history with Late Pleistocene glaciation.

Details from the field studies were also required to balance the construction of the models presented in Chapter 5. Factors of importance here are the rock mass properties and the way that the discontinuities correspond to localised structure. The symmetry of the massif and the loss of volume by cirque development is another consideration for the models.

The process flowchart developed in Chapter 2 is applied to the field examples presented here to assess the probable formative mechanism for the antiscarps mapped here and as an example of its use and application.

4.1 Kelly Range case study

The Kelly Range is located approximately 3km west of the village of Otira, Arthur's Pass, and is part of the chain of mountains which form the Southern Alps in the South Island of New Zealand (Figure 4.1). The approximately 10 km long ridgecrest trends NE-SW and is sub-parallel to the convergent plate boundary between the Pacific and Australian plates known as the Alpine Fault. The Kelly Range is 1394m above sea level at the peak, rising from a valley floor at about 320m at the junction of the Kelly Stream with the Otira River. The Kelly Stream extends upstream for approximately 6km to the southeast in the valley to

the east of the range and reaches an altitude of just over 800m. Typical slope heights are just over 1000m and have an approximate slope angle of 32°.

The antiscarps on the Kelly Range were the basis for the work undertaken by Beck (1968) on gravity faulting (Figure 4.2). Data collected from the field studies will be integrated into models, and includes a limited defect analysis, field mapping and field observations.

4.1.1 Geological setting

The Kelly Range is located in a geologically active area of the South Island of New Zealand within the Torlesse Group rocks typical of the Southern Alps and lies to the west of the main divide. Climatic variations on seasonal and geological time scales, tectonic forcing, seismic activity, and glacial activity all impact upon and have played a role in shaping the Kelly Range.

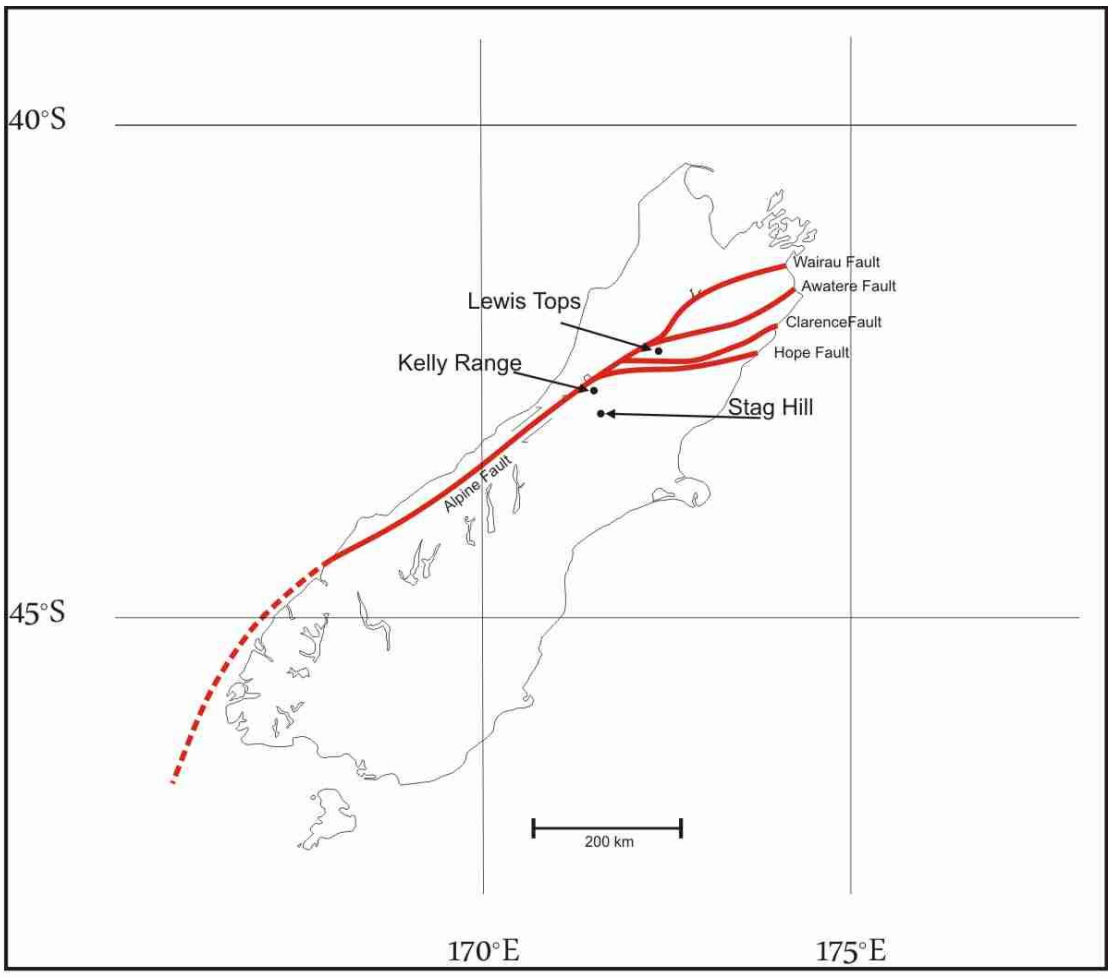

Figure 4.1: Locality map showing the New Zealand field areas and their proximity to the Alpine Fault and the faults of the Marlborough Fault Zone.

4.1.1.1 Lithology

The Kelly Range is primarily composed of highly fractured and sheared, bedded, weathered, very well indurated quartzofeldspathic sandstones and argillites of the Torlesse Group, colloquially referred to as greywacke (Figure 4.3). Low grade dynamic metamorphism is evident with the occurrence of poorly developed schist across the massif (Figure 4.4).

There is a thin soil cover over most of the range, with scree slopes and localised areas of slope colluvium.

Glacial till is observed on top of the ridge at the western end of the range with exposures up to 2m thick in places (Figure 4.5).

Estimated field strength is that of a very strong R5 rock, likely to have a UCS >200 MPa.

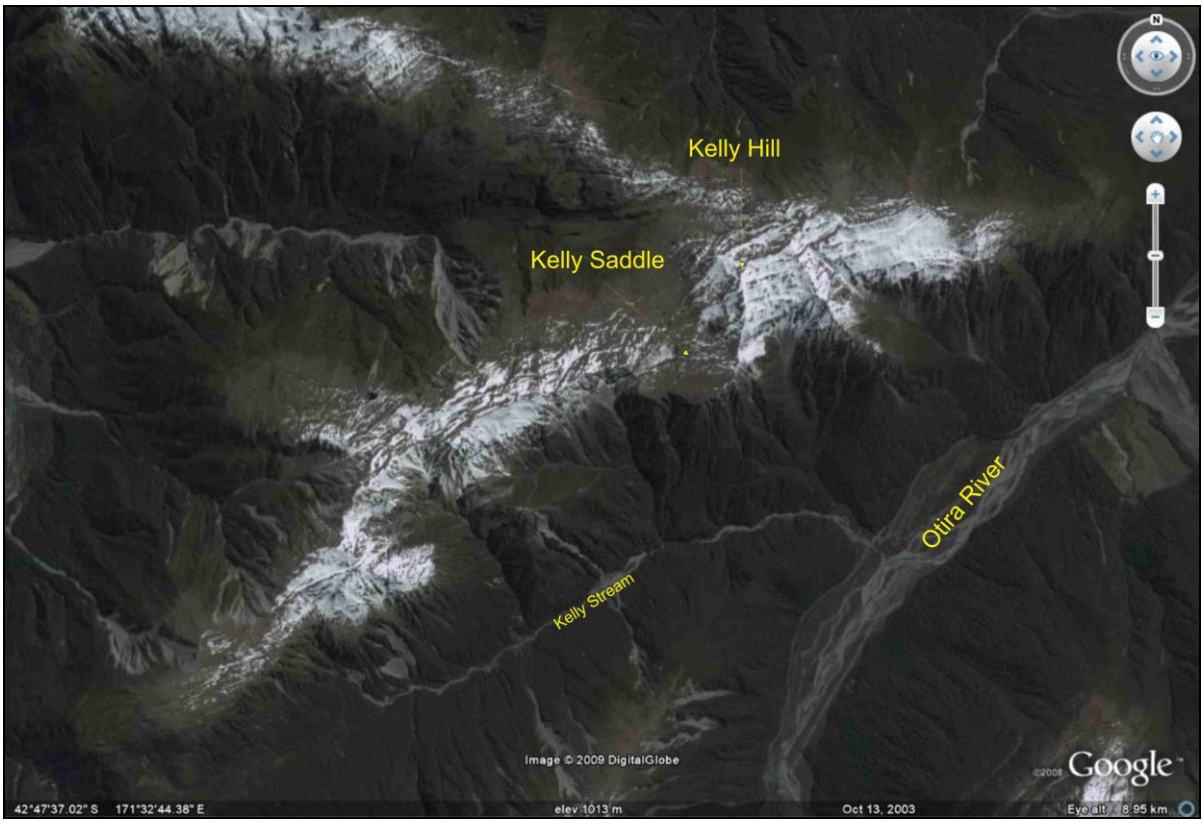

Figure 4.2: Google Earth image of Kelly Range. The snow cover helps to contrast the antiscarp features (refer to Figure 2.3 for an image centred on Kelly Hill).

Figure 4.3: Sheared and fractured weathered Torlesse quartzofeldspathic sandstone. Bedding is dipping moderately to the right in this photograph (bedding plane denoted by the arrows).

Figure 4.4: Poorly developed foliation within weathered Torlesse sandstone.

Figure 4.5: Till deposits on the ridge at the south western end of Kelly Range. The person in the photograph provides a scale of 2m. Glacial overtopping of the ridge is considered to have created the smooth nature of the slope above the incised till. The till extends to the break in slope to where it becomes the Torlesse bedrock.

4.1.1.2 Structure

The sandstones and argillites of the Torlesse Group are typically interbedded sedimentary rocks, although a poorly developed schistosity is observed on many outcrops along the ridge, indicative of low grade dynamic metamorphism. The interbeds are typically widely spaced, in the order of tens to hundreds of metres.

A pilot analysis of defect orientations on the Kelly Range, using Rocscience DIPS software, indicates a dominant defect set with a preferred strike of NE-SW (Figure 4.6). The strike of this dominant defect set parallels the trend of the ridge and is representative of the strike for both the SE and NW dipping antiscarp structures observed in the field. Some inferences could be made that there is be an association with the NE-SW trending Alpine Fault nearby. The three defect sets presented in Figure 4.6 were derived initially using a contour plot (Figure 4.7), and by then assigning search windows to calculate representative poles (Figure 4.8) prior to plotting the planes annotated with the dip and dip direction (Figure 4.9). Figure 4.10 and Figure 4.11 give an overview of the defect sets as seen in the field.

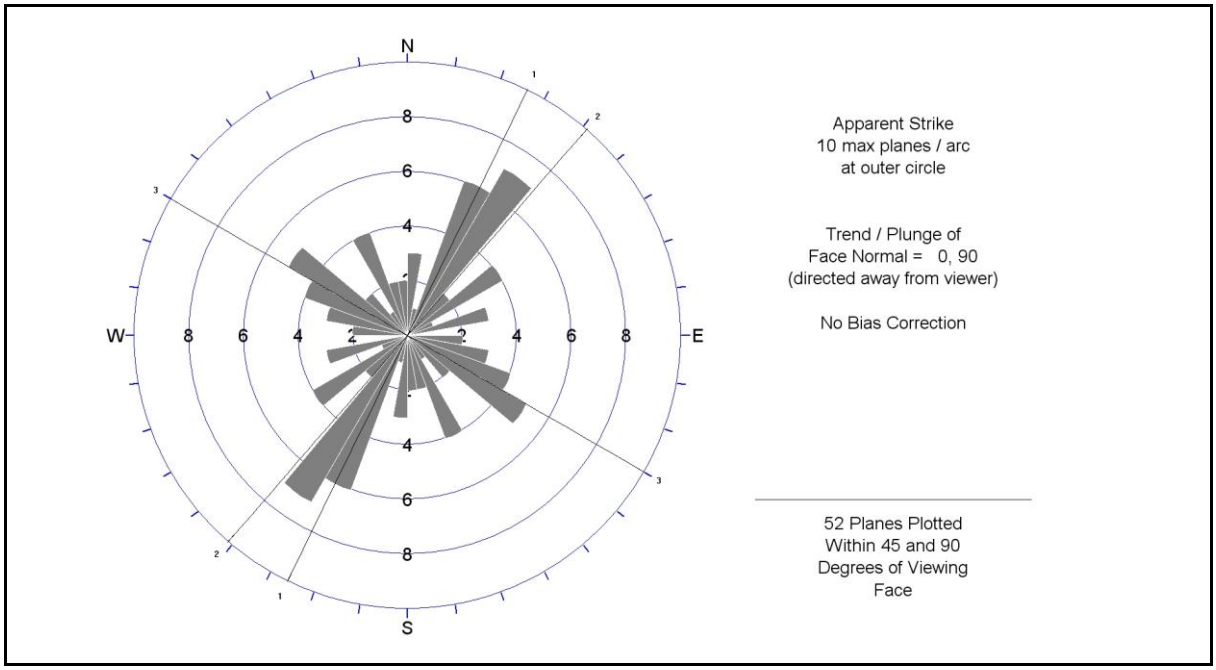

Figure 4.6: Rose diagram of the apparent strike calculated in DIPS using defect measurements from the Kelly Range. The preferred strike orientation is in a NE – SW direction with a second set of structures in the NW – SE. Three defect sets are identified in the DIPS data and the apparent strikes for each of these is represented by line across the stereonet with a corresponding set number on the perimeter.

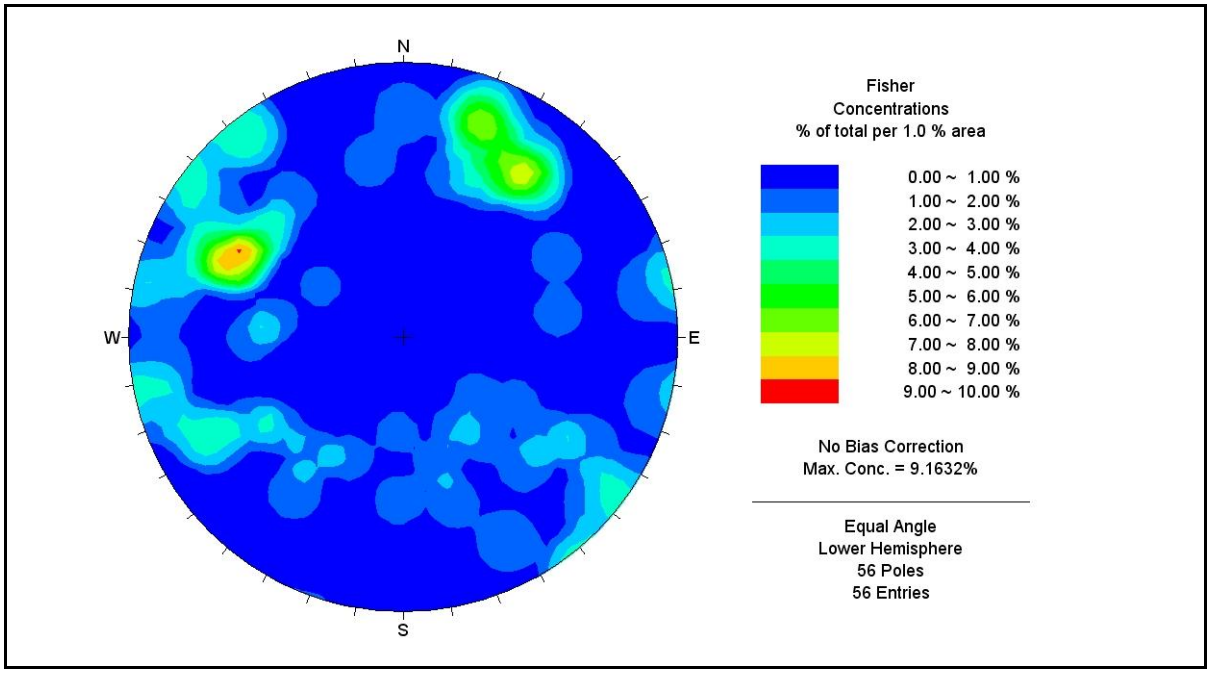

Figure 4.7: Initial pass of the Kelly Range discontinuity data presented as a stereonet contour plot.

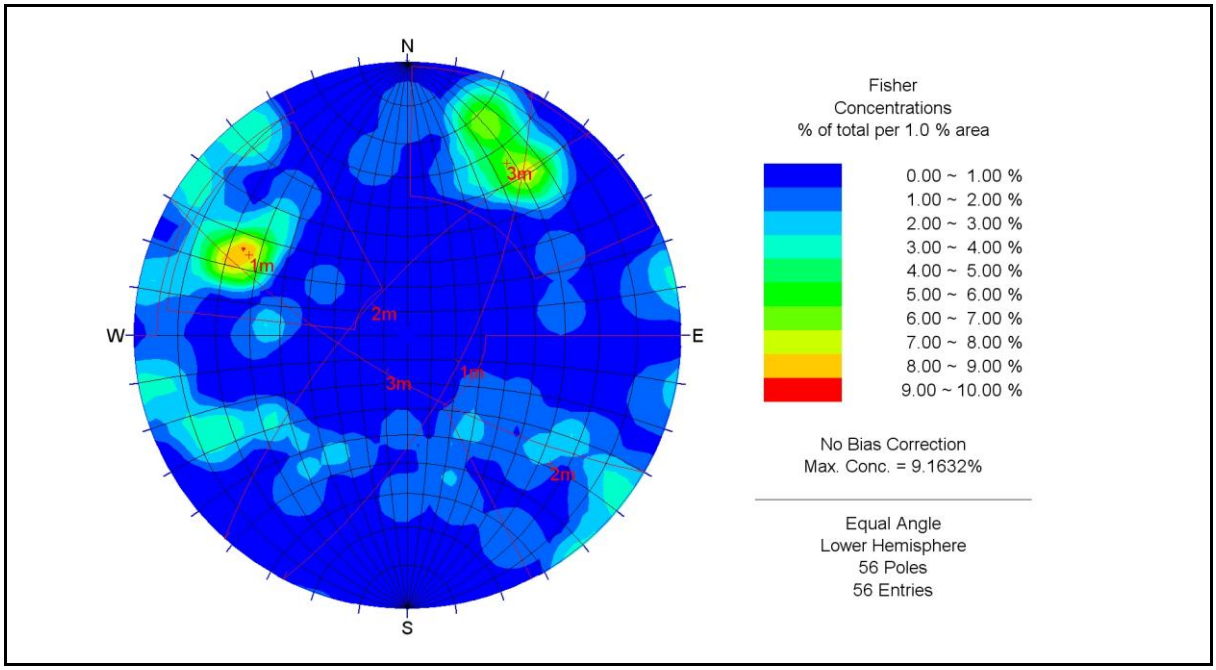

Figure 4.8: Search windows as used around data clusters to calculate representative poles, indicated by the crosses, for the Main Kelly Range discontinuity sets.

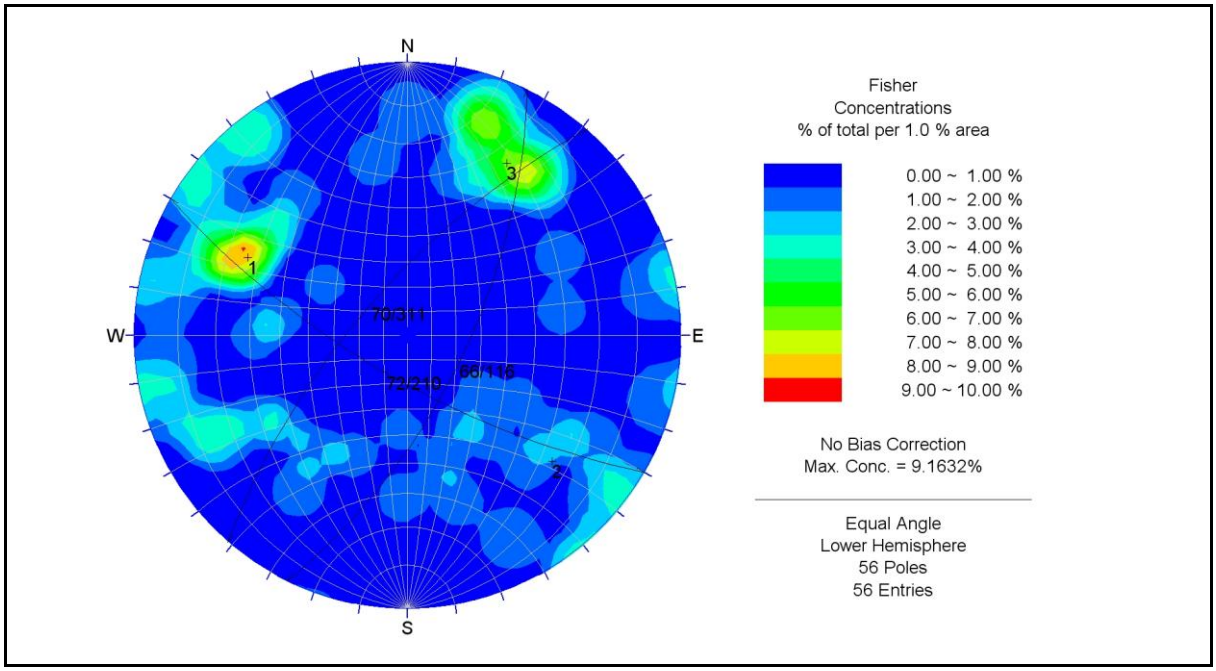

Figure 4.9: The three primary discontinuity sets. Poles 1 and 2 correspond to the structures associated with the SE dipping and NW dipping antiscarp sets respectively. Pole 3 is of a similar orientation to the exposed face just to the southwest of Kelly Hill (Figure 4.10).

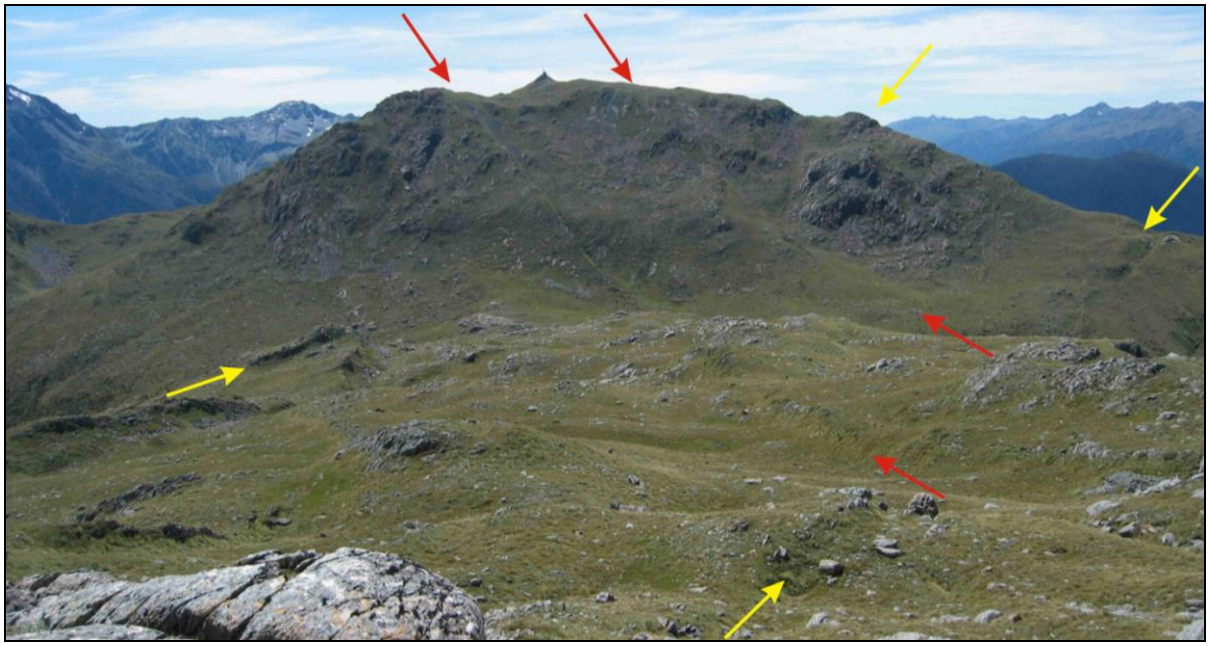

Figure 4.10: View to the north east from the top of the slope in Figure 4.12 on to the face below Kelly Hill. Structure Set 1 has an apparent southeast dip (red arrows) and Set 2 dips toward the northwest (yellow arrows). Structure set 3 parallels the slope face. Sets 1 and 2 can be easily tracked up the slope coming toward the front of the picture. Figure 4.12 shows the reverse view.

4.1.1.3 Climate

The Kelly Range is a typical New Zealand mountain range in that it is exposed to weather variations, both short term and on geological time scales. Seasonal winter snows are also common and during the warmer seasons there is full melt with lush snow grass cover. In parts of the Southern Alps this seasonal variation leads to freeze thaw fracturing of the rock mass but does not occur to the same extent on the Kelly Range, possibly due to its maximum elevation of 1394m asl.

Northwesterly wind flow is the prevailing direction for the winds here and across most of the South Island. The location of the Kelly Range on the western side of the Southern Alps main divide exposes it to orographic effects by water sourced from the Tasman Sea to the west.

Figure 4.11: This photograph is taken from Kelly Saddle, beneath the face shown in Figure 4.10, and allows a view up structure Set 3 which roughly parallel the slope. The tarn is a common feature associated with many antiscarps on the Kelly Range and at this locality is within Set 1.

4.1.1.4 Glacial history

The Southern Alps of New Zealand have been subject to multiple glacial events throughout their history. The most recent glacial event was the Otiran which spanned from 74 ka to 12 ka (Nathan et al. 2002). Glaciers would have been present in all of the valleys bounding the Kelly Range during the Otiran and would have extended well down the present day Taramakau Valley towards the West Coast.

Oversteepened slopes, till deposits on the ridge, and trim lines on both slopes either side of the Kelly Range and on all adjacent mountain ranges are indicative of the extensive glaciation throughout the region (Figures 4.13 and 4.15).

Figure 4.12: View to the southwest from Kelly Hill across the Kelly saddle (top of the hill in Figure 4.10). The smooth nature of the slope is indicative of glaciation and there is strong evidence that at some stage the Kelly Saddle has been under ice. The criss-cross pattern evident on the facing slope is due to the SW trend and plunge of the intersection between structure Set 1 (red arrows) and Set 2 (yellow arrows) (refer section 4.1.1.2) going into the slope.

Figure 4.13: View to the southwest across Kelly Stream from the top of the slope in Figure 4.12. A glacial trim line is clearly demarcated, not only on the opposing range but also on the southeast facing slope in the foreground, by a distinct steepening of the slope and also a vegetation change. Hanging valleys and cirques are also evident on the range in the background. Fluvial incision is an ongoing process through this area contributing to oversteepening of the valleys.

4.1.1.5 Tectonic history

The Kelly Range is proximal to the Alpine Fault which has accommodated approximately 400km of dextral slip. Oblique subduction of the Pacific plate beneath the Australian plate

along the east coast of the North Island has been transferred to the strike slip motion of the Alpine Fault via the four major faults that make up the Marlborough Fault Zone; from the north these are the Wairau, the Awatere, the Clarence and the Hope Faults. Currently the majority of the convergence is transferred via the Hope Fault which passes the northern end of Kelly Range to where it joins the Alpine Fault in the Taramakau Valley. Other minor faults are known within the region.

The Kelly Range is part of the Southern Alps which are the expression of ongoing uplift associated with the convergence of the Pacific Plate with the Australian Plate along the Alpine Fault.

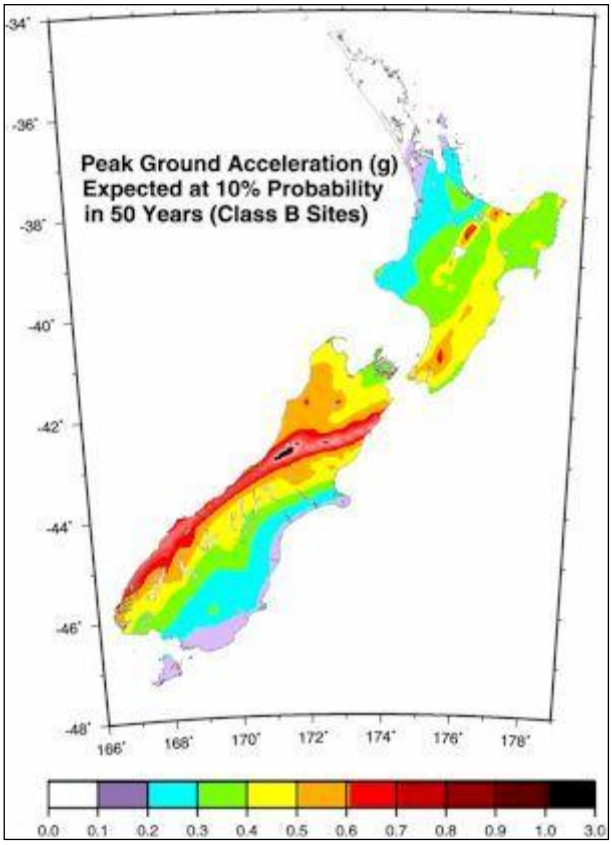

Figure 4.14: Peak ground accelerations (g) expected at 10% probability in 50 years for intermediate soil sites (from Stirling et al. 2002).

The Kelly Range lies within one of the most seismically active regions of New Zealand with major proximal earthquakes of M7.1 in 1929 and an M6.7 in 1994, the latter being the largest land based earthquake recorded in New Zealand for over 25 years (Arnadottir et al. 1995; Paterson 1996).

The Otira township several kilometres east of the Kelly Range is considered to be located in the highest hazard area in New Zealand with respect to expected peak ground acceleration associated with seismic events (Figure 4.14; Stirling et al. 2002).

4.1.2 Antiscarps

A geomorphological map is presented in Figure 4.15: Geomorphological map of the Kelly Range.Figure 4.15 and depicts the general distribution of the antiscarps on the Kelly Range and key features within the surrounding landscape.

Antiscarp development is concentrated in the upper third of the mountain range with no antiscarps observed below the bushline, which is typically coincidental to the break in slope (refer Figure 4.13), but that may be more a case of lack of exposure rather than absence. The Kelly Range antiscarps parallel the trend of the ridge and have observed lengths of 20m to 1500+m. Separation of the antiscarps from the slope ranges from 1m to 8m (Figure 4.16 to Figure 4.18).

To the east of Kelly's Hill there is a relatively even distribution of the Northwest facing Set 1 and Southeast facing set 2 antiscarps (refer Figure 4.10 and Figure 4.12). Towards the west in the middle of the range adjacent to Kelly saddle it is primarily the set 2 antiscarps that are observed. A series of minor scarps also adjacent to Kelly saddle have a sense of downthrow to the Northeast and have a similar strike to that of the slope beneath Kelly's Hill and are related to set 3 as outlined in Figure 4.10. Several structures are observed along the length of the Kelly Range have a similar orientation to that of the NW-SE striking set 3 structure and have a spacing of around 600m.

The predominance of the set 2 antiscarps continues through towards the western end of Kelly Range. Set 1 antiscarps are again observed on the most southwesterly corner of the range where there is an absence of set 1.

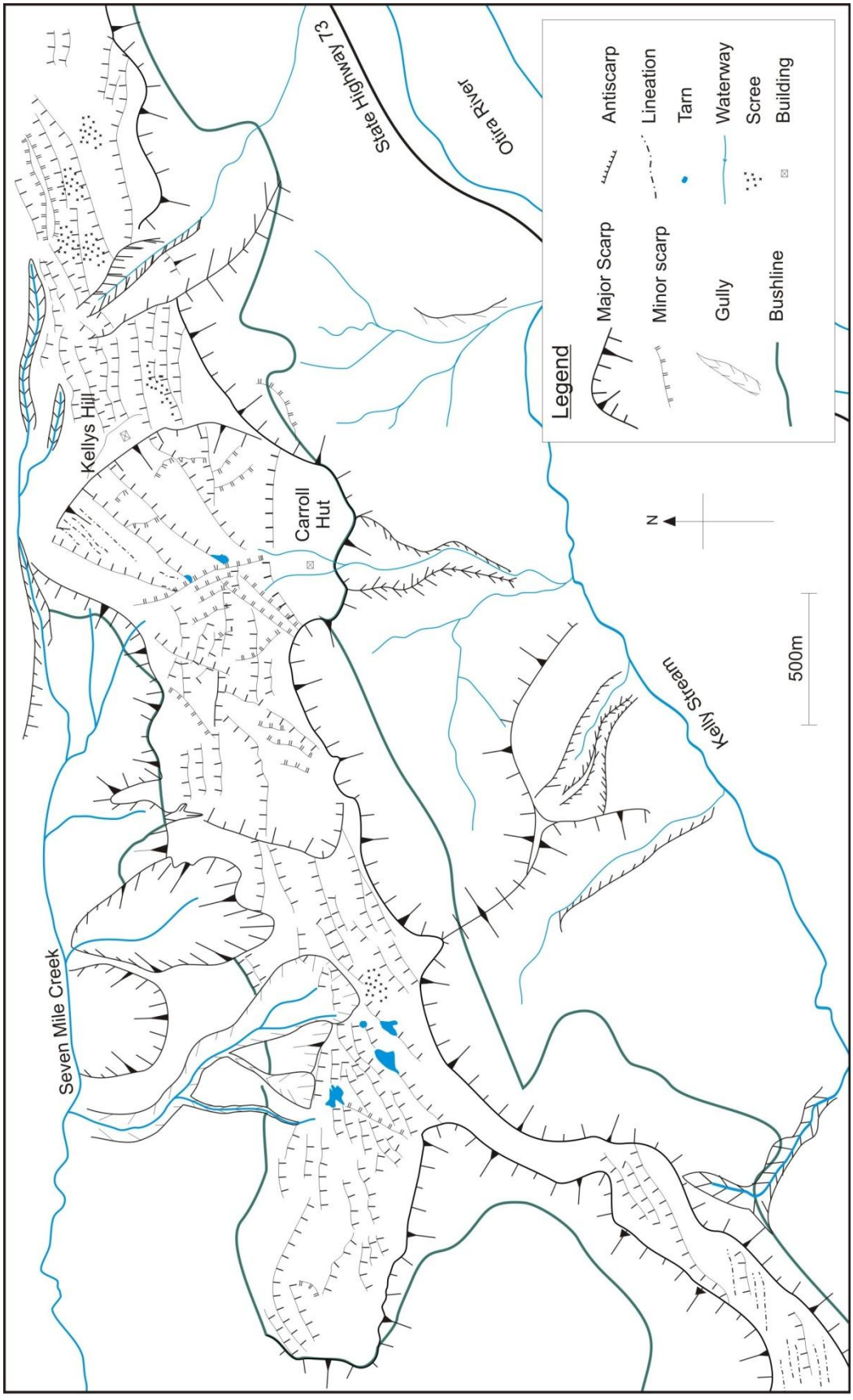

Figure 4.15: Geomorphological map of the Kelly Range.

All antiscarps appeared to have moved on discrete failure planes with no suggestion of translational movement. The antiscarps are clearly defined with any degradation limited to the top of the antiscarp face. The surface weathering of exposed rock within the antiscarps is similar to that of the surrounding rock.

Deformation rates are difficult to calculate because there are no constraints on whether formation is due to a single event or ongoing creep. Further errors for calculation are associated with not knowing which glacial event to correlate the onset of antiscarp formation to, although it is tentatively assigned to the end of the Otiran glacial event at 12 000 years BP (Suggate and Almond, 2005).

Movement associated with the antiscarps involves dislocation parallel to the two main defect sets identified in section 4.1.1.2. The deformation style is brittle with movement along existing defects.

The ridge shape is generally symmetrical, with the exception of areas that have been affected by localised glacial activity, incision, or slope instability. No slope bulging was observed.

Associated slope features include ridge rents, scree slopes, and numerous tarns (Figure 2.4 and Figures 4.18 to 4.21). The tarns are often elongated on the edge that is adjacent to an antiscarp. In some cases the tarn spans more than one antiscarp structure all the structures can be correlated to elongated sections of the tarn.

Graben style collapse of the ridge is also observed, primarily around Kelly Hill where there was good exposure and preservation of the ridge (Figure 4.23).

A schematic of the proposed evolution of the antiscarps on the Kelly Range is presented in Section 6.3.

Figure 4.16: An antiscarp at the southern end of Kelly Range related to structure Set 1. Approximately 2m of net separation along the scarp has occurred at this locality. View is to the north.

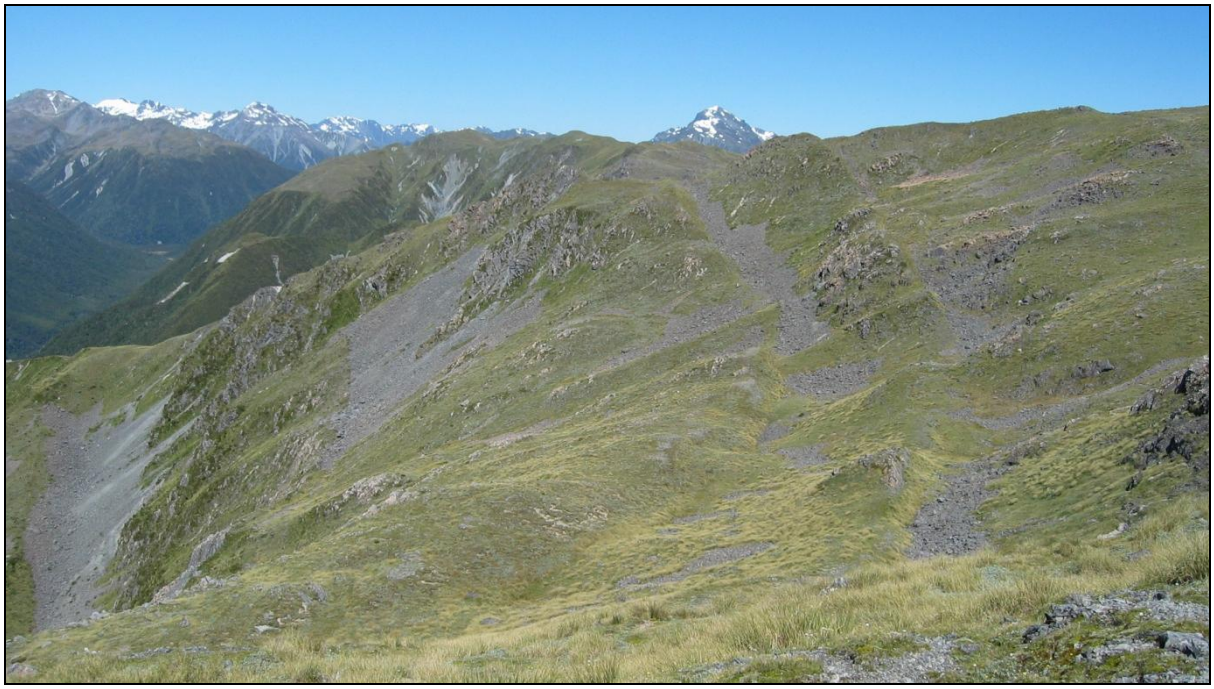

Figure 4.17: View south along structure Set 2 antiscarps on the slope to the east of Kelly Hill. Approximately 5m of separation is observed at this locality. Of note is the amount of infill, or lack of, within these antiscarps. Where there is a source rock for the production of scree the antiscarps act as a highly effective natural bund.

Figure 4.18: View to the south from the north end of the Kelly Range with Kelly Hill denoted by the communications aerial upon it. The antiscarps to the left of the peak are from Set 1 and have about 6m to 7m of displacement. There is a noticeable lack of scree or rock infill in the antiscarps on this side of the ridge (western slope).

Figure 4.19: View north towards Kelly Saddle with tarns formed within Set 1 structures.

Figure 4.20: Further to the south of Figure 4.19 with another tarn within western slope Set 1 antiscarps.

Figure 4.21: Another smaller tarn within western slope Set 1 antiscarps

Figure 4.22: View to the south with the tarn formed in Set 1 antiscarps. The antiscarp is to the right of the picture and has about 10m of displacement.

Figure 4.23: Graben style collapse of ridge at the northern end of the Kelly Range. View is to the north.

4.1.2.1 Classification

Application of the classification scheme presented in Chapter 3 indicates gravity faulting is the most likely mechanism for antiscarp formation at this locality based on the occurrence of multiple antiscarps, homogeneous massif, controlled by discontinuities, no rotation out of the slope, and displays graben style collapse features – Gravity faulting.

4.2 Beinn Fhada

Beinn Fhada is located on the west coast of Scotland in the Kintail region of the Highlands. Antiscarps have been observed in this region and discussed by numerous authors (Holmes and Jarvis 1985; Holmes and Jarvis 1986; Whiteside 1986; Jarman and Ballantyne 2002).

Beinn Fhada is 1032m high with other peaks on the range at 962m and 954m, to the east and to the west respectively, and has a typical slope angle of 40°, although it does flatten out towards the ridge crest.

Fieldwork on Beinn Fhada identified numerous antiscarps of 20m to 1200m+ in length on the southern slope which dips into Glen Licht (Licht Valley) at approximately 40°. The antiscarps are perpendicular to the slope with scarp amplitudes ranging from 1m to 10m.

4.2.1 Geological setting

Beinn Fhada is located in an area that has some of the highest relief in the western Highlands with numerous peaks at elevations >1000m within several kilometres of the coast. Glaciation

has been the primary shaper of the landscape, especially in the Late Pleistocene and has had a major impact at crustal scales with the glacial load placed on the land mass during this period. Much older Devonian faulting is also a feature of this landscape.

4.2.1.1 Lithology and structure

Beinn Fhada is located in Moine pelites and psammites of the Morar Division which is a part the Moine Succession (Figure 4.24). The gneissic texture of these rocks was evident in the outcrops (Figure 4.25). All rocks were typically very well indurated with many showing evidence of the low grade metamorphism that is associated with the rocks in this area. Rocks exposed in cirques in the northern slope of Beinn Fhada displayed a strong foliation that dipped steeply to the north (Figures 4.34 to 4.36).

Estimated field strength is that of a very strong R5 to R6 rock, likely to have a UCS ~250 MPa.

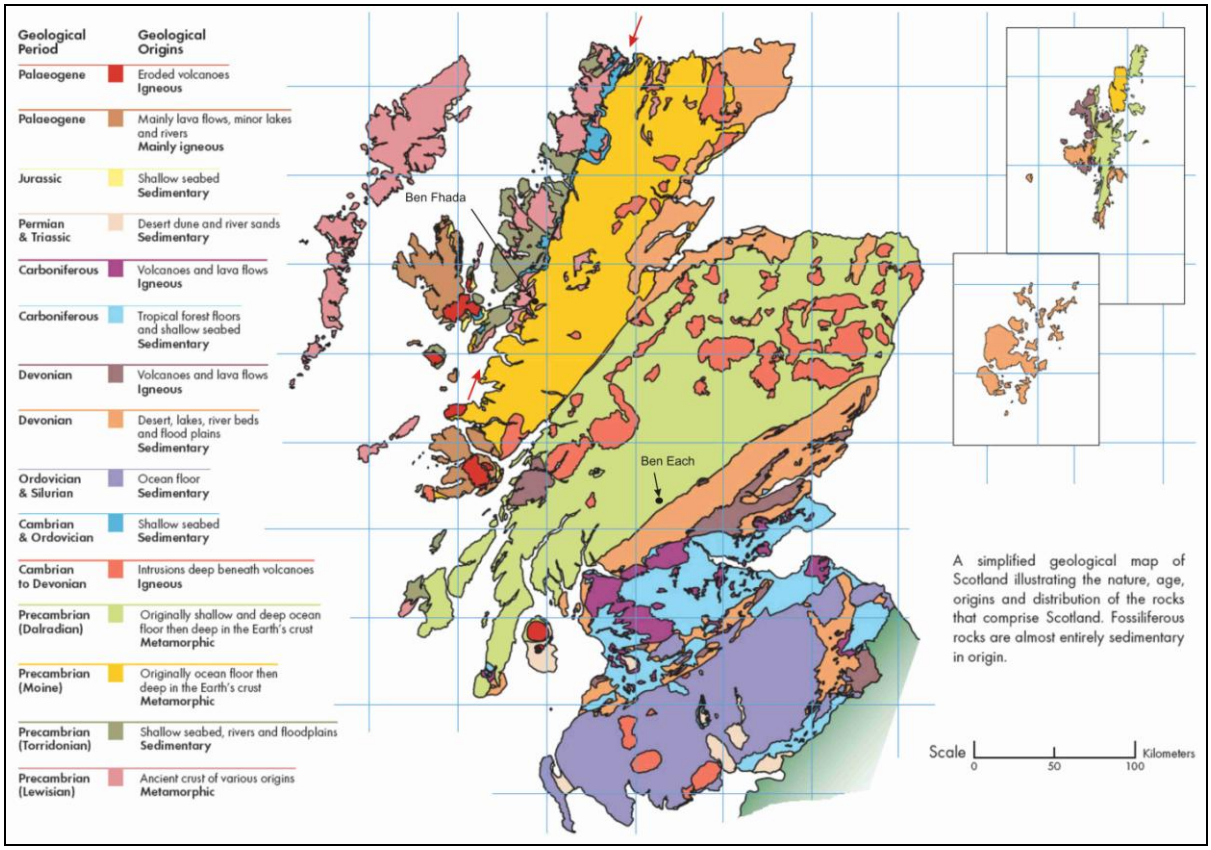

Figure 4.24: Geological map of Scotland. The Moine Thrust is denoted by the two red arrows (map from http://www.scottishgeology.com/geology/geology_of_scotland_map/scotland.html).

Figure 4.25: Psammite from Beinn Fhada with typical gneissic texture.

4.2.1.2 Glacial history

During the last major glacial (Late Pleistocene) there was an sheet ice over Scotland that between 29 ka and 22 ka joined with the Scandinavian ice sheet. By 15 ka to 14 ka there was an ice cap that covered most of Scotland which had melted by around 13ka, with a glacial readvance between 11 ka to 10 ka associated with the Loch Lomond stadial (Fenton 1992a).

A period of rapid isostatic uplift occurred during and directly following the retreat of the glacial ice with the majority of faulting observable within the region attributed to this event (Fenton and Ringrose 1992; Fenton 1992a; Fenton 1992b).

Numerous cirques are observed around the field area with oversteepened slopes, trim lines, and smoothed ridges indicating extensive glacial modification of the landscape.

4.2.1.3 Tectonic history

Scotland is a seismically quiet country by comparison with New Zealand, although compared to the rest of the United Kingdom the south western Scottish Highlands is one of the more seismically active areas. Paleoseismic studies indicate a correlation between the extent of the last glaciation and seismic activity (Davenport et al. 1989; Ringrose et al. 1991; Fenton 1992a; Fenton 1992b; Musson 1996). Figures of surface magnitude (M_S) = 7.0 and local

magnitude (M_L) > 5.0 are touted and are inferred based on slope failures, soft sediment deformation and fault rupture dimensions. Current indications are that the UK can expect an earthquake of 3.7 M_L every year, 4.7 M_L every 10 years and 5.6 M_L every 100 years (Musson 1996).

The Moine Thrust lies to the west of Beinn Fhada and is a 190km long fault trace that extends from Loch Eriboll on the North Coast to the Sleat Peninsula of Skye to the south-southwest. The Moine thrust is a 10km zone of low angle Devonian Nappe faults where Pre-Cambrian schists and gneisses are pushed over Cambrian and Ordovician quartzites, limestones and shales (Fenton 1992a; Musson 1996).

Faults that are associated with the post glacial rebound reactivated pre-existing faults within the region to accommodate movement.

No faults were observed in the field area during the period of fieldwork, or any evidence of recent seismic activity.

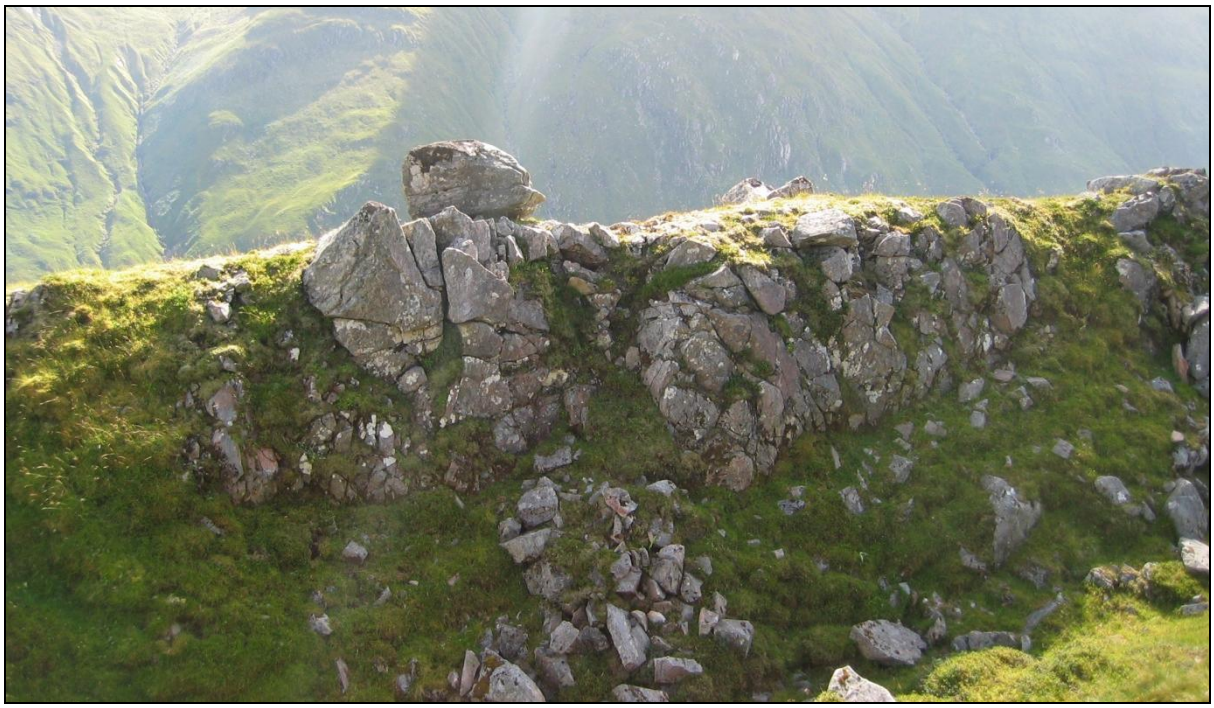

Figure 4.26: A precariously balanced rock on the crest of an antiscarp. The locality of this rock is suggestive of a very low probability of shaking being experienced within this region. It is inferred that this rock would most likely have been dislodged by relatively low levels of seismicity.

4.2.2 Antiscarps

A geomorphological map is presented in Figure 4.27 to illustrate the key features within the landscape that relate to antiscarps. Different zones can be identified within the Beinn Fhada massif and these correlate to a slope aspect. The southern slopes of the Beinn Fhada massif change aspect from west-southwest facing on the westernmost slopes (Zone A) through to south-southeast facing on the easternmost slopes (Zone D). Zone E on the top of the ridge is gently rounded with an overall shallow dip to the south. There is extensive cirque development to the north.

Antiscarps are primarily seen over the entire south-south west facing slope of Zone C and on the top of the massif in Zone E. Zone C antiscarps are subparallel linear features that extend along the strike of the slope from 20m to 1200m+ (Figure 4.28 to Figure 4.30). Scarp heights are greatest, in the upper sections of the slope, up to 10m in some cases, and are more muted in the lower slope and on the shallow ridgeline where heights are in the order of tens of centimetres (Figure 4.30 to Figure 4.36).

Slope bulging is not evident on Beinn Fhada. There is some downslope transfer of material that when coupled with scarp diffusion on the lower slope can appear to be minor bulging in the slope, especially in the interfluves. The increased scarp diffusion is attributed to proportionally larger catchment area above the scarp with decreasing elevation. There is also more material trapped in the antiscarps in the lower section of the slope than in the upper section because of the greater source area above. The more lush grass on the lower slope also attracts grazing livestock more readily than the drier grass present on the upper slopes where there is less water. Trampling by livestock movement also diffuses the appearance of the scarps in the lower section of the slope (Figure 4.30).

Deformation rates are poorly constrained with no controls on either the initiation of antiscarp formation or on how often movement may have occurred on the antiscarp. It is likely that the antiscarps formed soon after the end of the last glacial period in response to post glacial rebound where the elastic component of the previously compressed rock material is recovered.

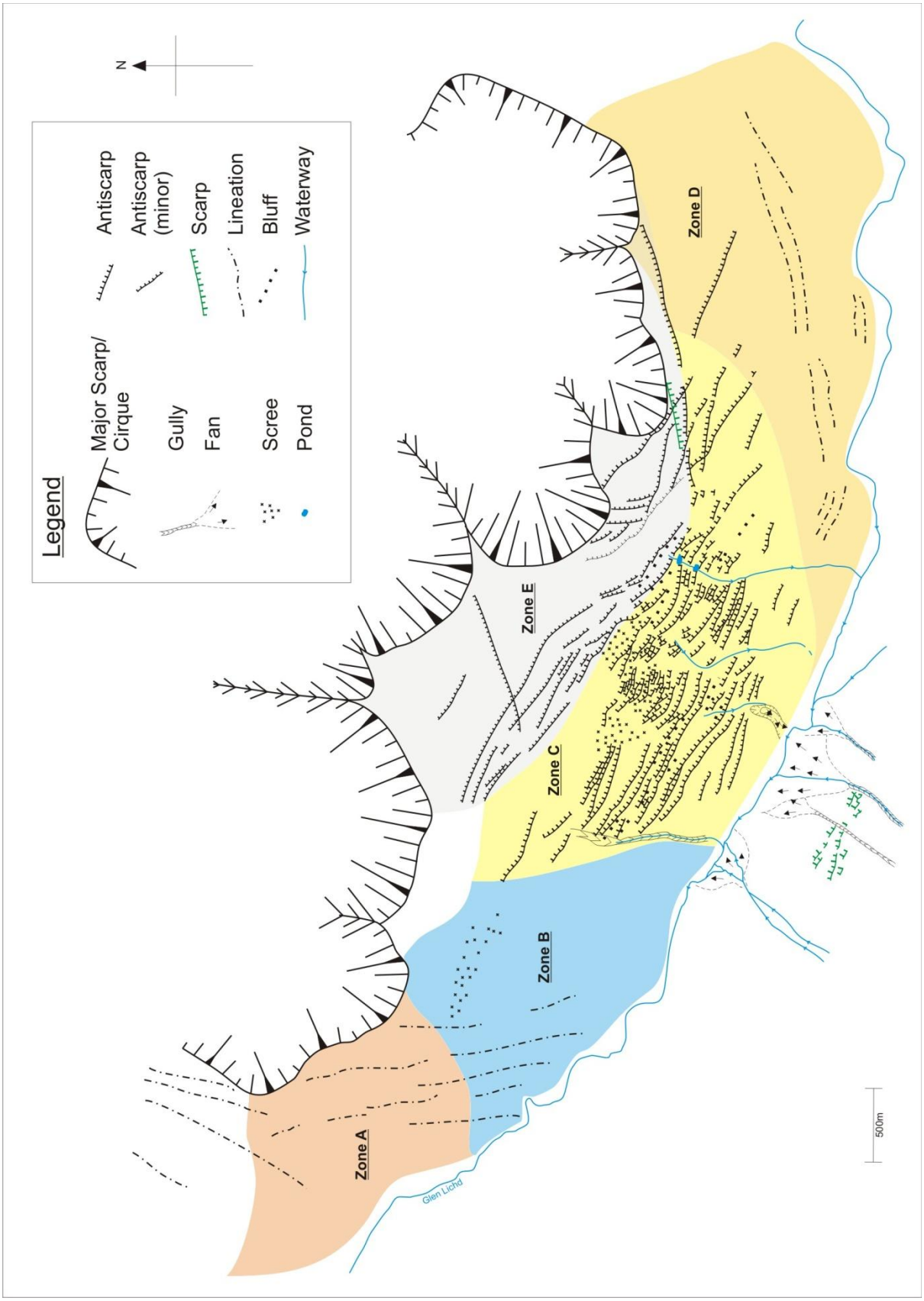

Figure 4.27: Geomorphological plan of Beinn Fhada.

There is no evidence of antiscarps on the northeast side of the ridge which is occupied by extensive cirque development which has removed millions of tonnes of material (Figure 4.36).

Antiscarps appear to exploit the exploiting existing discontinuities through the rock mass, in particular foliation (Figure 4.37 and Figure 4.38). Movement is considered to be brittle type failure involving flexural slip and is in response to unloading by mass wasting related to cirque development on the northern slopes coupled with an element of post-glacial rebound.

A schematic of the proposed evolution of the antiscarps on Beinn Fhada is presented in Section 6.3.

Figure 4.28: View to the northwest along the southwest slope of Beinn Fhada. Multiple linear antiscarps are evident running along the strike of the slope.

Figure 4.29: View to the southeast along the southwest slope. The even amount of displacement of the antiscarp along its length, even as it crosses undulations and interfluves across the slope, is well represented at this locality. This feature is one of the key arguments against the antiscarps here being a product of glacial action such as a trim line or selective plucking of material from within the antiscarp.

Figure 4.30: Increased degradation of the antiscarps in the lower section of the slope is attributed to inundation by surface processes, initially lower antiscarp heights, and trampling by livestock.

Figure 4.31: Some of the larger antiscarps observed on the slope with heights of around 10m. This is a different perspective of the antiscarps in Figure 4.29.

Figure 4.32: View to the northwest along another of the larger 10m high antiscarps. Note the lack of rockfall material or slope debris within the antiscarp; this is typical of the antiscarps

within the upper section of the slope. Infill in the lower slope antiscarps tends to be finer grained material rather than rocks.

Figure 4.33: A view downslope into the antiscarp in Figure 4.32. Sheep on the right of the antiscarp for scale.

Figure 4.34: View to the northwest along the southwest slope where it joins with the shallow ridgeline.

Figure 4.35: Upslope of Figure 4.34 towards the northeast. The ridge line along the Beinn Fhada massif is relatively subdued, where the low amplitude antiscarps have heights of as little as 20cm.

Figure 4.36: Further up the slope again looking along the ridge to the northwest. Note the three cirques on the northeast side of the ridge (right side of the photo) that have eroded all the way through to the ridgeline.

Figure 4.37: View northwest along the ridge looking into bedrock exposed within one of the cirques on the northeast slope. The foliation is steeply dipping to the northeast and is strongly aligned with the orientation of the antiscarps.

Figure 4.38: Another photo looking into a different cirque on the northeast slope. Again the foliation is dipping to the northeast and is sympathetic to the orientation of the antiscarp structures.

4.2.2.1 Classification

Multiple antiscarps, homogeneous massif, controlled by discontinuities, no rotation out of the slope, with large scale mass movement on the other side of the ridge – Unloading.

4.3 Ben Each

Ben Each is located approximately 30km to the northwest of Stirling in the Trossachs region of Scotland (Figure 4.24). The roughly 5km long massif is asymmetrical and is aligned in a north –south direction. The massif is 813m high and has the Burn of Ample flowing to the North in the adjacent 340m high valley giving an approximate western slope height of 470m.

The visit to Ben Each was a day trip involving a walk over the western slope of the massif and notes made on observed features.

4.3.1 Geological setting

4.3.1.1 Lithology

The observed rocks are sheared and fractured, bedded, indurated to well indurated quartzose sandstones with a poorly developed foliation. The surface cover consists of a thin top soil on most of the upper slope areas with the presence of peat within some antiscarps and on parts of the lower slopes.

Estimated field strength is that of a very strong R5 rock, likely to have a UCS ~200 MPa.

4.3.1.2 Structure

Ben Each is an asymmetrical massif with antiscarps on the western slope and bluffs and minor cirques on the east. Both slopes have been glacially modified at some stage in their past.

At least two discontinuity sets are present in the massif, these being bedding and a pervasive joint set respectively. The antiscarps observed here appear to utilise the existing discontinuities.

Tension cracks were observed cutting across the summit and were aligned with the bedding orientations within the area (Figure 4.39).

4.3.1.3 Glacial history

As with Ben Fhada the last glacial had a major impact on shaping the landscape throughout this area. U-shaped valleys, glacial trim lines are indicative of the glacial history of this valley. Cirques have developed on the west side of the massif but these were not observed in any detail.

Figure 4.39: This photo is taken from above the face in Figure 4.40. There is an obvious tension crack behind the face that is dilated, with a second tension crack also apparent just below the summit.

4.3.1.4 Tectonic history

There were no major tectonic lineaments observed within the area during this period of field work. It is assumed that there would have been some degree of post-glacial rebound associated with deglaciation around 13ka and that minor faults would have accommodated much of the movement.

4.3.2 Antiscarps

Two antiscarp sets were observed on the western slopes of the Ben Each massif. The primary set are a ridge parallel set, A1, with an oblique set, A2, plunging to the south at approximately 45° (Figures 4.38 and 4.39). The antiscarp sets exploit the prominent bedding and joint discontinuities in the massif.

Antiscarp heights vary between 2 and 12m in the upper sections of the slope where they are more pronounced (Figures 4.40 to 4.43). Some antiscarps have a muted appearance due to partial infilling with peat and/or slope colluvium, and may be accompanied by degradation of the headscarp itself.

Figure 4.40: The exposed face in this photograph is on the ridgeline near the summit of Ben Each. The structure exposed in this face is bedding and the orientations are coincidental to the same structures associated with the A2 antiscarp sets.

Figure 4.41: Another outcrop showing the discontinuity set that aligns with the A2 antiscarp set.

Figure 4.42: View towards the north with A2 antiscarps cutting across from the top right to the bottom left corner. Antiscarp heights are approximately 2m here.

Figure 4.43: Looking towards the north along remnants of A1 set antiscarps. Two A2 antiscarps cut down across the picture from the top right corner towards the bottom left. This picture is downslope from Figure 4.42. Antiscarp heights are less than 1m here and appear quite muted.

Figure 4.44: Looking down the south plunging A2 set into the intersection with the A1 set. Both sets appear to offset each other which is common for the intersections observed on this slope. The variable antiscarp heights of the intersections suggest movement on the different sets may have been contemporaneous or that movement varies between the two sets. Typical heights in this area ranged from 1m to 8m.

Figure 4.45: 12m high oblique antiscarp associated with the A2 set. Person in centre of the photo is approximately 1.8m tall for scale.

No indicators for determining or constraining deformation rates were identified at this site, although there may be a possibility of chronostratigraphic horizons within some of the antiscarps which could be targeted by trenching. No offset of the peat material was noted on any of the observed antiscarps, suggesting peat deposition postdates antiscarp formation.

Several springs were identified in the lower section of the slope and align with the general trend of antiscarp set A1 (Figure 4.46). This suggests that groundwater exploits the fracture network associated with the antiscarps at this locality (Figure 4.47).

No bulging of the slope was observed.

Figure 4.46: Barren patch in bottom of photograph is one of several springs coming through and removing fines, leaving patches of cobbles and gravel. The springs are in alignment with the projection of a linear feature upon the slope that is aligned with the trend of the antiscarps on the slope. The heather on the slope (darker brown pink flowered shrub) sits within the lineation up the centre of the picture which is a poorly developed, or infilled, antiscarp.

Figure 4.47: Another of the springs along the same alignment as the one identified in Figure 4.46.

4.3.2.1 Classification

Multiple antiscarps, homogeneous massif, controlled by discontinuities, very limited rotation out of the slope, and with large scale mass movement on the other side of the ridge – Unloading.

4.4 Lewis Tops

The Lewis Tops are adjacent to the Lewis Pass which is the lowest point across the Southern Alps in this region at 864m (Figure 4.1). The ridgeline is aligned roughly east-west and has been shaped by the extensive glaciation and tectonic activity within the region.

The antiscarps on the Lewis Tops were brought to my attention by Rob Langridge from GNS Science in Wellington, New Zealand, where he was interested in them as being an indicator of paleoseismicity in this area.

4.4.1 Geological setting

The field area is located adjacent to several major faults including the Alpine Fault and several strands of the Marlborough Fault Zone. Antiscarps observed follow discontinuities within the rock mass and appear as both ridge parallel and oblique sets.

Rocks exposed in the Lewis Tops show a high degree of fracturing, likely to be associated with tectonic uplift, glacial history and seasonal cycles of freeze-thaw.

4.4.1.1 Lithology

The highly sheared and fractured rocks of the Torlesse Group are exposed within scree slopes, outcrops and antiscarps on the Lewis Tops and are typical of the rocks common along the length of the Southern Alps. The Torlesse Group at this locality is represented by bedded, very well indurated argillites and quartzofeldspathic sandstones. A thin soil cover is present over the majority of the upper ridge.

A poorly developed foliation is apparent in many of the outcrops and is indicative of low grade dynamic metamorphism.

Estimated field strength is that of a very strong R5 rock, likely to have a UCS >200 MPa.

4.4.1.2 Structure

Bedding tends to dip moderately to the south with a prominent joint set steeply dipping to the north. A second discontinuity set dips steeply towards the northwest and is expressed as an oblique antiscarp set with an antiscarp spacing between 150m and 200m.

Typical slope angles are between 20° and 30° over the upper section of the southern slope and across ridge, with the incised lower southern slope and the oversteepened northern slope approaching angles of 40°.

4.4.1.3 Glacial history

The Lewis Pass region has a similar glacial history to the rest of the Southern Alps of New Zealand in that Otiran glaciation from 74 ka to 12 ka was the last glacial period.

Oversteepened slopes with smoothing of the flattened upper slopes are indicative of the incised glaciated valleys. Other glacial features within the area adjacent to the Lewis Tops include trim lines in the surrounding valleys and on the adjacent mountains, cirque development, and hanging valleys.

4.4.1.4 Tectonic history

Uplift in the region has been driven by the convergence of the Pacific Plate with the Australian Plate.

The southwest north east trending Alpine Fault is to the west and intersects in the north with the Wairau Fault, which is the most westerly of the faults within the Marlborough Fault Zone (MFZ). Other faults of the MFZ such as the Awatere also passes to the north while the Clarence and the Hope faults lie to the south.

The region is subject to many shallow earthquakes and also large peak ground accelerations associated with the proximal faults referred to above (Figure 4.14).

4.4.2 Antiscarps

Antiscarps on the Lewis Tops are seen in the upper third of the roughly east west trending massif on both sides of the asymmetric ridge. There are more antiscarps apparent on the southern slope, including both ridge parallel and oblique antiscarps (Figure 4.48). The northern slope has extensive scree slope development upon it and is slightly steeper than the southern slope (Figures 4.48 and 4.49).

There is no available data on the initiation of antiscarp formation. Inferences are made from the glacial features on the slope that antiscarps post date the glacial event that covered the Lewis Tops. There are further complications in establishing a deformation rate as there are also no controls on whether the formative event is a single event displacement or ongoing creep.

Figure 4.48: Intersection between an oblique antiscarp with a ridge parallel antiscarp. The ridge parallel antiscarp extends along the slope in both directions while the oblique antiscarp terminates at this intersection. Both people in this photo are approximately 1.8m tall. The ridge parallel antiscarp is approximately 0.5 m at this locality with the oblique antiscarp ranging between 1m and 1.5 m. (Reproduced from Figure 2.2B).

Figure 4.49: View to the west of the northern slope. Of note is the development of scree slopes. There are remnants of antiscarps evident in the outcrop adjacent to the scree slope.

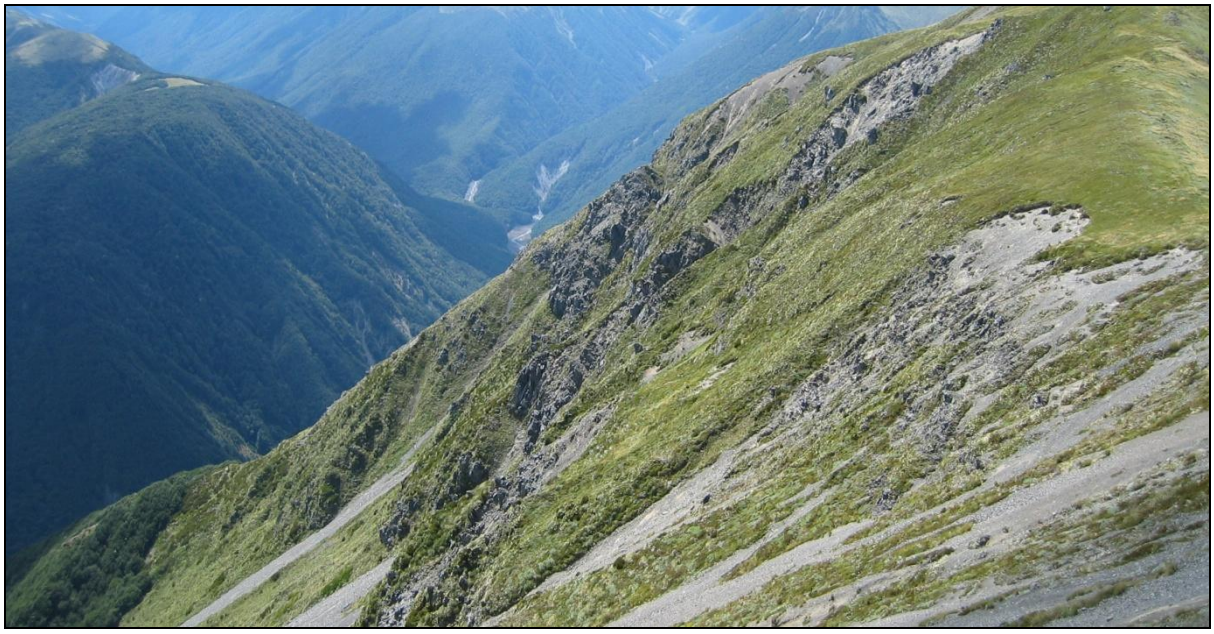

Figure 4.50: View to the east along the northern slope.

There is no evidence of bulging in the lower slopes on either side of the ridge although vegetation cover and shallow slope failures may hide or have removed any evidence of their presence.

Antiscarps range in length from 150m to traces in excess of 2km for those that are ridge parallel. The oblique antiscarps tend to be shorter and are in the order of tens of metres to 300m long, and tend to truncate against the ridge parallel sets (Figure 4.48). Typical scarp heights were in the region of 1m to 3m.

Numerous tarns that have formed within antiscarp related depressions on the ridge (Figures 4.50 to 4.53). Trenching through some of these tarns may provide some insights into rates of formation and possibly some paleoseismic data. Some initial small test holes on the edges of the tarns did not intersect anything of note but they were on the margins of the tarns where a full sedimentation record may not be intersected.

Movement style is attributed to be brittle failure that utilised existing defects. There are some similarities to the deformation processes of both Beinn Fhada and the Kelly Range. The scree and extensive oversteepening on the northern slope are comparable to the cirque development on Beinn Fhada in that they are both indicative of large volumes of material removed from the slope. The presence of antiscarps on both the northern and southern slopes however is more similar to the Kelly Range example.

Figure 4.51: View to the west along the southern slope. Multiple 1.5 -5m high ridge parallel antiscarps are obvious extending from the lower left of the photograph and extending right along the slope towards Lucretia in the centre background. Several oblique sets are also present with the tarn in the centre lower section of the photo formed against one that extends from the lower right corner up towards the left. Several other oblique antiscarps are also apparent along the slope following the same orientation.

Figure 4.52: Tarn within ridge parallel antiscarp set. The slope has a chopped up appearance with the interaction between the parallel and oblique sets. Scarp heights on both sets range between 1 to 5m.

Figure 4.53: Large tarn within a ridge parallel antiscarp.

Figure 4.54: Series of tarns within an oblique antiscarp this locality is approximately 250m to the northeast of the same oblique antiscarp in Figure 4.51.

4.4.2.1 Classification

Multiple antiscarps, homogeneous massif, controlled by discontinuities, no rotation out of the slope, and displays graben style collapse features – Gravity faulting coupled with unloading.

4.5 Stag Hill

Antiscarps on Stag Hill were observed from the Cass Saddle to the northwest (Figure 4.1). Attempts to access the outcrops proved unsuccessful due to extensive gullies blocking the route and poor access from the Cass Saddle, however much information was gained from the observations made from afar.

Stag Hill is 1631m asl elevation and has a distinct break in slope around 1400m asl where the upper slope flattens out to approximately 21° and the lower slope is about 37°, potentially approximating the angle of repose for the material. The overall slope length is approximately 1300m.

4.5.1 Geological setting

Stag Hill is similar to the Kelly Range (Section 4.1) in that it is located in a geologically active area of the South Island of New Zealand. It lies approximately 30km to the southeast of the main divide within Torlesse Group rocks and is subject to climatic variations on seasonal and geological time scales, tectonic forcing, seismic activity, and glacial activity.

4.5.1.1 Lithology

Stag Hill is composed of highly fractured and sheared, bedded, weathered, very well indurated quartzofeldspathic sandstones and argillites of the Torlesse Group. The argillites are typically thinner, with thickness from several metres to tens of metres, than the sandstone beds, which are in the order of tens to hundreds of metres. Minor jasper occurrences are observed in some outcrops adjacent to Stag Hill

There is a thin soil cover over most of the range, with scree slopes and localised areas of slope colluvium.

Estimated field strength is that of a very strong R5 rock, likely to have a UCS >200 MPa.

4.5.1.2 Structure

Gullying is apparent on many of the slopes surrounding Stag Hill and provides good exposure of the bedded Torlesse argillites and sandstones (Figure 4.55). Only one set of antiscarps

were observed at this locality and have the scarp face aligned with the northwest moderately dipping bedding.

4.5.1.3 Glacial history

Smoothing of the upper slope sections is thought to be related to the Otiran glacial period from 74 ka to 12 ka. Other noted glacial features within the region are the hanging valley associated with the Cass Saddle, minor cirque development, and remnant trim lines on some slopes.

Figure 4.55: View to the southwest from Cass Saddle towards Stag Hill.

4.5.1.4 Tectonic history

No faults were observed during the foray into the Stag Hill area although there are many known and established faults within the area.

The far field tectonic loading associated with the convergence of the Pacific and Australian Plates impacts upon this region by the uplift which is expressed as the Southern Alps.

4.5.2 Antiscarps

As with the other sites presented in this chapter, there is great difficulty in establishing deformation rates as there is no control on whether movement is ongoing creep or a single event displacement.

Antiscarps strike sub-parallel to the slope and are only identified above the break in slope where it flattens out towards the ridge. Any antiscarps that may have formed on the lower section of the slope would probably have been removed or buried by ongoing slope processes, as evident by the extensive development of scree slopes, or may be obscured by the native forest. Antiscarps were only observed on the southeastern slope of the asymmetric ridge.

Slope bulging was not evident although this could be attributed to any bulging being obscured by scree or forest rather than absence.

The antiscarps exploit the bedding as a failure surface and are indicative of a brittle deformation style.

Air photos indicate antiscarp lengths are in the vicinity of 300m to 1500m. Scarp heights were determined from a distance, approximately 2.5km away on Cass Saddle, and appear to be in the vicinity of 2m to 10m.

4.5.2.1 Classification

Multiple antiscarps, homogeneous massif, controlled by discontinuities, no rotation out of the slope, and displays graben style collapse features – Gravity faulting coupled with unloading.

4.6 Comments on the field studies

The focus of this chapter was to present field based observations and measurements from a variety of spatially separate areas where antiscarps are observed. Two main antiscarp formative processes stand out from the field examples examined here, these being gravity faulting and unloading.

There were several commonalities observed across the different field sites

- Rock strengths typically R5
- Glacial activity is observed with indications that the entire massif has been under ice at some stage.
- Close proximity to known faults/ fault zones.
- Slope modification has occurred as a direct result of glacial activity

Major differences observed related to massif symmetry, or asymmetry, and the extent that a slope had been modified by surface processes to remove large volumes of material.

There is difficulty in identifying a single process as being more prevalent than another. For example, gravity is acting at all times and across all massifs and so gravity faulting could be considered to be an integral part of all non seismic antiscarps. In fact with reference to Chart 1 it is apparent that most antiscarps are considered to be related to a gravity driven mechanism. Also, there is little to no control on at what stage of a massifs evolution that antiscarps may form, seismically related antiscarps excluded, and so there is difficulty in teasing out the contribution of post-glacial rebound following deglaciation.

A secondary aim has been to obtain enough data on which to base both physical and numerical models. The Kelly Range was used by Beck (1968) as the basis for his work on gravity faulting and after assessing the area it is proposed to utilise this massif as the template for both physical and numerical models, also addressing gravity faulting.

Beinn Fhada had some spectacular cirques that had developed on the northern slopes and in the process had removed millions of tonnes of material. Numerical models that will be used to assess the role of unloading as an antiscarp formative process will base aspects of the initial setup on this massif.

5 Antiscarp modelling

Physical and numerical modelling of antiscarps were undertaken to test whether antiscarps can form solely under the influence of gravity, and also if their formation can be attributed to removal of large volumes of material from the slope.

The modelling undertaken here aims to clarify the extent that gravity contributes to antiscarp formative processes. Determining a response from the mountain/slope under static conditions does not factor in perturbations to the system from loading/unloading, seismic events, or far-field tectonic stresses.

Where modelled antiscarps form solely under gravity the conclusion is simply that it is possible for antiscarps to form without an external perturbation. Both physical and numerical models are utilised to test the role of gravity.

Unloading by rapid incision or cirque formation is proposed to alter the stress fields within the massif by allowing stress relief expressed as movement into the area where the mass has been removed. Numerical models are used to test antiscarp development under an unloading scenario.

Two dimensional (2D) models were used for both the physical and numerical modelling and assessed the models as an infinite slope because there is not expected to be significant variance in rock mass conditions throughout the massif. Antiscarps can effectively be modelled in 2D because they typically extend laterally along a slope, and as such the rock mass on either side of any proposed section through a massif should have equivalent values and conditions.

5.1 Physical modelling using base friction models

A base friction approach was used to physically model antiscarps by simulating the effects of gravity through a cross section of a model massif. The base friction model works on the premise that a shear force along the base of a two dimensional model as it is moving relative to a planar surface will act as a proxy for gravity (Bray and Goodman, 1981; Goodman, 1976; Goricki and Goodman, 2003; Yeung, 1999).

The base friction models are used in this study to model deformations in the rock mass rather than to assess the strength of the modelled rock materials. No scaling of the rock mass properties was undertaken and to extract quantitative values from the models requires scaling of

the material properties of the elements. Thus all results extracted from these models are only qualitative and indicate deformations possible under a gravity load.

The models were idealised massifs with a symmetrical cross-section that is intersected by two discontinuity sets.

5.1.1 Base friction table set-up

There are two options for constructing a base friction table; the first is has the table moving beneath a static model, and the second is where the model is moved over a static table. Initial tests were undertaken using the latter method with the view to constructing a friction table with a moveable surface if large displacements were required to induce deformation within the model. The preliminary tests using the static table with a sliding model yielded satisfactory results and this method was adopted for the testing undertaken here. The static table is also a more cost effective method.

The table was a standard flat office desk approximately 1200 x 600mm with a textured melamine surface (Figure 5.1). The sliding frame consisted of a 1m long tee square that was positioned hard against the left hand side of the table with the model then constructed against the top edge. Sliding the tee square up the table provided the movement necessary to generate friction along the base of the model.

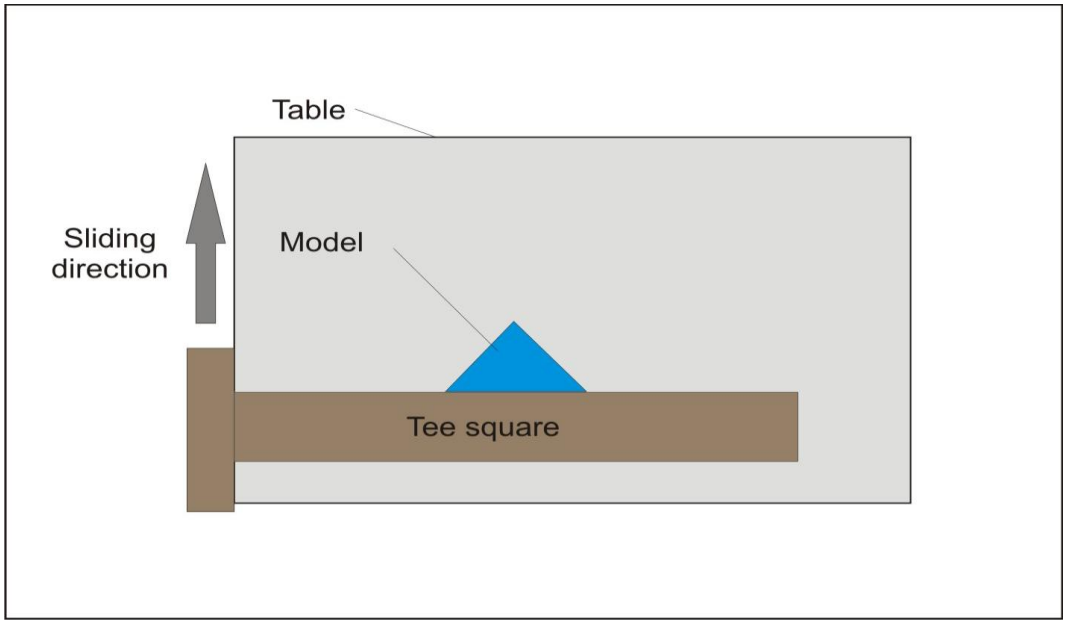

Figure 5.1: Setup for the base friction table modelling.

5.1.2 Model construction

The materials used to construct the models were selected to have low deformation values so that any motion generated would be along the discontinuities rather than through deformation or rupture of the material itself. The scale of the model also lent itself to selecting non-deforming elements because minor deformation in the element translates to excessive deformation within the proposed massif.

Individual elements were used for model construction to simulate a rigid rock material, rather than using modelling materials such as plasticine or flour and oil mixtures and then cutting in the discontinuities. A variety of materials were used for the elements in the experiments, ranging from coins and hexagonal nuts to plastic geometric pattern blocks.

The cross sectional models constructed for the experiment were built using a number of regularly shaped elements to represent defect-ridden massifs. Each element was an individual unit that when stacked together with other like elements, in a similar fashion to building blocks, formed the massif. Discontinuities are either at 30° or 60° relative to the base for all element shapes. The hexagonal models also incorporate either a horizontal or a vertical defect set depending on the stacking relative to the sliding frame of the tee square (Figure 5.2).

The stepped interface between elements in the models that use the circular and hexagonal elements have a higher cohesion value for the overall discontinuity path in comparison to the linear discontinuities represented in the models that use the diamond shaped pattern blocks.

5.1.3 Base friction tests and test properties

The base friction testing utilised a minimum of 20 runs for each of the different models to ensure that the results were repeatable and consistent. The photosets of the base friction tests (Appendix A) are representative of a typical test for the respective model photographed.

Testing of the models assumed that the discontinuities in the models are clean and open with no infill and that they are not subject to cementation or annealing. Tensile strength within the modelled rock mass is zero.

Attempts were made to test various friction angles by wedging the edge of the tee square to rotate the angle of the discontinuities within the model. In doing so the load upon the modelled massif was also rotated giving an oblique gravitational load across the model and negated this approach. A series of models was then tested using elements cut from 3mm thick MDF board at various angles to construct sliding models. There was much difficulty in being able to achieve a

consistent finish on the edges of the elements which led to a lot of variability in the results. These tests were abandoned when it became apparent that they were not consistently reproducible. No range of values for the internal friction within the models could be determined however whether a model failed or not on discontinuities of a known angle could be used to place constraints on the internal friction angle.

Indicative values for cohesion can be determined using the Mohr-Coulomb failure criterion (Hoek, 1990; Sjöberg, 1997). Where

$$\tau = \sigma_n \tan\varphi + c$$

and can be rearranged as

$$c' = \tau - \sigma_n \tan\varphi$$

Where:

τ = shear strength

σ_n = normal stress

φ = internal friction angle

c = cohesion

c′ = effective cohesion

When no load is being placed on the model then $\sigma_n = 0$, so c′ will be equal to the y-intercept of the failure envelope.

5.1.4 Hexagons

Two modelled massifs were constructed using steel M4 hexagonal nuts as the elements, Hex-A and Hex-B (Figure 5.3). Hex-A incorporated two opposed 30º discontinuity sets and a vertical set; Hex-B incorporated two opposed 60º discontinuity sets and a horizontal set.

No deformation was observed in the Hex-B model. The lack of movement suggests cohesion on the modelled discontinuities is likely to be in excess of 60 º.

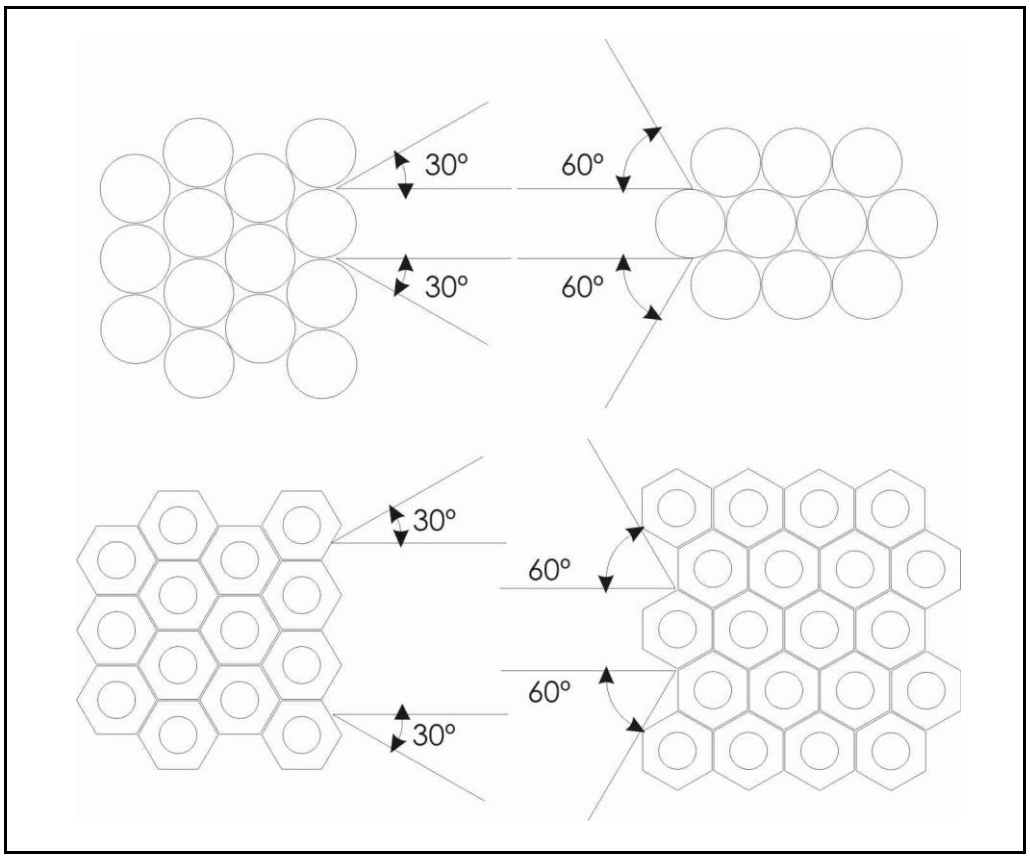

Figure 5.2: The primary discontinuity angles for different shaped elements depend on the relationship of how the elements are stacked relative to the model. The diagram here depicts how a 90 ° rotation of either circular or hexagonal stacked elements result in either a 30° or 60° primary discontinuity angle. For the hexagonal elements there is also a vertical or horizontal secondary discontinuity formed in the Hex-A and Hex-B models respectively.

Hex-A deformed as a block flexure topple where columns of elements bent out of the slope and then broke along existing joints. Dilation within the model was observed after the model had slid 120mm, with the equivalent of large tension cracks or ridge rents evident in the upper slope at 150mm. Distinct flexural topple was observed after sliding of 170mm and progressed through to major slope failure by around 300mm. Antiscarps formed on both slopes of Hex-A.

There was no deformation attributable to the 30º discontinuity set in Hex-A.

The Hex-A and Hex-B models were only tested using a fixed base, meaning the models were not free to spread at the base, and were not assessed using semi-confined or unconfined scenarios.

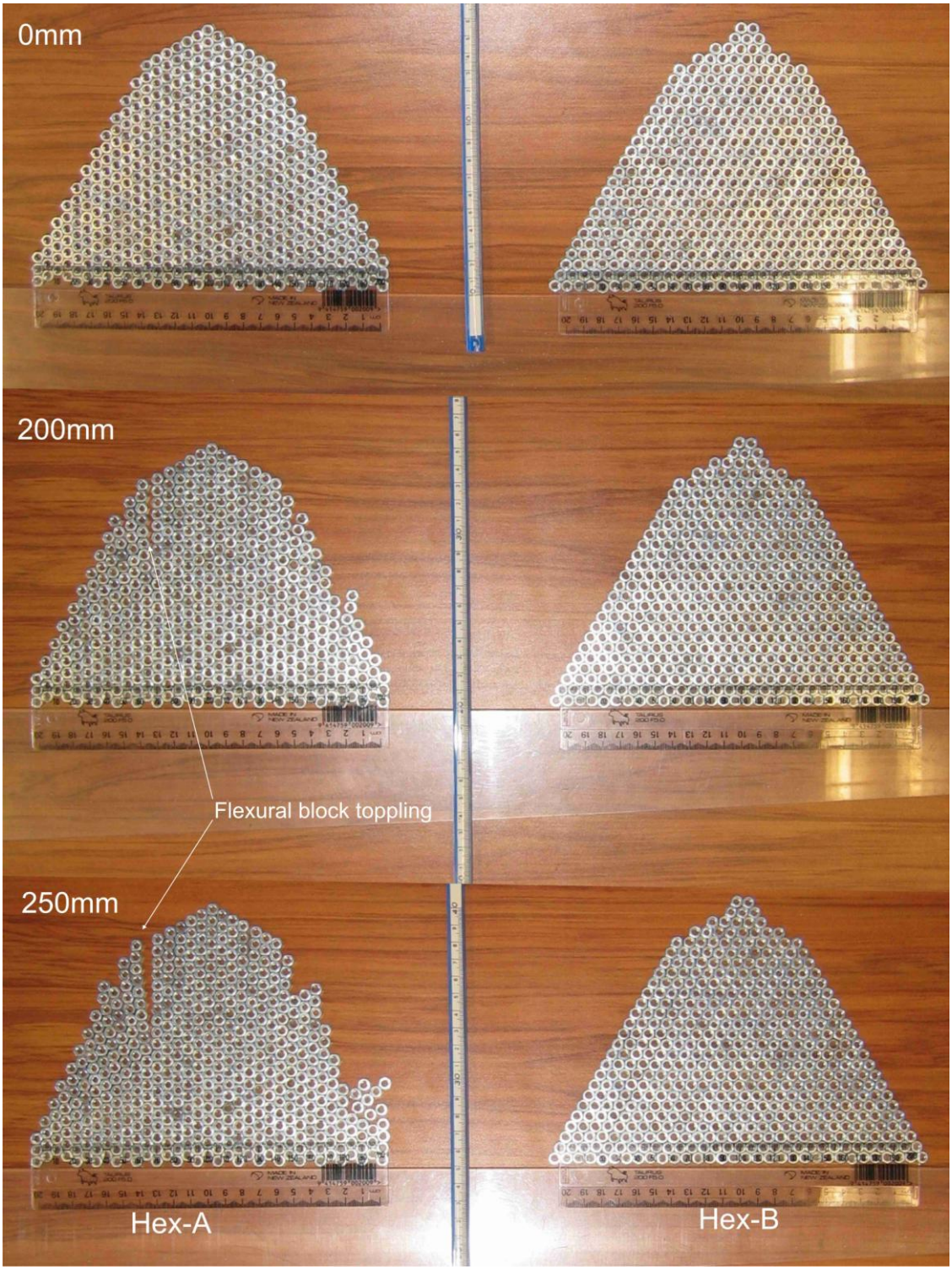

Figure 5.3: Hexagonal base friction models. Both models have a 60° lower slope section with an upper slope of 30°.

5.1.5 Circles – 30º models

A model was constructed using New Zealand 5 cent coins, a redundant circular coins with a diameter of 19mm, to form a massif that had lower slopes at 60°and an upper slope section that flattened out to 30°. Two opposed 30° discontinuity sets were the primary defects within the model with a secondary vertical defect set (Figure 5.4).

Frictional values for the primary defect set are a function of the undulatory nature of the model discontinuity imposing cohesion coupled with the numerous voids in the model reducing friction.

Figure 5.4: 30° circular element model with secondary vertical discontinuity set. The red blocks in this model are attached to the sliding frame and prevent the base from spreading.

5.1.5.1 Confined base

Failures occurred rapidly with most movement observed on the 30° defect set with a dominant failure surface daylighting in the lowest unconfined section of the slope. The lower internal section of the model formed a static pyramid with slope angles of 30º that keyed into the fixed corners of the base and did not move. The lower section of this model appears to bulge as the translating elements move downwards and are pushed outwards by the static pyramid with

further lateral movement driven by the elements moving over the asperities of the corrugated failure path (Figure 5.5).Voids were created as the coins stepped along the failure path and generated phases of model expansion and contraction.

Some flexural block toppling was observed on the vertical discontinuity set but was limited to the upper sections of the translating material. The rounded shape of the circular elements was not as effective as the hexagonal elements for maintaining integrity of the columns during toppling. The toppling process here was primarily that of block toppling rather than flexural block toppling as observed in the hexagonal elements.

The ridge of the model also maintains a high level of integrity and moves into the massif in response to the downslope lateral displacement as a horst block within a graben.

The antiscarps that form within this model are analogous to gravity faults and incorporate aspects of block toppling and slope bulging.

5.1.5.2 Semi-confined base

A semi-confined base was tested to assess the response of the massif to an initial period of lateral extension as an attempt to emulate unloading. Movement at the base was constrained to the equivalent of one element on either side of the model. Initial deformation within the model is focused along the base with block toppling occurring along the slopes (Figure 5.6).

Large voids develop as sliding progresses with the elements locking up as the extension along the base stops. The central portion of the model remained relatively coherent with a 30º pyramid forming within the lower section once the base locked up. Slope bulging occurs in response to the lateral displacement of the elements.

The ridge forms a crude horst block as the model evolves that moves down into the massif as the voids are created. Block toppling occurs down the entire slope including on the surface of the horst.

Antiscarps are poorly developed and are related to gravity faulting with overprinting by block toppling (Figure 5.6).

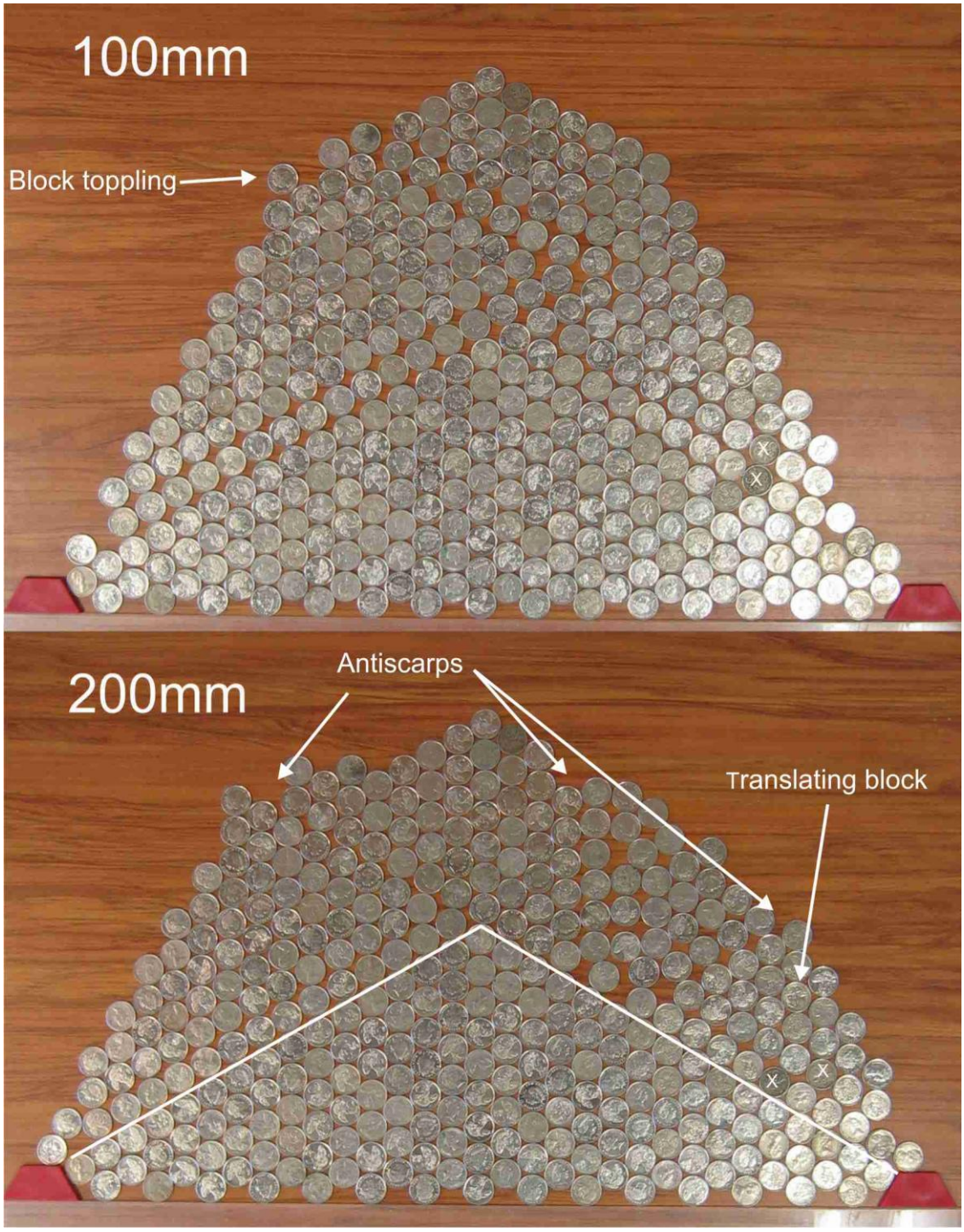

Figure 5.5: Stages of development in the confined 30º circle model

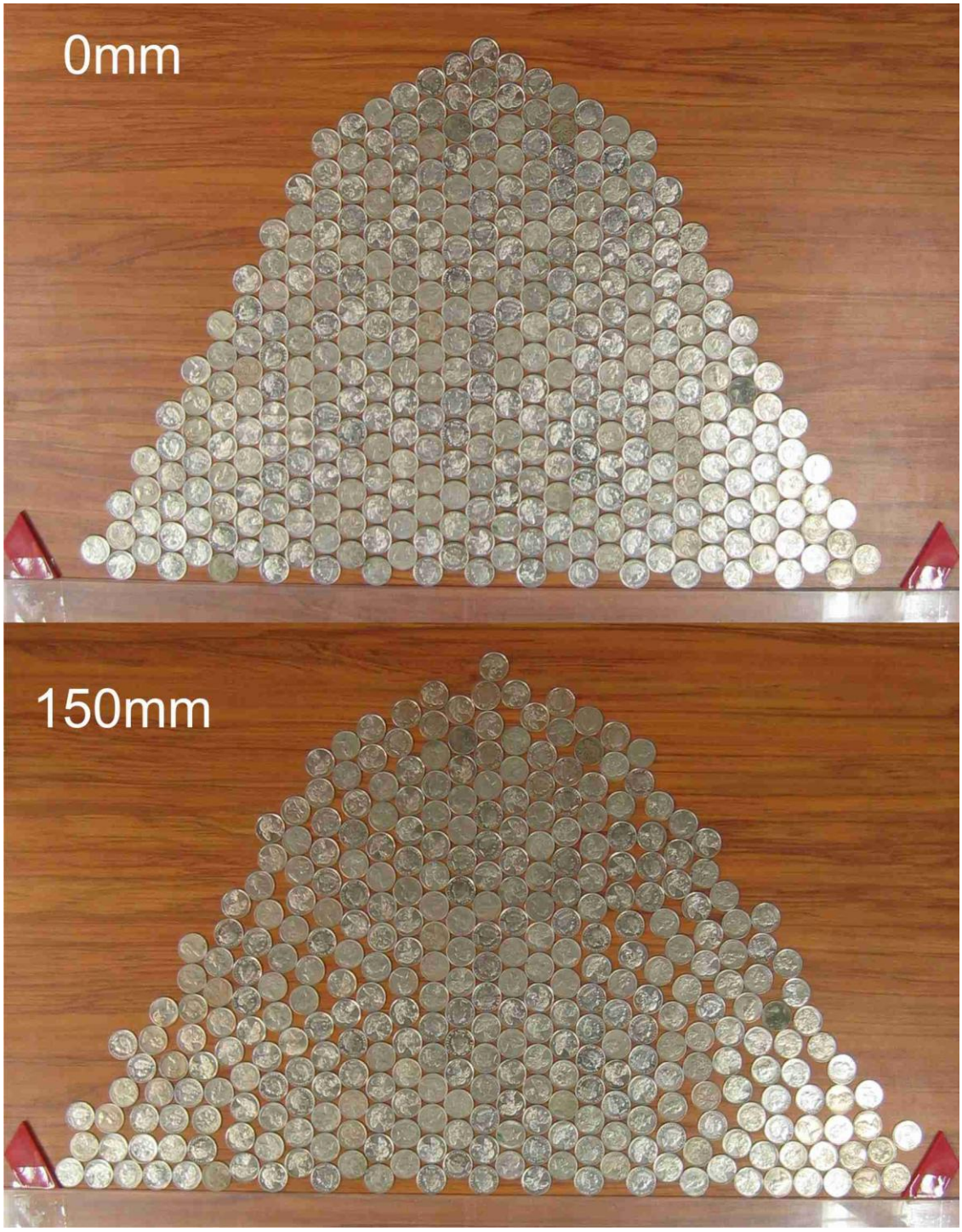

Figure 5.6: Initial semi-confined 30º circle model with the deformed model after 150mm of movement. The shallow block topples are evident down the slopes with a wide diamond shaped horst formed in the upper section of the model and a 30º pyramid formed at the base once the elements were no longer able to move laterally along the base.

5.1.5.3 Unconfined base

Deformation within the lower section of the model was more obvious where the base of the model was unconfined than for the confined and semi-confined scenarios. Most of the observed dilation, and therefore movement, was located around the periphery of the model with lateral movement along the base creating bulging in the lower slope. The core of the model underwent very little deformation (Figure 5.7).

Multiple 30° discontinuities were accommodating the deformation with dilation along all the associated defects due to the elements stepping over each other.

Translation and block topples were the key processes but there were no conclusive antiscarps formed within these models.

5.1.6 Circles – 60º models

An equilateral triangle was constructed using New Zealand 5 cent coins to form a massif with slopes at 60°. Two opposed 60° discontinuity sets were the primary defects within the model with a secondary horizontal defect set (Figure 5.8).

5.1.6.1 Confined base

No deformation was observed in the 60º model when the base was confined.

5.1.6.2 Semi-confined base

Movement at the base was constrained to the equivalent of one element on either side of the model. The response throughout the entire model was relatively uniform with dilation occurring in all parts of the model as lateral spreading at the base was accommodated. Gravity faulting occurred in response to the voids created during the initial phase of the spreading but ceased once the base became confined.

Crude antiscarps formed in response to the gravity faults but were overprinted as flexural block toppling occurred down the slope as the model equilibrated (Figure 5.9) reducing the angle of the discontinuity to around 50°.

The apparent bulging in the lower section of the right hand slope in Figure 5.9 is the equivalent of a landslide deposit rather than actual bulging.

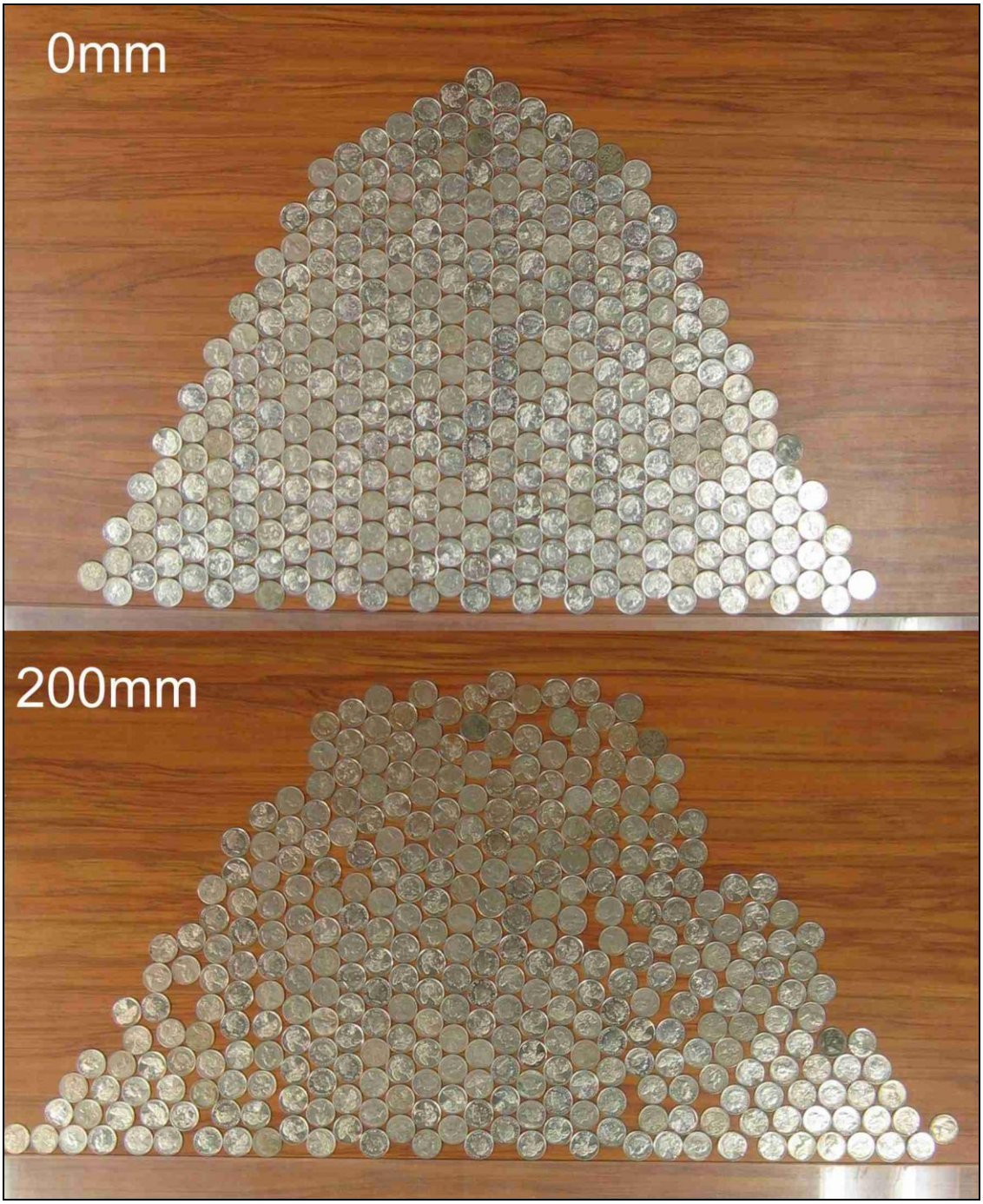

Figure 5.7: Unconfined 30º circle model with the initial condition and after a 200mm shift

Figure 5.8: Circular element model with confined base and incorporated 60° and vertical discontinuity sets.

Figure 5.9: Semi-confined 60º circle model

5.1.6.3 Unconfined base

The initial response to application of the simulated gravity load by sliding is uniform dilation throughout the model (Figure 5.10).

A conjugate set appears to develop at around 70mm of sliding which has a rudimentary graben and associated antiscarps on both slopes to form gravity faults that exploit the voids created by lateral extension of the model mass (Figure 5.11).

Figure 5.12 shows the model after 120mm of sliding with antiscarps in the upper massif attributed to gravity faults and there is flexural toppling down the slope with the discontinuities shallowing from 60° to 50° in places. The circular elements are unable to give any indication of low amplitude antiscarps that may form in response to the flexural toppling. Topple blocks are unable to form as the extension of the modelled massif supports the flexure and prevents the blocks from dislocating.

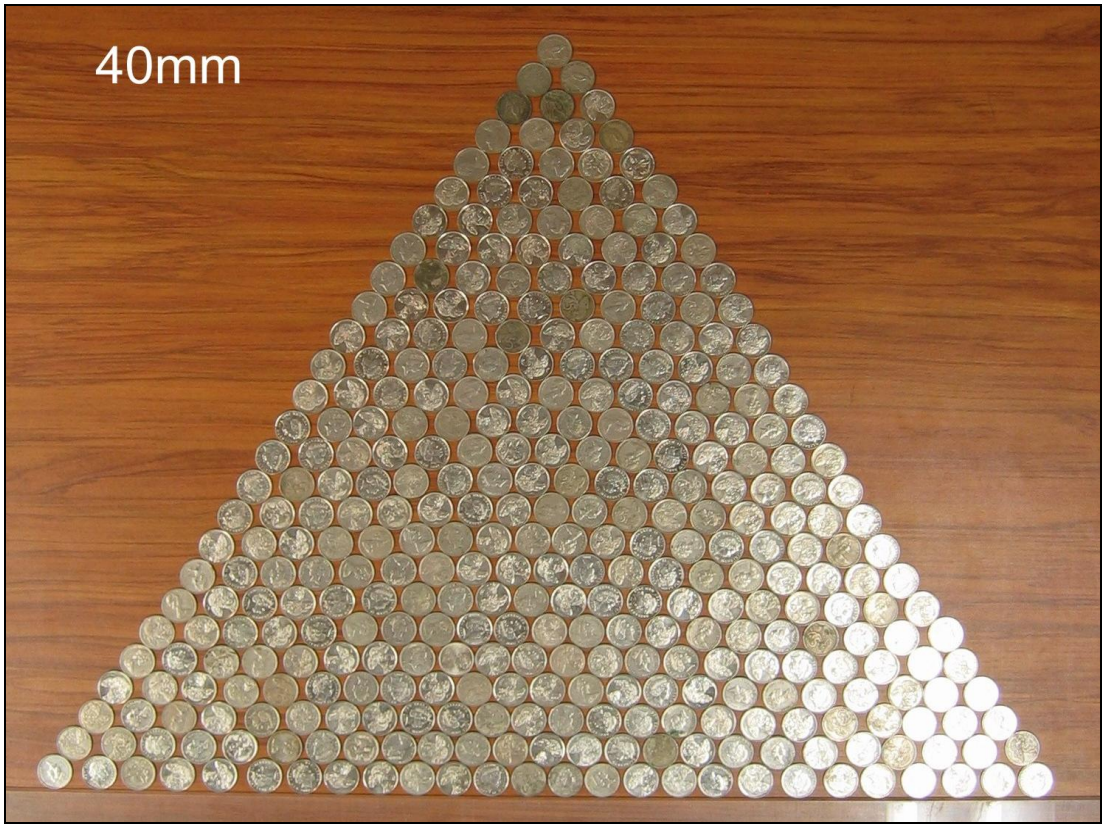

Figure 5.10: Unconfined 60º circle model after 40mm of sliding.

Figure 5.11: Unconfined 60º circle model after 80mm of sliding.

Figure 5.12: Unconfined 60º circle model after 120mm of sliding.

5.1.7 Diamonds – 30° models

Plastic pattern blocks were used to construct a massif that had 30° slopes and opposing 30° planar discontinuities. The diamond blocks had internal angles of 120° and 60° (Figure 5.13). The model was confined at the base so no lateral spreading could occur.

No deformation was observed in the 30° diamond model.

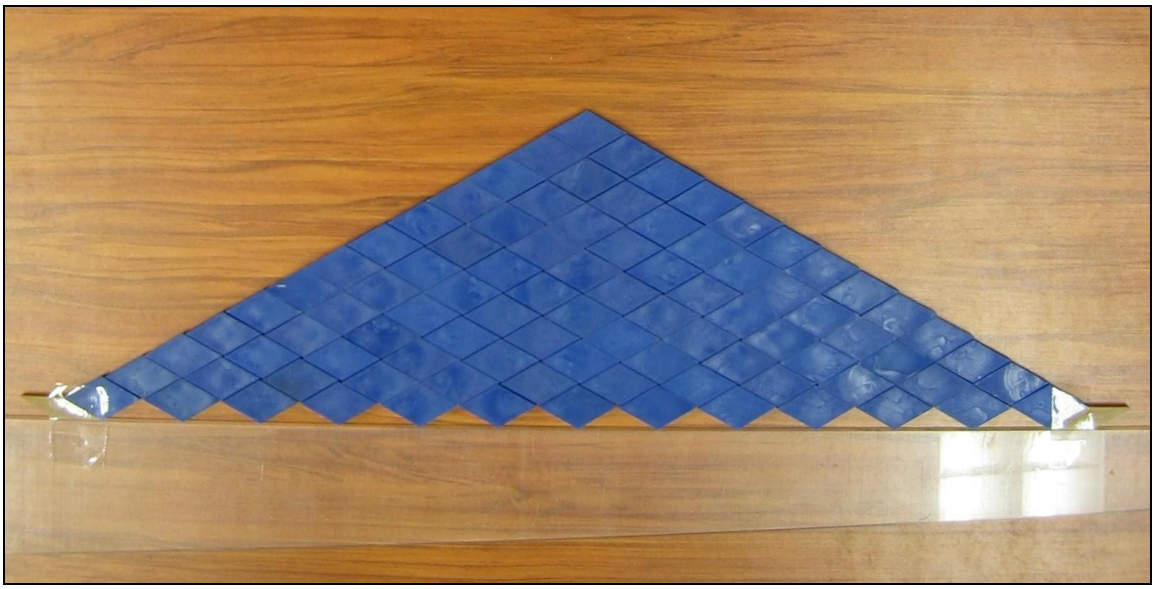

Figure 5.13: 30° diamond pattern blocks

5.1.8 Diamonds – 60° models

Plastic pattern blocks were used to construct a massif that had 60° slopes and opposing 60° planar discontinuities (Figure 5.14). The model was confined at the base so no lateral spreading could occur.

Gravity faulting and minor rotation of elements on the slope occurred very rapidly with obvious antiscarps formed within 10mm of movement. Figure 5.15 shows the model after 20mm of sliding; multiple antiscarps can be seen on both slopes and the graben style gravity faulting is observed as elements, or element clusters, that are moving in to the voids which are opening up during sliding of the model.

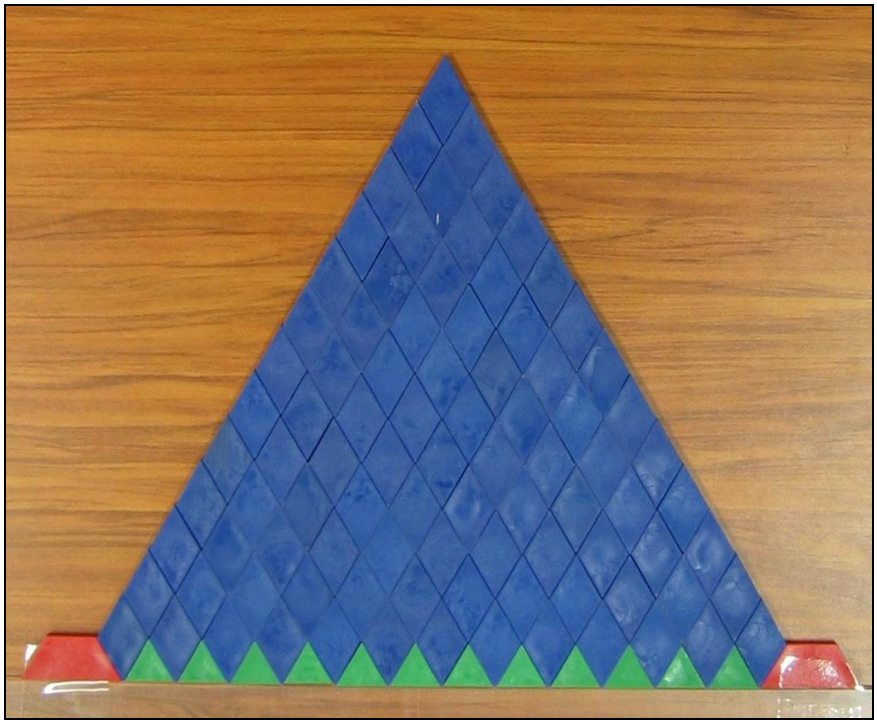

Figure 5.14: 60° diamond model.

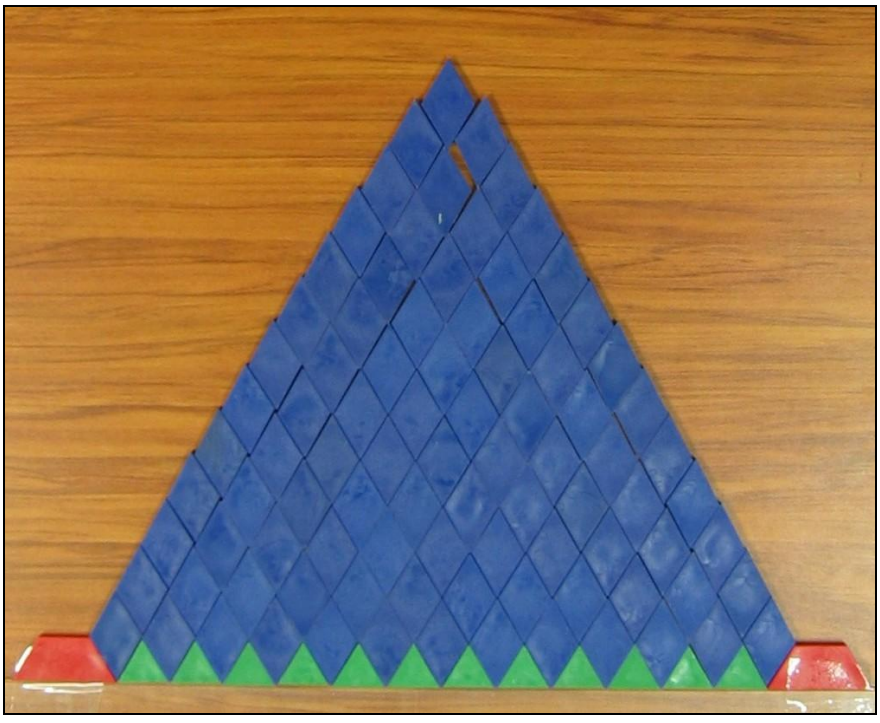

Figure 5.15: 60° diamond model after 20mm of sliding.

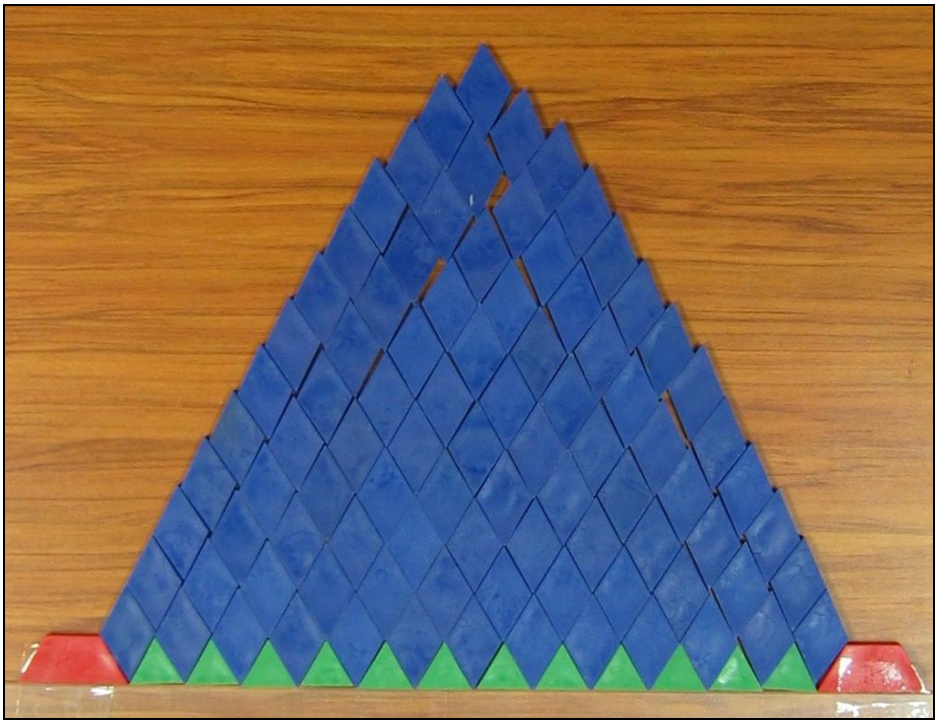

Figure 5.16: 60° diamond model after 120mm of sliding.

Ongoing sliding enhances the existing antiscarp features (refer Figure 5.15) by the increasing the quantity, size, and distribution of voids, and greater displacement of the blocks within the gravity faults (Figure 5.16). Antiscarp amplitudes have also increased.

5.2 Base friction modelling summary

Antiscarps formed early in the models that used the diamond shaped blocks and achieved the majority of associated displacement during the early stages of model testing. These models had much lower frictional values along the modelled discontinuities than the models that had interlocking elements.

Antiscarps also developed in the models that utilised the hex nuts and the coins albeit under conditions that involved both translation along discontinuities that daylighted the slope, the models with discontinuities of 30°, and also toppling, especially where there was a vertical defect set incorporated into the model.

The 60° models for the hexagonal and circular elements underwent no observable change for the confined models. In comparison to the pattern blocks which exhibited significant deformation of the elements near the slope there appears to be some disparity. It is likely that the element shape contributed to the differences between the models with the hex nuts

interlocking and with difficulty in seeing small scale deformation by rotation near the surface in the circular elements.

No toppling occurred within either of the diamond block models. There was some rotation of the elements adjacent to the slopes but it was not about the base so does not constitute toppling. The role of toppling in antiscarp formation may be more significant than was previously considered.

The semi-confined and unconfined circular element models allowed the model to undergo expansion at the base. The hexagonal elements did not use semi or unconfined because of difficulties in setting up the models.

Voids were created in all models where there was movement of the elements. The material strength of the elements used in the models was too high to allow any deformation to occur to or within the element. Comminution or flow of material from the elements was therefore not possible and the voids could not be filled. Voids at depth are not uncommon but as an analogue to the real world the quantity of the voids produced in some of these models appears to be excessive. It is normal for discontinuities to become less rough with ongoing movement and therefore not requiring the stepping over of the elements as seen in these models.

The base friction physical modelling indicates that antiscarps can form solely under a gravitational load.

5.3 Numerical modelling

Numerical models are a way of obtaining approximate solutions to problems encountered in the analysis of slope stability. They can be used to simulate rock masses and then test these masses under different failure criterion and under varying properties. The rapidity that a simulation can be run is one of the distinct advantages of undertaking numerical modelling, especially where the analysis is a parametric one. Finite Element Models (FEM) were chosen for the testing undertaken here because they are able to deal with the complexity inherent in using multiple variable factors under different boundary conditions and produce robust results.

Numerical modelling of antiscarps was undertaken to assess the response of a model massif to a simulated gravitational load and also to the removal of a large section of the model slope. The modelling was a qualitative analysis that utilised varying rock mass properties.

Two different FEM software packages were used to undertake the numerical modelling, these being Plaxis v6.1 and FLAC 2D v3.40. Both FEM packages utilised two dimensional models with integrated discontinuities and assume an infinite slope scenario.

FEM models allow some prediction of rock mass response to applied stresses by showing how the theoretical stresses vary in response within the model. Outputs from various models include deformed grids, displacement vectors and stress contours.

5.4 Plaxis

Plaxis v6.1 was used as an initial approach to finite element modelling of a mountain massif with incorporated defects. Plaxis v6.1 is a DOS based programme that required an older computer with a specific internal architecture in order to run. DOS emulators were tried but proved to be ineffective. Outputs from the program were consequently limited as they were designed for use with specific plotters although several figures were extracted and prepared as jpg files by using a plot simulator. Even though the programme version was old in technological terms the abilities of the Plaxis programme were more than adequate for the models proposed, and many of the algorithms are still in use in newer versions.

Plaxis v6.1 models are limited to a total of 50 elements and so only very basic grids could be constructed. These basic models were used as a first pass to assess if antiscarps could be reproduced within numerical models, with the forward plan being to undertake further modelling with a more modern FEM programme if successful.

5.4.1 Grid construction

One grid was developed for the modelling of a plane strain model and was constructed so that the model could be tested for both a massif under gravity and also as a massif with a large volume removed.

The model massif had a 45° slope and incorporated one defect set with a dip of 65° (Figure 5.17). Discontinuities were built into the model along the interfaces between adjacent polygons, where the boundary between the two polygons represents a discontinuity and shear parameters can be applied.

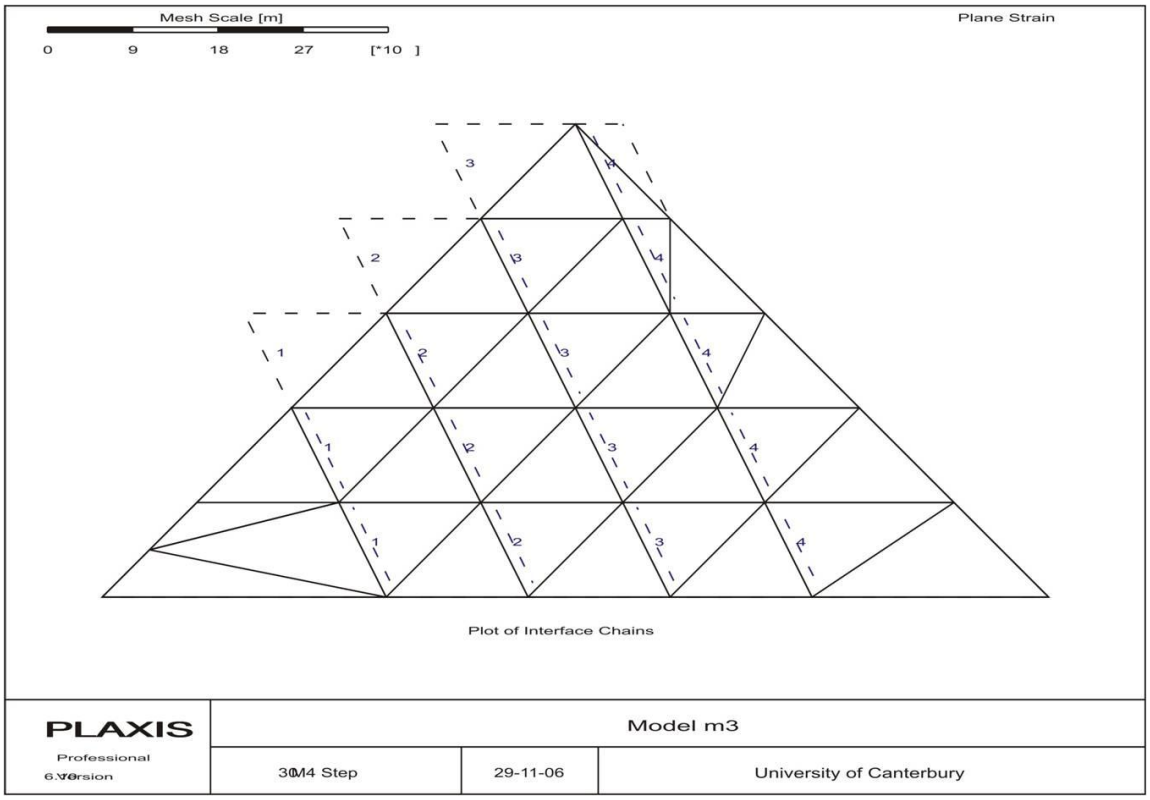

Figure 5.17: Plaxis cross-section developed using version 6.1. The dotted lines represent the polygon boundaries and have been assigned low shear strength values to simulate discontinuities within the model. Where the dotted lines extend beyond the model is an artefact of the model and reflects null zones associated with the construction of the original polygons.

Plaxis automatically generated the elements, also known as the mesh, within the polygons. A 15-node element was used in the analyses to increase the sensitivity of the coarse grids created in the version of Plaxis used here and is equivalent to four 6-node elements.

The completed grid had a total of 38 elements, 4 of which were null values that were required for the initial construction of the grid but are not utilised in the model calculations.

The boundary conditions for the model assume that there is no deformation of the base and that the corners of the models are fixed and as such will not move.

5.4.2 Material values

A Mohr-Coulomb model was used to represent the material properties in the FEM. This model requires five parameters; Young's modulus (E), Poisson's ratio (v), the friction angle (φ), and a dilatancy angle (ψ). A strength reduction factor (R_{inter}) and a real interface thickness (δ_{inter}) is applied to the interfaces to simulate low values of friction and cohesion. Typical values for the material properties used in the Plaxis models are presented in Table 5.1.

Table 5.1: Typical Plaxis model input values

Property	Value
Young's Modulus (E)	7×10^7 kN/m^2
Poisson's ratio (v),	0.3
Cohesion (c)	100 kN/m^2
Friction (φ)	30°
Dilatancy angle (ψ)	0°
Interface strength (R_{inter})	0.5
Real interface thickness (δ_{inter})	0

Different iterations of the models utilised different material values. Some models were designed with material properties that allowed the mesh to deform plastically with very little shear strength assigned to the interfaces to allow the mesh to deform easily and exploit the modelled discontinuities. Antiscarp forming displacements were also observed in models based on stiffer materials but due to the scale of the displacement they were difficult to see without zooming in or using a displacement contour plot.

5.4.3 Plaxis gravity models

Gravitational acceleration was set to the default value of 9.8 ms^{-2} and is directed coincidental to the negative y-axis to simulate the load acting on the massif.

A deformed mesh output is presented in Figure 5.18 and depicts antiscarps having formed on the left slope in response to deformation within the material inducing movement along the modelled discontinuities. The response is exaggerated in this figure due to the low values used to model the rock mass by comparison to typical values for an R5 rock.

5.4.4 Plaxis volume removal models

A secondary objective for the modelling was to assess the model response to the removal of a large volume of material to emulate cirque development. Figure 5.19 presents a deformed mesh that has tested the removal of a large section of the massif and uses the same rock mass

properties as the previous model. The base of this model was also fixed and no point along the base was allowed to deform.

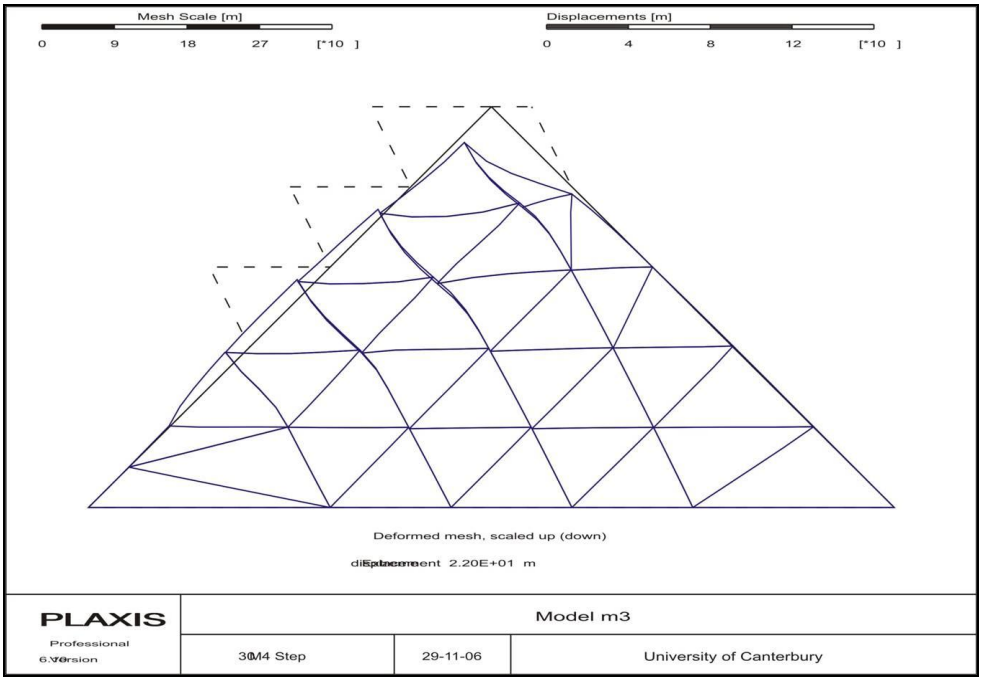

Figure 5.18: Deformed mesh output from Plaxis. Antiscarps have formed on the left slope and exploit the discontinuities.

Although the massif and cirque morphology are idealised the resultant deformation is considered to be representative of what could feasibly be expected. There is bulging of the slopes on both sides of the model with the peak rotating towards the right as the material moves towards the zone of free air left by the removed section of the massif.

Poorly developed antiscarps are apparent on the left slope and are aligned with the discontinuities.

Both of the Plaxis models indicate that low shear strength discontinuities and a material that is able to deform under gravity both contribute to the formation of antiscarps. The coarseness of the mesh available in Plaxis v6.1 produces low resolution model outputs relative to the scale of the massif that is being modelled.

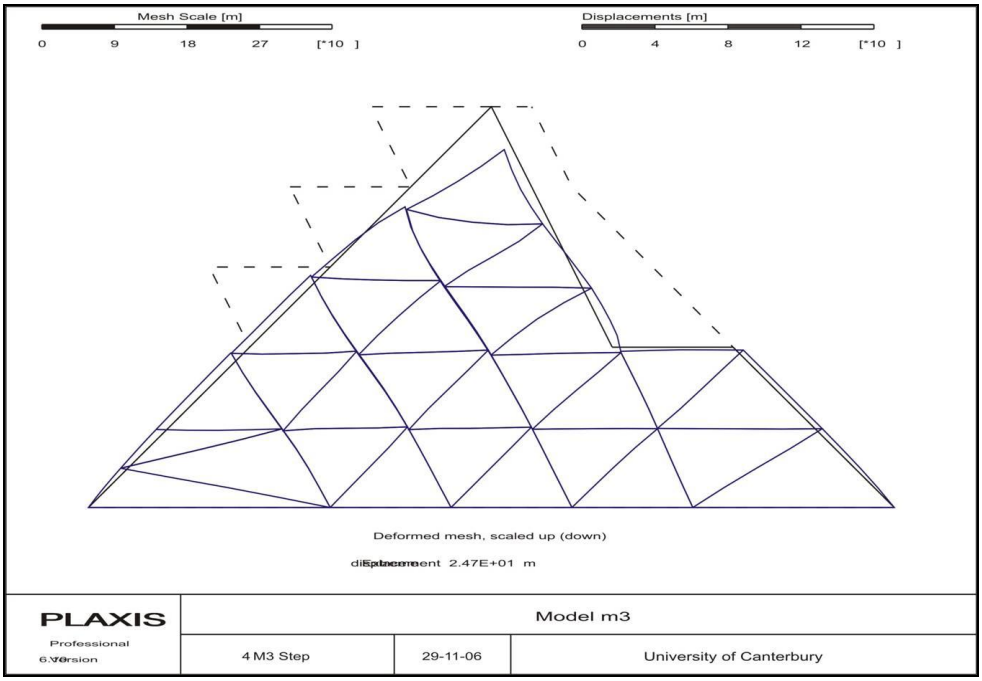

Figure 5.19: Deformed mesh output from Plaxis where the model has been constructed to assess the response of the massif to the removal of a large volume of material.

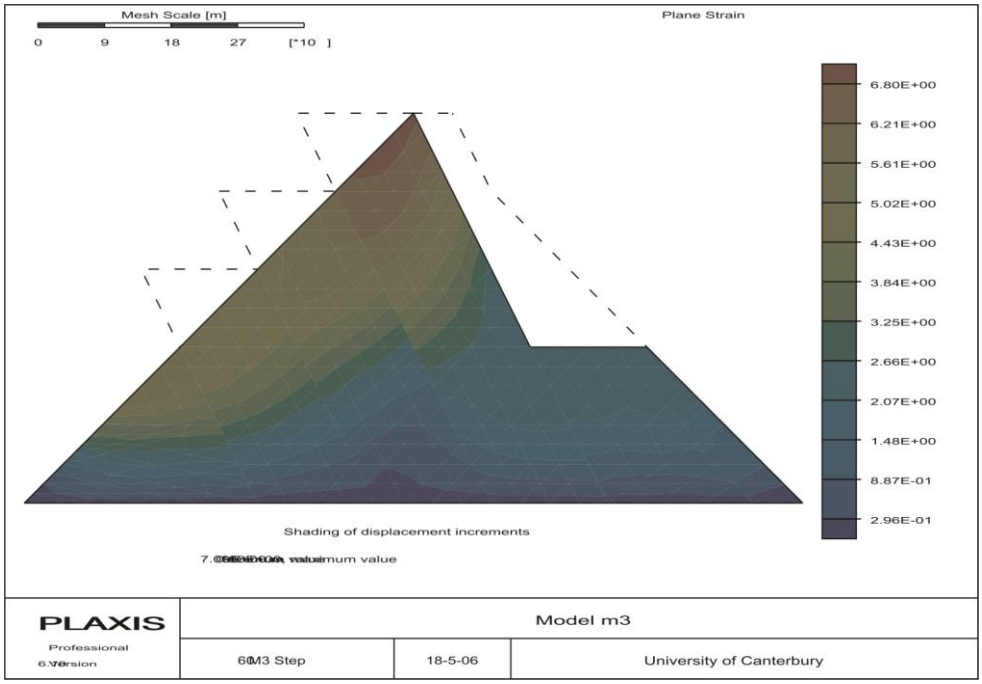

Figure 5.20: Displacement contours are shaded within the original mesh without any deformation applied to the mesh itself. Displacement decreases downslope with the majority of the movement occurring adjacent to the ridge.

5.5 FLAC 2D

FLAC 2D finite element modelling was undertaken in an effort to extend upon the data developed using the Plaxis FEM programme. FLAC modelling was undertaken at the University of Otago and utilised the copy of FLAC 2D v3.40 within their department. The decision to use FLAC was based on its ability at the time to be able to model with a much larger number of elements than Plaxis allowing greater resolution within the model. Only a gravity model was constructed using FLAC, no cirques were modelled.

5.5.1 Grid construction

The FLAC model was a symmetrical FEM that was based in part on aspects of the Kelly Range with the incorporation of a discontinuity set dipping at 60° and utilises 25º slope angles. A series of polygons were designed to create the outer boundary of the model. No internal material boundaries were required as the model was based on a homogeneous material.

Interfaces were then incorporated by using a coordinate system to locate them within the model. Several iterations of the model attempted to use ubiquitous joints to provide a second orientation of weak planes to accompany the constructed interfaces. The ubiquitous joint models allow the user to add an element of anisotropy to the model by embedding penetrative weak planes at a specific orientation. Unfortunately these models were unable to run and the error could not be isolated.

The mesh was then generated and material properties assigned.

5.5.2 Material values

A Mohr-Coulomb material was utilised for the modelling. The properties required by the FLAC models are different from those used in the Plaxis models and are presented in Table 5.2.

A large cohesion value was used to force initial elastic behaviour within the material and prevent slope failure when initialising the gravity stresses.

5.5.3 FLAC Gravity models

The output taken from the FLAC 2D models is that of a displacement vector (Figure 5.22). While there is no actual deformation of the grid to form antiscarps their presence can be inferred from analysis of the displacement vectors, where the sense of displacement is indicative of toppling. The direction of the flexural topple relative to the low shear strength interfaces would form antiscarps.

Table 5.2: Typical material properties associated with the FLAC model. Properties were constantly varied across models.

Property	Value
Bulk modulus	100 MPa
Shear modulus	30 MPa
Density	1500 kg/m3
Friction	20°
Cohesion	1.0×10^4 MPa
Tensile strength	1.0×10^4 MPa
Gravity	9.81m/s2
Young's Modulus (E) - Torlesse	70GPa

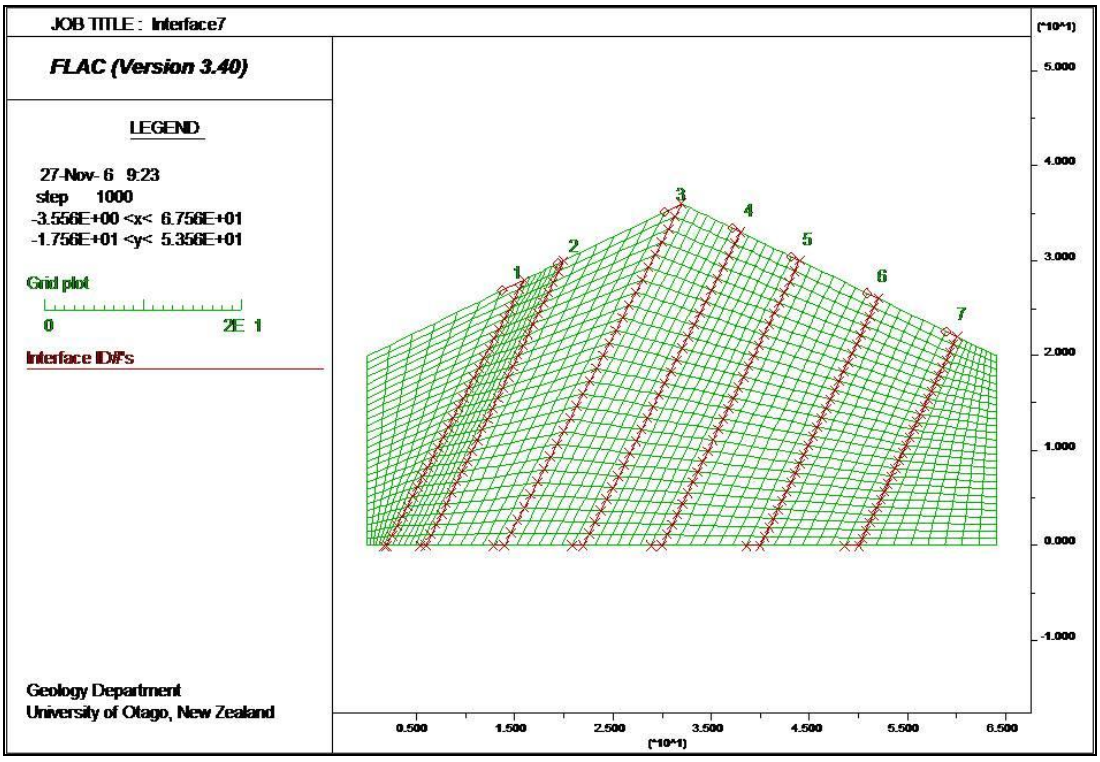

Figure 5.21: Meshed FLAC model with the interfaces used to simulate discontinuities outlined in red.

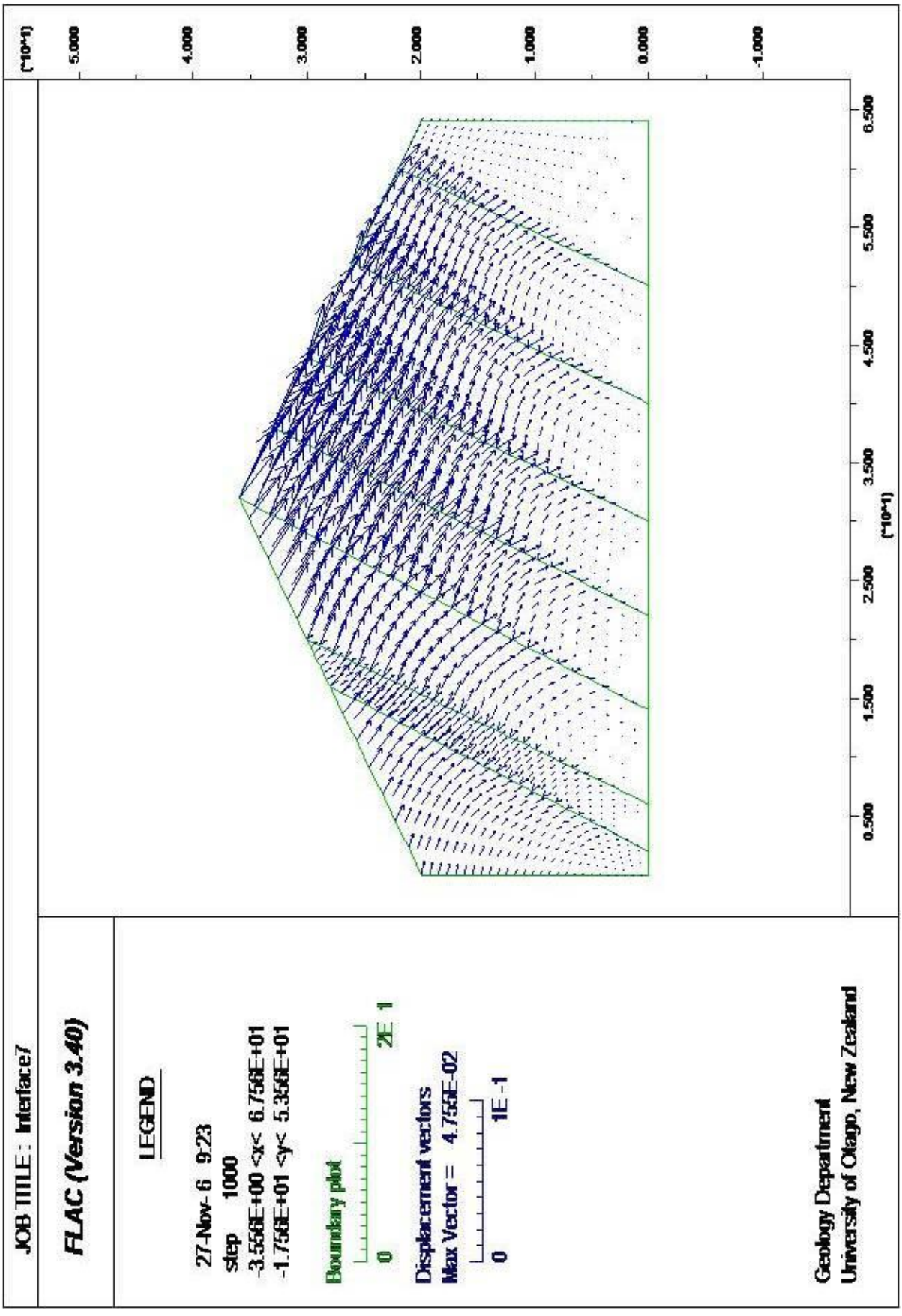

Figure 5.22: Displacement vectors indicative of a toppling style of slope deformation.

5.6 Numerical modelling summary

Numerical modelling using finite element models provided valuable information on the role of gravity in the formation of antiscarps. Even though the difficulties in getting sensible feedback from the models increased in line with the complexity of the model the data returned is robust.

It is difficult to represent small scale slope deformations when modelling. For example a 10m antiscarp on a 1000m high massif is the equivalent of having a feature that in size is only 1% of the actual model. The use of low density materials in some of the numerical model iterations was undertaken just to get the modelled massif to yield and create some deformation for analysis.

The material in both models is the equivalent of an extremely weak to weak rock suggesting R0 to R2 class rocks. In comparison to the R5 rocks that predominate in the observed field examples the weak rocks represented by the models would be less likely to be preserved in an alpine environment.

The ability to use only one discontinuity set was limiting in that many of the field examples typically had two discontinuity sets. This was a user limitation in the case of the FLAC models.

5.7 Modelling conclusions

Both the physical and numerical modelling undertaken here produced models that were able to generate antiscarp type deformations solely under a simulated gravitational load. The setup of all models used here was focused on achieving a well constrained qualitative outcome rather than on quantifying the scope of the parameters.

The two dimensional models utilised here were a simple approach and provided some base conditions that can be used to direct future approaches to modelling similar structures. The use of pliable materials in the base friction analyses may be able to provide better constraints on the internal deformations and the production of voids within the models.

The base friction models will never be able to be undertaken in 3 dimensions but with the constant improvements in computing power the application of 3D numerical models is becoming more common and programmes are more readily available. The modelling of large scale removal of material from a massif could benefit from being undertaken using a 3D model as it would allow insights into variability along a model massif to large scale perturbations.

6 Discussion

The aim of this section is to address the three approaches used in this study towards understanding antiscarp formation; these are antiscarp classification, identification of the primary antiscarp formative process, and antiscarp modelling. Some of the ideas and observations in earlier sections of this thesis are revisited and addressed here with comparisons made between the modelling, classification and field data.

During the course of this research programme on antiscarps numerous thoughts, observations, and queries were made and have contributed to the conclusions drawn. Limitations of the study are also identified and as with many studies there are new questions that are raised and new ideas are developed. Further areas of research arising from this study on antiscarps are identified and presented here

6.1 Antiscarp features and processes

6.1.1 Discontinuities

Discontinuities predate the surface expression of antiscarp features and are considered necessary for the formation of antiscarps because they provide a set of surfaces with lower shear strength parameters than the bounding rock material allowing them to be a preferential zone for movement.

A question that is raised is the relationship between discontinuity sets and the length of the antiscarps formed. Where the discontinuities are laterally persistent, for example a well formed bedding surface or schistosity, the expectation is that the antiscarps will also be of significant continuous length. Where the discontinuities have low persistence, for example a jointed granite or quartz diorite, then the expectation is that there will be multiple discontinuous antiscarps.

6.1.2 Post-glacial rebound

Post-glacial rebound is postulated as a viable mechanism for the formation of most of the antiscarps referred to in Chapter 4 in that it suggests that antiscarps form rapidly following deglaciation and they are likely to occur as single event displacements. Most of the antiscarps observed cut through or across glacial features implying that they post-date the last glacial maximum. The postulation that antiscarps are the product of a single event does not correlate

with the proposition by the majority of the authors in Chart 1 that antiscarps are likely to be related to processes that operate at the rate of creep.

Where an antiscarp is the product of post-glacial rebound it can be inferred that the rock material within which the antiscarp has formed is highly resistant to erosion and degradation because of the length of time that it has been exposed. Typical field estimated strength of the rock material within which antiscarps were observed was R5 (Table 2.1), which is indicative of a very hard rock material.

6.1.3 Seismicity

Seismicity is not a necessary factor for the formation of antiscarps and is not deemed to be a significant factor either. While there may be some reactivation or induction of movement associated with a seismic event there is no need or requirement to have a seismic input for most antiscarps to form. The key exceptions are surface ruptures or fault scarps that have an antiscarp morphology.

Antiscarps are an unreliable proxy for use as paleoseismic indicators and it is not recommended to adopt them as such without first ascertaining that they are indeed the product of coseismic activity. The main argument against a seismic relationship for the formation or evolution of most antiscarps is that the seismically-related antiscarps typically have a singular trace associated with a fault surface, or produce ridge rents with a low amplitude antiscarp, if any (Chart 1). There are few modern analogues for relating antiscarp formation or evolution to seismic events and those that do are fault traces or ridge rents.

Practitioners should exercise caution when considering the seismic significance of antiscarps, and investigation techniques similar to those used in the paleoseismic study of tectonic faults should be adopted prior to assigning a seismic source (McCalpin 1999). It is not recommended to use antiscarps as an indicator of seismicity nor should they be perceived as representative of a hazard without detailed investigation.

6.1.4 Ridge rents

Ridge rents are a feature that have been associated with seismic activity and where observed they often exhibit small displacements, in the order of centimetres. While there is a possibility that over time they may evolve into larger-scale antiscarps there is no evidence thus far to support such a proposition. It is highly likely that ridge rents do not develop far

beyond minor vertical displacement unless they are the initial expression of a fault that has undergone, or will undergo, further movement.

The ability to gather observations on this possible phenomenon is limited by the frequency of the event and the need for a baseline to build successive measurements upon. Further complications arise where slope processes occur at a greater rate than any movement on the ridge rent and either obliterate or mask them.

6.1.5 Cirques and large scale volume removal

Cirques appear in a massif as an area where there has been a large volume of material removed by glacial activity. Numerical models indicate that antiscarps can develop on the opposite side of a ridge as the massif responds to the removal of the mass by relaxing into the created void. The presence of cirques is indicative that the massif has undergone some glacial activity. Caution should be taken to ensure that the antiscarps formed are related to the cirque and not to post-glacial rebound. If there are other related antiscarps along the slope of a similar scale that do not have a relationship to any cirque, or large scale removal of material, then the antiscarps are probably associated with a different process.

6.1.6 Rock mass homogeneity

All the field studies and all of the modelling were from, or were based on, homogeneous massifs. Antiscarps related to processes such as sackung or spreading, where a less competent lower unit is required, were neither observed nor modelled during the course of this study. There are higher levels of complexity associated with modelling heterogeneous materials that could not readily be incorporated into the modelling undertaken here.

6.2 Movement rates and exposure time

There is a large window of time within which the antiscarps assessed in this study were considered to form, this being sometime since the last glacial maximum. There is also no constraint on whether the movement is a singular event or if it is ongoing.

The lack of any distinct chronological markers means that any time constraints are often taken from associated features such as the offset of a glaciated surface or of a dated fault scarp. The poor constraint on timing of antiscarp formation and on any associated ongoing movement rates, or periodicity, poses problems for constraining antiscarp evolution. It is difficult to understand the roles of different processes and their levels of input when there is

often no ability to determine whether the antiscarp is a singular event or the product of creep or episodic movement.

The antiscarps observed in the field studies are thought to be the product of a single event, or a series of events within a short time frame, and the different formative processes operated while the massif was going through a cycle of strain recovery shortly after a deglaciation event. The rate of antiscarp formation on the geometric block base friction models indicate that the majority of the movement is generated at the onset of the gravity loading and dissipates very quickly with only minor amounts of ongoing displacement observed as sliding of the model progressed. The geometric block base friction model supports the proposition that antiscarps are primarily related to a single event displacement.

Where antiscarps are formed by a single event there are rock mass properties required that must be associated with the massif upon which the antiscarps have formed. These are that the rock material must be durable enough to maintain the antiscarp profiles for the period of time since deglaciation, and also that the material needs to have an elastic component to generate the rebound. As outlined in section 6.1.2 the majority of the rocks within the field study areas where antiscarps were observed have field estimated strengths of R5 and so should have a high level of resistance to erosion or degradation.

Tarns that form adjacent to antiscarps are identified in many of the field sites. Trenching of these tarns may provide some constraints on the timing of events associated with the formation of the antiscarps, any ongoing rates of movement, and the response of the antiscarp to seismic events.

6.3 Antiscarp evolution

The Kelly Range and Beinn Fhada field examples have been instrumental in the development of ideas on antiscarp formation and evolution. The following section provides a brief discussion on the proposed evolution of the antiscarps at these two localities.

6.3.1 Kelly Range example

Figure 6.1 is a schematic representation of a proposed mode of evolution for antiscarps at the Kelly Range locality in Arthurs Pass, New Zealand (refer Section 4.1).

Part A of Figure 6.1 is a representation of a possible initial condition for the Kelly Range during the last glacial maximum where the glaciers have overwhelmed the massif across the

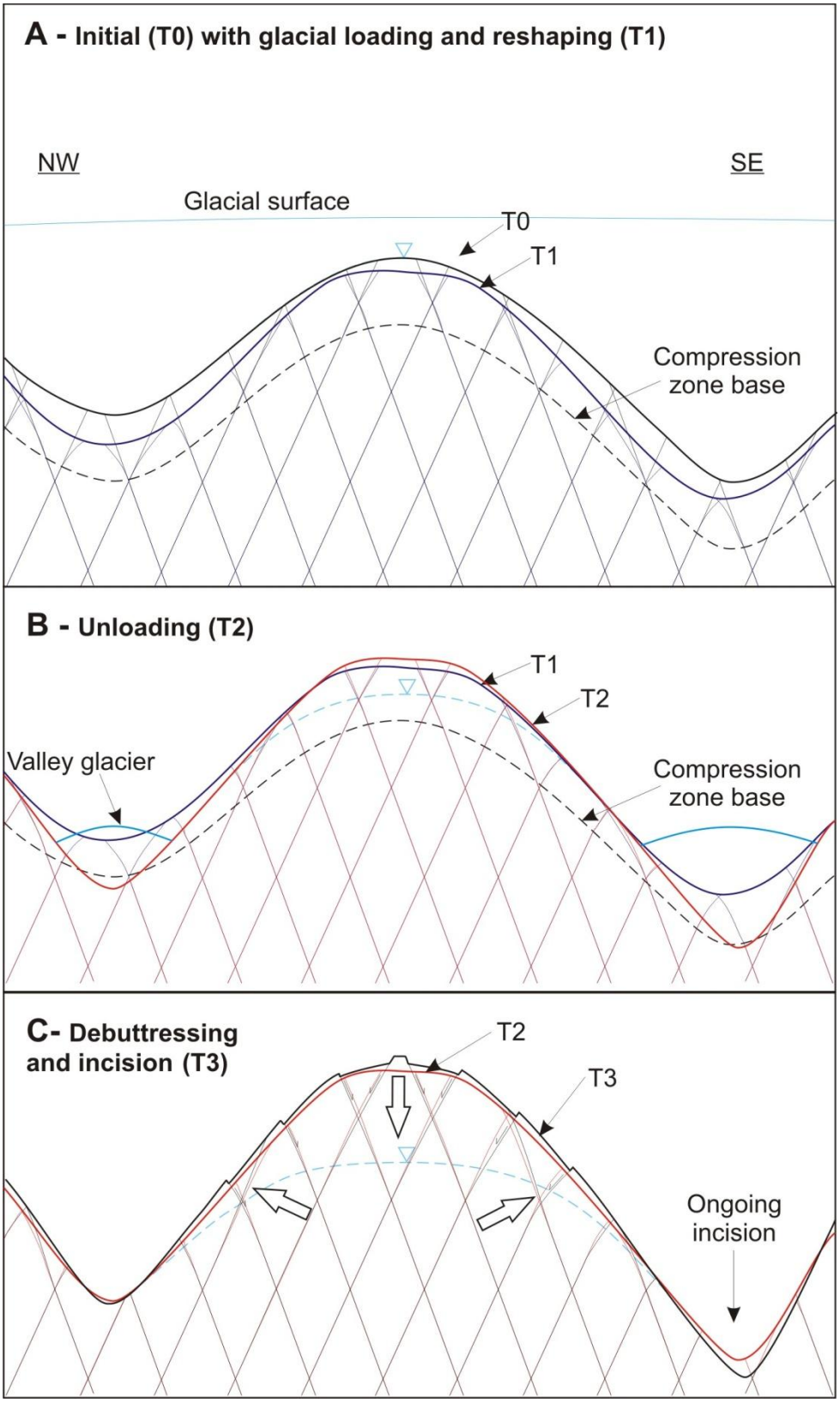

Figure 6.1: Schematic of antiscarp evolution from the Kelly Range.

a smoothed ridge profile, slopes steepened by glaciation and a net shrinking of the massif representing the elastic component of the deformation induced by the glacial load. A lower

saddle and for the section south of the main peak. T0 is the initial surface with T1 illustrating bound surface has been used to represent the depth at which the glacial loading is considered to not significantly impact upon the massif with all deformation occurring in the zone above. The two intersecting joint sets observed in the field studies are represented here with the folding of the T1 discontinuities based on a combination of compression and removal of material from the massif during glaciation. Movement and readjustment of the massif is accommodated along the discontinuities throughout the compressive phase of deformation. The massif is considered to be fully saturated with the water table at the surface at this point in time. The colour used for the discontinuities for each of the time steps is matched to that of the respective surface colour.

The surface for T2 presented in Part B is used to represent a time when the main glacial event has finished and there are still smaller glaciers within the valleys that are continuing to incise the valley systems, oversteepen the lower slopes in the process, and will still provide a buttressing effect to the toe of the adjacent slope. The main load has been removed from the upper section of the massif and there has been some recovery of the elastic component of the deformation. The movement associated with the post-glacial rebound is proposed to be accommodated along the discontinuities. The discontinuities have now accommodated movement both during the compression and unloading phases and are now preconditioned as the most likely path for future movement. The water table is lower but is still elevated and will generate high pore pressures in the mid to lower slopes which will contribute to overall slope instability.

The T3 surface has antiscarps formed on both sides of the massif. Incision has been continuous and has oversteepened the slopes and the cessation of glaciation in the valleys has removed the buttress from the slopes. The post-glacial debuttressing in concert with ongoing post-glacial rebound has allowed the massif to relax outward with a graben forming along the ridge. The large arrows within the massif indicate the broad sense of movement of different parts of the massif in response to the gravity driven graben driving lateral movement in the lower section which is also responding to the debuttressing. The sense of motion of the discontinuity bound blocks at the slope surface is based on observations taken from the base friction modelling of the pattern blocks where there was similar rotation of elements out of the slope. In Figure 6.1 the elements are deformed with no obvious voids incorporated or required. The lateral movement within the massif is also in accordance with the results taken

from the numerical models. The water table has lowered in line with surrounding base levels and is no longer considered to have a significant impact on slope stability.

6.3.2 Beinn Fhada example

A schematic representation of the proposed evolution of the antiscarps at Beinn Fhada is produced in Figure 6.2 with the following text referring to the diagram. The different values of T in the diagram represent different time steps with T0 being the initial and T3the final.

T0 represents a proposed initial condition prior to the last glacial maximum where sheet glaciation covered the entire massif. During the emplacement of the ice sheet the bounding valleys were deepened by erosion and also compressed by loading. Compression of the rock mass by the glacial load has been maintained in the upper section of the massif where it is postulated that deformation did not go beyond the base of the compression zone. The discontinuities representing the foliations within the rock mass bend during the compression phase. T1 represents the cross-sectional profile at peak load. The water table is considered to be at the surface.

Following and during deglaciation the recoverable elastic component of deformation within the compression zone is recovered to bring the slope profile to that of T2. Flexural slip along the foliation is likely to occur and weakens and preconditions the rock mass for failure along the discontinuities. The elevated water table raises pore pressures within the massif and assists in driving the rock mass to failure especially now that the glacial buttress has been removed. Glaciers in the valleys and on the slopes continue to remove material from the massif and can oversteepen the slopes and also produce cirques.

T3 represents a mass wasting event, in the case of Beinn Fhada this is considered to be the formation of a series of extremely large cirques on the northern flank. The stress differential created by removing the large volume of material from the slope allows movement from the lower section of the massif as it equilibrates. Antiscarps form on the southern slope in response to the stress adjustment and overall movement in the massif to the north. The antiscarp faces are the foliated surfaces preconditioned during the compression and unloading. In the early stages of the mass wasting process the water table will still be elevated and will contribute to destabilising the massif but will continue to drop over time.

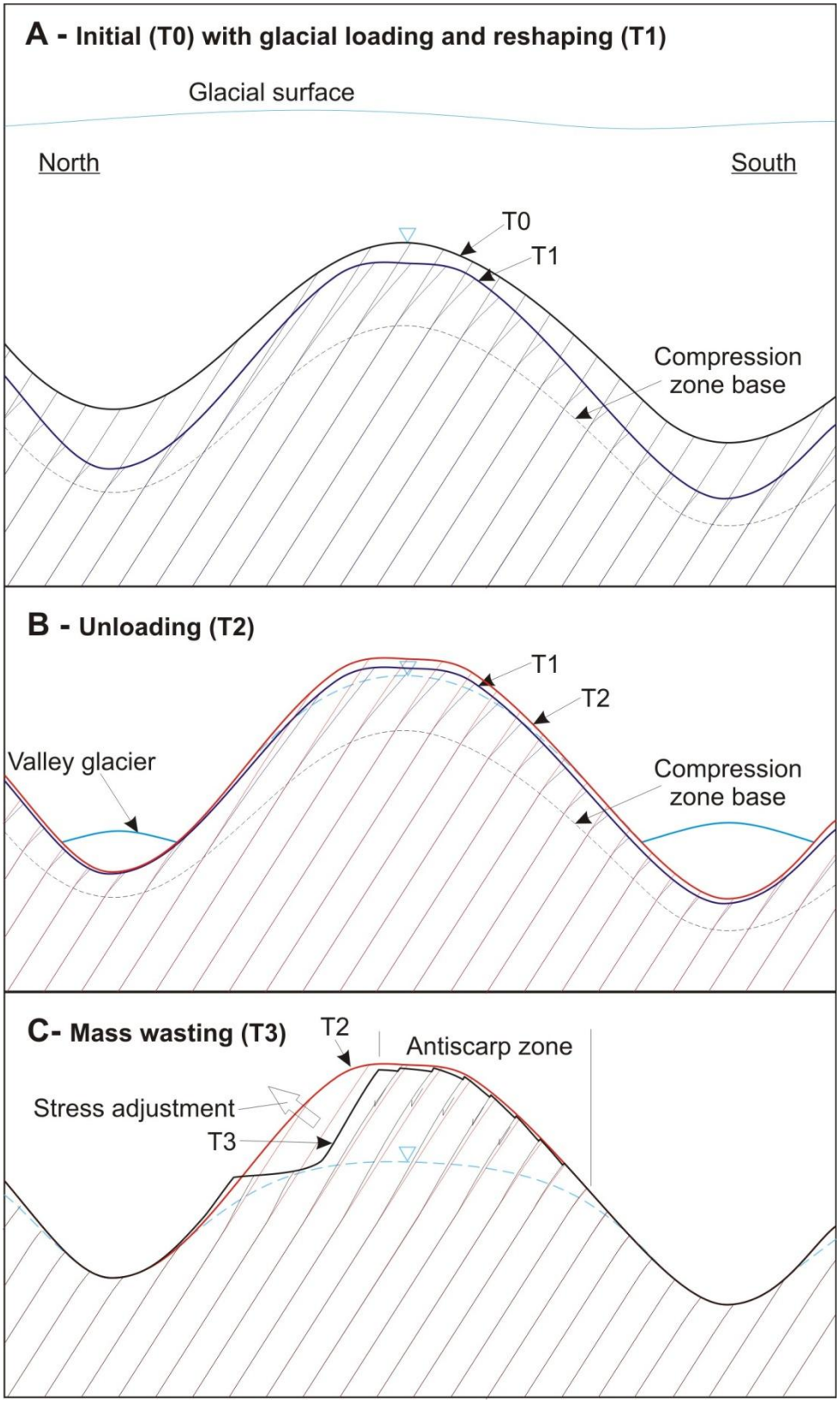

Figure 6.2: Evolution of antiscarps at Beinn Fhada.

6.4 Antiscarp classification

The collation of the antiscarp-related literature assisted in providing a broad summary of the multiple and various conditions under which antiscarps may form. The side-by-side comparison of the contributing factors for antiscarp formation as presented in Chart 1 has been beneficial in helping to understand the subtle differences between the different processes. The aim of using antiscarp as a geomorphological term that can be further defined by adopting a process based term, where the processes can be identified, has been successfully achieved. The presentation of this proposed classification now requires peer review to ascertain the rigour of the divisions made and to encompass different perspectives on the categorisation of antiscarp processes.

The antiscarp formational process flowchart constructed and presented in Chapter 3 was successfully applied to all of the field study areas presented in Chapter 4. The flowchart is based on values and observations taken from an extensive literature review so its successful application to field based-examples is an initial verification of its suitability for the identification of antiscarp formative processes. The true test of the veracity of the flowchart will be its application to previously unreported or unexplored antiscarps prior to field investigations.

6.5 Field studies

While only a limited number of the possible processes have been observed, a conscious effort was made to ensure that antiscarps that were observed in the field were addressed without bias. The application of the antiscarp formation flowchart to the antiscarps observed in the field studies undertaken in New Zealand and Scotland allowed all possible processes to be identified, but due to the qualities inherent to the locations visited, only gravity faulting and unloading processes were encountered. It was not possible to visit enough sites to allow observation of the full suite of antiscarp processes as part of the field study programme.

6.6 The role of gravity

Models indicate that it is possible for antiscarps to form solely under a gravitational load. This observation from the modelling is a qualitative one and is difficult to quantify because in most cases it is unlikely that gravity is working in isolation The models used were unable to incorporate the level of complexity required to be able to test the role of multiple factors and so are only able to provide a base condition.

6.7 Water

Water is a key factor in slope stability analyses and it is likely that elevated water tables will assist in driving slope instability. The water tables presented in the evolution of the antiscarps in Figure 6.1and Figure 6.2 are elevated in both scenarios in the early periods of deformation within the massif. Many observations on the timing of antiscarp formation regard them as being a feature that formed soon after the last glacial maximum and that they often have not moved significantly since their initial flourish. The fact that water tables are elevated during the peak period for antiscarp formation is not coincidental but there do need to be other factors such as discontinuities conducive to movement within the massif, seismicity, or oversteepened slopes to exploit the water.

6.8 Future work

Further work has been identified by this study as being able to provide better constraints on the data that is available and also on the data that has been used and is presented here.

6.8.1 Trenching of tarns

The poor constraints on timing may benefit from the trenching of antiscarp-related tarns for chronostratigraphic information. In some tarns there may even be the possibility of getting a varve count which would provide a minimum age for some antiscarp structures.

Any trenching should also be undertaken with a focus on identifying any paleoseismic indicators such as displaced or truncated stratigraphy, soft sediment deformation, and gravel or cobble horizons indicative of a proximal sediment source. At present there is no correlation between the antiscarps observed in the field studies and seismicity and it is envisaged that trenching for paleoseismic data will provide firmer constraints of the role of seismicity in antiscarp formation and evolution.

6.8.2 Numerical modelling

The numerical modelling undertaken as a part of this study was very basic with the sole focus on assessing whether or not antiscarps could form under a gravity load both with and without the removal of large volumes of material.

With advances in both computing power and also in how numerical modelling can be applied to large-scale problems it is considered that a more thorough analysis of antiscarp formation can be undertaken. Models now are able to better utilise greater levels of complexity such as

improved definition of joint sets, the application of several different loads (e.g. a constant far field tectonic load coupled with a transient glacial load), and multiple material properties much more readily than their earlier counterparts.

Numerical modelling could be targeted towards different aspects of antiscarp formation such as the modelling of sackung-style slope deformations that require two distinct material properties, or even dynamic modelling to simulate repeated seismic loading of a massif.

There is also scope to assess the response of a massif to cycles of glacial loading and unloading with a focus on understanding the role of post-glacial rebound.

6.8.3 Physical modelling

Some thought was given to constructing a physical model that was able to expand in such a way that it would simulate the response of a massif to post glacial unloading and replicate strain recovery and/or rebound adjustment. Ideas included the use of a swelling material that would expand when wet and using an inflatable sac or balloon encased within a deformable material to elicit a volume increase.

While such a model was not constructed as a part of this study it is considered that an expanding model may be able to provide some insight as to the location on the slope that deformations are most likely to occur and also whether antiscarps will actually form under such a scenario.

7 Summary and conclusions

7.1 Study objectives

Two key objectives have been the focus of this study. These are:

1. to provide a systematic approach to identify and communicate antiscarp features and the related processes, and to facilitate the identification of the primary antiscarp formative process; also

2. to assess the role of gravity in antiscarp formation and to determine whether they can form solely under gravity using physical and numerical models.

These objectives are now addressed and conclusions drawn from them.

7.2 Literature review and antiscarp classification

The review of literature related to antiscarp occurrences and associated processes was undertaken in order to gather as much information as possible and to understand how the current nomenclature is being used. Several terms are used in a such a way that their meaning has become dilute and they were being used to explain phenomena beyond their original intent. In particular is the term “sackung” which is where antiscarps form in response to plastic deformation in an underlying less-competent unit (Zischinsky 1966). Sackung has progressively been used to describe antiscarps that are related to other types of slope deformation such as spreading, translational failures, rotational failures, sliding on high angle fault surfaces, reactivation of pre-existing fractures, oversteepening by incision, toppling, reactivation of conjugate tectonic faults, and surface rupture of a fault trace (Beget 1985; Savage and Varnes 1987; Varnes et al. 1989; Sorriso-Valvo et al. 1999; Ferrucci et al. 2000; Varnes et al. 2000; Agliardi et al. 2001; Kellogg 2001; Schwab and Kirk 2002; Jibson et al. 2004; Rizzo and Leggeri 2004; Hippolyte et al. 2006). The term antiscarp has been introduced in this study as a way to counter the use of key terms being used to represent more than the processes that they were originally based on. An antiscarp is defined here as any uphill-facing scarp that is observed within the landscape and as it solely addresses uphill facing scarps as a morphological feature there is no specific process implied. Antiscarp has not been defined in any of the literature researched in line with this project and it is likely that this is the first time that a definition has been provided for its use. The adoption of a

morphological term as a descriptor for uphill facing scarps gives greater explanatory power to the process-based terminology when it is correctly applied to features that have been formed by that process.

It was decided to classify antiscarps by the primary process under which they formed because in general most antiscarps are already being referred to by specific process-based terms. The key processes are presented in Chapter 2, and where possible the terminology currently in use was retained and clear definitions provided for their ongoing application. The key processes were integrated into a chart (Chart 1) which enabled comparisons to be made across a number of different factors that were identified during the review as being related to antiscarps.

A flow chart was developed to assist in identification of the probable formative process for antiscarps. Application of the flowchart to field study areas indicate that it is robust and is acceptable as a first approach to determining the dominant antiscarp forming process.

The key outcomes from the literature review are:

- the extraction of important antiscarp related terms from the available literature and presentation within Chart 1,
- the introduction of antiscarp as a morphological term for the description of uphill facing scarps and clear definitions for the scope of existing terms, and
- the production of a flowchart that enables the identification of the primary antiscarp formative process.

7.3 Field studies

Antiscarps were identified and studied in multiple sites in the South Island of New Zealand and in the Highlands of Scotland. Gravity faulting and unloading are the two key processes that were observed at all of the localities studied.

All areas showed signs of extensive glaciation in the past with the ridges on all of the observed massifs indicating that they had been under ice at some stage and all slopes also showing signs extensive glacial modification.

An estimated field strength of R5 was observed for rocks at all study localities regardless of lithology.

The main difference between the observed massifs was the massif symmetry, or asymmetry, and the removal of large volumes of material at some localities. Typically the asymmetric massifs had either been subject to widespread cirque development (both Ben Each and Beinn Fhada) or to extensive incision creating oversteepened slopes (both Lewis Tops and Stag Hill). Only the Kelly Range example could really be referred to as a symmetrical massif.

Application of the primary formative process flowchart was in agreement with observations made at each of the study areas as to the main process associated with the antiscarps observed.

The Kelly Range was utilised as a basis for idealised models to test the potential for the gravity faulting postulated by Beck (1968). Similarly some models were based on the asymmetric massif of Beinn Fhada to test the effect of removing large volumes of material.

7.4 Modelling

Base friction modelling and finite element modelling (FEM), using Plaxis and FLAC 2D, was undertaken to assess if antiscarps can form solely under gravity. The FEM were also used to evaluate the response of a modelled massif that incorporated a cirque.

The base friction models were constructed using a variety of different shaped elements such as circles, hexagons, and diamond shaped blocks to form the models. Antiscarps formed in all of the models tested that had modelled the dip of discontinuities of 60°. The antiscarps that displayed the most obvious displacement were the diamond blocks, probably due to the more regular failure surface. Some of the antiscarps that formed in the circular-element models were difficult to see.

The meshes constructed and tested in the FEM incorporated one discontinuity set and all returned deformed grids or vector displacements that represented the formation of antiscarps when solely under a gravitational load.

The mesh that was used to model the massif with the cirque also displayed significant deformation of the mesh where there was movement out of the massif into the area where the cirque had been cut. This model too was tested solely under a gravitational load.

7.5 Key outcomes

The key outcomes of this study are:

- the introduction of the term antiscarp and the associated literature review where key factors relating to antiscarps are extracted and collated to form Chart 1,
- the provision of key definitions for the application and scope of identified antiscarp formational processes,
- the construction of a flowchart that assists in identifying the primary process for the formation of antiscarps, and the successful application of the flowchart to field study areas,
- identifying that antiscarps can form solely under gravity based on both physical and numerical modelling.

8 References and bibliography

Adhikary, D. P., et al. (2001). "A numerical study of flexural buckling of foliated rock slopes." International Journal for Numerical and Analytical Methods in Geomechanics **25**(9): 871-884.

Agliardi, F., et al. (2001). "Structural constraints on deep-seated slope deformation kinematics." Engineering Geology **59**(1-2): 83-102.

Agliardi, F., Crosta, G.B., Zanchi, A., and Ravazzi, C., 2009, Onset and timing of deep-seated gravitational slope deformations in the eastern Alps, Italy: Geomorphology **103**, p. 113-129.

Aksoy, H. and M. Ercanoglu (2007). "Fuzzified kinematic analysis of discontinuity-controlled rock slope instabilities." Engineering Geology **89**(3-4): 206-219.

Ambrosi, C. and G. B. Crosta (2006). "Large sackung along major tectonic features in the Central Italian Alps." Engineering Geology **83**(1-3): 183-200.

Amoruso, A., et al. (2005). "Faulting geometry for the complex 1980 Campania-Lucania earthquake from levelling data." Geophysical Journal International **162**(1): 156-168.

Apuani, T., et al. (2007). "Stress-strain-time numerical modelling of a deep-seated gravitational slope deformation: Preliminary results." Quaternary International **171-172**: 80-89.

Arnadottir, T., et al. (1995). "Deformation associated with the 18 June 1994 Arthur's Pass earthquake, New Zealand." New Zealand Journal of Geology and Geophysics **38**: 553-558.

Augustinus, P. C. (1995). "Glacial valley cross-profile development: the influence of in situ rock stress and rock mass strength, with examples from the Southern Alps, New Zealand." Geomorphology **14**(2): 87-97.

Bachmann, D., et al. (2004). "influence of weathering and pre-existing large scale fractures on gravitational slope failure: insights from 3-D physical modelling." Natural Hazards and Earth System Sciences (NHESS) **4**(5/6): 711-717.

Ballantyne, C. K. (2002). "Paraglacial geomorphology." Quaternary Science Reviews **21**(18-19): 1935-2017.

Baron, I., et al. (2005). "Numerical analysis of deep-seated mass movements in the Magura Nappe, Flysch Belt of the Western Carpathians (Czech Republic)." Natural Hazards and Earth System Sciences (NHESS) **5**(3): 367-374.

BCHF_Ltd. (1994). Otira Viaduct and Approaches - Geotechnical Report, prepared for Transit NZ by Beca Carter Hollings & Ferner Ltd., Christchurch.

Beck, A. C. (1968). "Gravity faulting as a mechanism of topographic adjustment." New Zealand Journal of Geology and Geophysics **11**(1): 191-199.

Beget, J. E. (1985). "Tephrochronology of antislope scarps on an alpine ridge near Glacier Peak, Washington, U.S.A." Arctic and Alpine Research **17**(2): 143 - 152.

Berardino, P., et al. (2003). "Use of differential SAR interferometry in monitoring and modelling large slope instability at Maratea (Basilicata, Italy)." Engineering Geology **68**(1-2): 31-51.

Bertolini, G., et al. (2005). "Landslides in Emilia-Romagna region (Italy): Strategies for hazard assessment and risk management." Landslides **2**: 302-312.

Bhasin, R., et al. (2004). "Insights into the deformation mechanisms of a jointed rock slope subjected to dynamic loading." International Journal of Rock Mechanics and Mining Sciences **41**(Supplement 1): 587-592.

Bhasin, R. and A. M. Kaynia (2004). "Static and dynamic simulation of a 700-m high rock slope in western Norway." Engineering Geology **71**(3-4): 213-226.

Bieniawski, Z. T. (1989). Engineering rock mass classifications : a complete manual for engineers and geologists in mining, civil, and petroleum engineering. New York, Wiley.

Bovis, M. J. (1982). "Uphill-facing (antislope) scarps in the Coast Mountains, Southwest British Columbia." Geological Society of America Bulletin **93**(8): 804-812.

Bovis, M. J. and S. G. Evans (1996). "Extensive deformations of rock slopes in southern Coast Mountains, southwest British Columbia, Canada." Engineering Geology **44**(1-4): 163-182.

Bray, J. W. and R. E. Goodman (1981). "The theory of base friction models." International Journal of Rock Mechanics and Mining Science & Geomechanics Abstracts **18**(6): 453-468.

Brideau, M.-A., et al. (2007). "Geomorphology and engineering geology of a landslide in ultramafic rocks, Dawson City, Yukon." Engineering Geology **89**(3-4): 171-194.

Bromhead, E. N. (2004). Landslide slip surfaces: their origins, behaviour and geometry. Landslides : evaluation and stabilization = Glissement de terrain ; evaluation et stabilisation. W. A. Lacerda. Leiden ; London, A. A. Balkema. **1:** 3-22.

Brook, M. S., et al. (2004). "Rock strength and development of glacial valley morphology in the Scottish Highlands and northwest Iceland." Geografiska Annaler. Series A: Physical Geography **86**(3): 225-234.

Brown, M. (1997). Engineering geology of the Kelly Range, Arthur's Pass National Park, South Island, New Zealand. New Zealand Geomechanics News. **54:** 43 - 45.

Brown, M. E. D. (1998). Structural and engineering geology of the Kelly Range, Arthur's Pass National Park, South Island. Geology department. Auckland University of Auckland

Bruckl, E. and J. Bruckl (2006). "Geophysical models of the Lesachriegel and Gradenbach deep-seated mass-movements (Schober Range, Austria)." Engineering Geology **83**(1-3): 254-272.

Brückl, E. P. (2001). "Cause-Effect Models of Large Landslides." Natural Hazards **23**(2): 291-314.

Cadoppi, P., et al. (2007). "Litho-structural control, morphotectonics, and deep-seated gravitational deformations in the evolution of Alpine relief: A case study in the lower Susa Valley (Italian Western Alps)." Quaternary International **171-172**: 143-159.

Chamberlain, C. G. (1996). Seismic hazard from cross-faulting in North Canterbury : Broader implications from the Arthur's Pass earthquake sequence of 18 June 1994. Department of Geological Sciences. Christchurch, New Zealand, University of Canterbury. **M.Sc. Engineering Geology:** 2 Volumes

Chemenda, A., et al. (2005). "Three-dimensional physical modeling of deep-seated landslides: New technique and first results." Journal of Geophysical Research **110**(F04004).

Chigira, M. (1992). "Long-term gravitational deformation of rocks by mass rock creep." Engineering Geology **32**(3): 157-184.

Chigira, M. and H. Yagi (2006). "Geological and geomorphological characteristics of landslides triggered by the 2004 Mid Niigta prefecture earthquake in Japan." Engineering Geology **82**(4): 202-221.

Clague, J. J. and S. G. Evans (1995). The role of geomorphology in assessing landslide potential and behaviour. International Symposium on Prediction of Rapid Landslide Motion, September 1995, Kyoto, Japan.

Clifford, T. N. (1957). "The stratigraphy and structure of part of the Kintail district of southern Ross-shire : Its relation to the Northern Highlands." Quarterly Journal of the Geological Society **113**(1-4): 57-92.

Clough, C. T., et al. (1909). "The Cauldron-Subsidence of Glen Coe, and the Associated Igneous Phenomena." Quarterly Journal of the Geological Society **65**(1-4): 611-678.

Clough, C. T. and W. Pollard (1899). "On Spinel and Forsterite from the Glenelg Limestone (Inverness-shire)." Quarterly Journal of the Geological Society **55**(1-4): 372-380.

Cook, G. K. (2001). Rock mass structure and intact rock strength of New Zealand greywackes. Department of Geological Sciences. Christchurch, New Zealand, University of Canterbury. **M.Sc. Engineering Geology:** 471 + 1 sheet.

Cossart, E., et al. (In Press (2007)). "Slope instability in relation to glacial debuttressing in alpine areas (Upper Durance catchment, southeastern France): Evidence from field data and 10Be cosmic ray exposure ages." Geomorphology **In Press, Corrected Proof**.

Cruden, D. M. and X.-Q. Hu (1999). "The shapes of some mountain peaks in the Canadian Rockies." Earth Surface Processes and Landforms **24**(13): 1229-1241.

Cruden, D. M., et al. (1993). "Rock topples in the highway cut west of Clairvaux Creek, Jasper, Alberta." Canadian Geotechnical Journal = Revue Canadienne de Geotechnique **30**(6): 1016-1023.

Dahle, H., et al. (2005). Numerical study of stability for the Oppstadhornet rock-slope failure. Landslides and Avalanches ICFL 2005, Norway, Taylor & Francis Group, London.

Davenport, C. A., et al. (1989). Geological investigations of late and post glacial earthquake activity in Scotland Earthquakes at North-Atlantic Passive Margins: Neotectonics and

Postglacial Rebound (NATO ASI series. Series C, Mathematical and physical sciences). S. Gregersen and P. W. Basham. **266:** 175-194.

Davies, T. R., et al. (2006). "Rapid block glides: slide-surface fragmentation in New Zealands Waikaremoana landslide." The Quarterly Journal of Engineering Geology and Hydrogeology **39**: 115-129.

De Freitas, M. H. and R. J. Watters (1973). "Some field examples of toppling failure." Geotechnique **23**(4): 495-513.

Di Luzio, E., et al. (2004). "Influence of structural framework on mountain slope deformation in the Maiella anticline (Central Apennines, Italy)." Geomorphology **60**(3-4): 417-432.

Dramis, F. and A. M. Blumetti (2005). "Some considerations concerning seismic geomorphology and paleoseismology." Tectonophysics **408**(1-4): 177-191.

Dramis, F. and M. Sorriso-Valvo (1994). "Deep-seated gravitational slope deformations, related landslides and tectonics." Engineering Geology **38**(3-4): 231-243.

Eusden, J. D., et al. (2000). "Structural evolution and landscape development of a collapsed transpressive duplex on the Hope Fault, North Canterbury, New Zealand." New Zealand Journal of Geology and Geophysics **43**(3): 391-404.

Fenton, C. H. (1992a). Holocene Seismotectonic Activity in the Area of Glen Shiel. Neotectonics in North West Scotland: A Field Guide. C. H. Fenton. Glasgow, University of Glasgow**:** 61-67.

Fenton, C. H. (1992b). Postglacial Faulting in Scotland: An Overview. Neotectonics in North West Scotland: A Field Guide. C. H. Fenton. Glasgow, University of Glasgow**:** 4-15.

Fenton, C. H. and P. S. Ringrose (1992). Glacio-isostatic Faulting and Paleoseismicity in the Area of Glen Roy. Neotectonics in North West Scotland: A Field Guide. C. H. Fenton. Glasgow, University of Glasgow**:** 41-53.

Ferrucci, F., et al. (2000). "Seismic prospecting of a slope affected by deep-seated gravitational slope deformation: the Lago Sackung, Calabria, Italy." Engineering Geology **57**(1-2): 53-64.

Firth, C. R. and I. S. Stewart (2000). "Postglacial tectonics of the Scottish glacio-isostatic uplift centre." Quaternary Science Reviews **19**(14-15): 1469-1493.

Genevois, R. and R. W. Romeo (2003). "Probability of Failure Occurrence and Recurrence in Rock Slopes Stability Analysis." International Journal of Geomechanics **3**(1): 34-42.

Gerbault, M., et al. (2003). " Numerical models of lithospheric deformation forming the Southern Alps of New Zealand." Journal of Geophysical Research **108**(B7).

Giraudi, C. (1995). "Considerations on the significance of some post-glacial fault scarps in the Abruzzo Apennines (Central Italy)." Quaternary International **25**: 33-45.

Goodman, R. E. (1976). Methods of geological engineering, West Publ. Co., St. Paul, Minn., United States (USA).

Goodman, R. E. and J. W. Bray (1976). Toppling of Rock slopes. Rock Engineering for Foundations & Slopes: Specialty Conference on Rock Engineering for Foundations and Slopes, Boulder, Colorado, American Society of Civil Engineers, .

Goricki, A. and R. E. Goodman (2003). "Failure Modes of Rock Slopes Demonstrated with Base Friction and Simple Numerical Models." Felsbau **21**(2): 25-30.

Grasselli, G. and P. Egger (2003). "Constitutive law for the shear strength of rock joints based on three-dimensional surface parameters." International Journal of Rock Mechanics and Mining Sciences **40**(1): 25-40.

Greif, V., et al. (2006). "Failure mechanism in an extremely slow rock slide at Bitchu-Matsuyama castle site (Japan)." Landslides **3**(1): 22-38.

Grollimund, B. and M. D. Zoback (2000). "Post glacial lithospheric flexure and induced stresses and pore pressure changes in the northern North Sea." Tectonophysics **327**(1-2): 61-81.

Guterman, V. G. (1980). "Model studies of gravitational gliding tectonics." Tectonophysics **65**(1-2): 111-126.

Gutierrez-Santolalla, F., et al. (2005). "Geomorphology and geochronology of sackung features (uphill-facing scarps) in the Central Spanish Pyrenees." Geomorphology **69**(1-4): 298-314.

Hamel, J. V., et al. (1974). "Some field examples of toppling failure [discussion and reply]." Geotechnique **24**(4): 691-693.

Hippolyte, J.-C., et al. (2006). "The recent fault scarps of the Western Alps (France): Tectonic surface ruptures or gravitational sackung scarps? A combined mapping, geomorphic, levelling, and 10Be dating approach." Tectonophysics **418**(3-4): 255-276.

Hippolyte, J.-C., Bourlès, D., Braucher, R., Carcaillet, J., Léanni, L., Arnold, M., and Aumaitre, G., 2009, Cosmogenic 10Be dating of a sackung and its faulted rock glaciers, in the Alps of Savoy (France): Geomorphology **108**, p. 312-320.

Hoek, E. (1990). "Estimating Mohr-Coulomb friction and cohesion values from the Hoek-Brown failure criterion." International Journal of Rock Mechanics and Mining Science & Geomechanics Abstracts **27**(3): 227-229.

Hoek, E. (2000). Rock Engineering - Course notes, Evert Hoek Consulting Engineer Inc.**:** 313.

Hoek, E. and J. W. Bray (1981). Rock slope engineering. London, Institution of Mining and Metallurgy.

Hoek, E. and E. T. Brown (1980). Underground excavations in rock. London, The Institution of Mining and Metallurgy.

Holmes, G. and J. Jarvis (1986). "Discussion on 'Large-scale toppling within a sackung type deformation at Ben Attow, Scotland': G. Holmes & J. Jarvis reply." Quarterly Journal of Engineering Geology and Hydrogeology **19**(4): 439-b-.

Holmes, G. and J. J. Jarvis (1985). "Large-scale toppling within a sackung type deformation at Ben Attow, Scotland." Quarterly Journal of Engineering Geology and Hydrogeology **18**(3): 287-289.

Houtgast, R. F., et al. (2005). "Late Quaternary evolution of the Feldbiss Fault (Roer Valley Rift System, the Netherlands) based on trenching, and its potential relation to glacial unloading." Quaternary Science Reviews **24**(3-4): 489-508.

Hudson, J. A. and J. P. Harrison (1997). Engineering rock mechanics : an introduction to the principles. Tarrytown, NY, Pergamon.

Hurlimann, M., et al. (2006). "The deep-seated slope deformation at Encampadana, Andorra: Representation of morphologic features by numerical modelling." Engineering Geology **83**(4): 343-357.

Hutri, K.-L. and J. Antikainen (2002). "Modelling of the bedrock response to glacial loading at the Olkiluoto site, Finland." Engineering Geology **67**(1-2): 39-49.

Jaeger, C. (1972). Rock mechanics and engineering. Cambridge [Eng.], University Press.

Jahn, A. (1964). "Slopes morphological features resulting from gravitation." Zeitschrift für Geomorphologie - Supplementband 5 **5**: 59-72.

Jarman, D. (2002). "Rock slope failure and landscape evolution in the Caledonian Mountains, as exemplified in the Abisko area, northern Sweden." Geografiska Annaler, Series A: Physical Geography **84**(3-4): 213-224.

Jarman, D. (2003a). Paraglacial landscape evolution. The Quaternary of the Western Highland Boundary: Field Guide. D. J. A. Evans, Quaternary Research Association**:** 50-68.

Jarman, D. (2003b). Tullich Hill Rock Slope Failures. The Quaternary of the Western Highland Boundary: Field Guide. D. J. A. Evans. London, Quaternary Research Association**:** 200-208.

Jarman, D. (2003c). The Glen Shiel Rock Slope Failure Cluster. The Quaternary of Glen Affric and Kintail: Field Guide. R. Tipping. London, Quaternary Research Association**:** 165-183.

Jarman, D. (2003d). The An Sornach Rock Slope Failure. The Quaternary of Glen Affric and Kintail: Field Guide. R. Tipping. London, Quaternary Research Association**:** 63-74.

Jarman, D. (2006). "Large rock slope failures in the Highlands of Scotland: Characterisation, causes and spatial distribution." Engineering Geology **83**(1-3): 161-182.

Jarman, D. and C. K. Ballantyne (2002). "Beinn Fhada, Kintail; an example of large-scale paraglacial rock slope deformation." Scottish Geographical Journal **118**(1): 59-68.

Jarman, D. and E. Read (2003). Postglacial Rock Slope Failure and Slope Features in Glen Strathfarrar. The Quaternary of Glen Affric and Kintail: Field Guide. R. Tipping. London, Quaternary Research Association**:** 119-121.

Jibson, R. W. (1996). "Use of landslides for paleoseismic analysis." Engineering Geology **43**(4): 291-323.

Jibson, R. W., et al. (2004). "Landslides triggered by the 2002 Denali Fault, Alaska, earthquake and the inferred nature of the strong shaking." Earthquake Spectra **20**(3): 669-691.

Jibson, R. W., et al. (2006). "Large rock avalanches triggered by the M 7.9 Denali Fault, Alaska, earthquake of 3 November 2002." Engineering Geology **83**(1-3): 144-160.

Kamenov, B., et al. (1977). "Conditions for the origin, mechanism and dynamics of block landslides in Bulgaria." Bulletin of the International Association of Engineering Geology **16**: 98-101.

Kellogg, K. S. (2001). "Tectonic controls on a large landslide complex: Williams Fork Mountains near Dillon, Colorado." Geomorphology **41**(4): 355-368.

Kimber, O. G., et al. (1998). "Mechanisms of Failure and Slope Development in Rock Masses." Transactions of the Institute of British Geographers **23**(3): 353-370.

Kinakin, D. and D. Stead (2005). "Analysis of the distributions of stress in natural ridge forms: implications for the deformation mechanisms of rock slopes and the formation of sackung." Geomorphology **65**(1-2): 85-100.

Kirkbride, M. P. and C. R. Warren (1999). "Tasman Glacier, New Zealand: 20th-century thinning and predicted calving retreat." Global and Planetary Change **22**(1-4): 11-28.

Klemann, V. and D. Wolf (1998). "Modelling of stresses in the Fennoscandian lithosphere induced by Pleistocene glaciations." Tectonophysics **294**(3-4): 291-303.

Korup, O. (2005a). "Large landslides and their effect on sediment flux in South Westland, New Zealand." Earth Surface Processes and Landforms **30**(3): 305-323.

Korup, O. (2005b). "Geomorphic imprint of landslides on alpine river systems, southwest New Zealand." Earth Surface Processes and Landforms **30**(7): 783-800.

Korup, O. (2005c). Large Rock-Slope Failures in the Southern Alps of New Zealand. Geophysical Research Abstracts, European Geosciences Union, 2005.

Lee, C. F., et al. (1996). "Evolution and origin of the ground fissures in Xian, China." Engineering Geology **43**(1): 45-55.

Lensen, G. J. (1975). Earth-deformation studies in New Zealand. Recent crustal movements. N. Pavoni and R. Green. New York, Elsevier Sci. Publ. Co.

Lensen, G. J. (1976). "Earth deformation in relation to town planning in New Zealand." Bulletin of the International Association of Engineering Geology **14**(25th International Geological Congress, Sydney, Australia. August 1976. Symposium 113. Geological hazards and the environment): 241-247.

Liu, H. Y., et al. (2004). "Numerical simulation of shear fracture (mode II) in heterogeneous brittle rock." International Journal of Rock Mechanics and Mining Sciences **41**(Supplement 1): 14-19.

MacLaughlin, M. M. and D. M. Doolin (2006). "Review of validation of the discontinuous deformation analysis (DDA) method." International Journal for Numerical and Analytical Methods in Geomechanics **30**: 271-305.

Maffei, A., et al. (2005). "From the geological to the numerical model in the analysis of gravity-induced slope deformations: An example from the Central Apennines (Italy)." Engineering Geology **78**(3-4): 215-236.

Mahr, T. (1977). "Deep-reaching gravitation deformations of high mountain slopes." Bulletin of the International Association of Engineering Geology **16**: 121-127.

Mahr, T. and A. Nemčok (1977). "Deep-seated creep deformations in the crystalline cores of Tatra Mountains." Bulletin of the International Association of Engineering Geology **16**: 104-106.

Marinos, V., et al. (2005). "The geological strength index: applications and limitations." Bulletin of Engineering Geology and the Environment **64**(1): 55-65.

Marone, C. (1998). "Laboratory-derived friction laws and their application to seismic faulting." Annual Review of Earth and Planetary Sciences **26**: 643-697.

Martino, S., et al. (2004). "Quaternary mass movements controlled by a structurally complex setting in the central Apennines (Italy)." Engineering Geology **72**(1-2): 33-55.

McCalpin, J. P. (1996). "Tectonic geomorphology and Holocene paleoseismicity of the Molesworth section of the Awatere Fault, South Island, New Zealand." New Zealand Journal of Geology and Geophysics **39**(1): 33-50.

McCalpin, J. P. (1999). Criteria for determining the seismic significance of sackungen and other scarplike landforms in mountainous regions. Reprinted and reformatted from

Appendix A, p. A-122 to A-142 in "Techniques for identifying faults and determining their origins" U.S. Nuclear Regulatory Commission NUREG/CR-5503.

McCalpin, J. P. and E. W. Hart (2000). Annual Project Summary - Ridgetop splitting, spreading, and shattering related to earthquakes in southern California, GEO-HAZ Consulting, Inc. Downloaded from http://www.geohaz.com/ on 13/08/2004**:** 6.

McLean, G. W. (1986). Structure and metamorphism near the Alpine & Awatere Faults, Lewis Pass. Department of Geological Sciences. Christchurch, New Zealand, University of Canterbury. **M.Sc. Geology:** 179 + 5 maps.

Mendum, J. R. (1979). "Caledonian thrusting in NW Scotland." Geological Society, London, Special Publications **8**(1): 291-297.

Merritts, D. J. and M. Ellis (1994). "Introduction to special section on tectonics and topography." Journal of Geophysical Research **99**(B6): 12,135-12,141.

Mokudai, K. and M. Chigira (1999). Evolution of ridge-top linear depressions and a disintegration process of mountains. Slope stability engineering : Proceedings of the International Symposium on Slope Stability Engineering : , 8-11 November, 1999 Matsuyama, Shikoku, Japan.

Montgomery, D. R. (2002). "Valley formation by fluvial and glacial erosion." Geology **30**(11): 1047-1050.

Morner, N.-A. (1995). "Paleoseismicity--The Swedish case." Quaternary International **25**: 75-79.

Moro, M., et al. (2007). "The relationship between seismic deformation and deep-seated gravitational movements during the 1997 Umbria-Marche (Central Italy) earthquakes." Geomorphology **89**(3-4): 297-307.

Muir-Wood, R. (2000). "Deglaciation Seismotectonics: a principal influence on intraplate seismogenesis at high latitudes." Quaternary Science Reviews **19**(14-15): 1399-1411.

Musson, R. M. W. (1996). "The seismicity of the British Isles." Annali Di Geofisca **39**(3): 463 - 469.

Nathan, S., et al. (2002). Geology of the Greymouth area. Lower Hutt, New Zealand, Institute of Geological and Nuclear Sciences.

Nemčok, A. (1972). "Gravitational Slope Deformation in High Mountains." International geological congress, twenty-fourth session, Canada, 1972 - Congres geologique international, Vingt-quatrieme. **24**(Engineering Geology--Geologie de l'Ingenieur, Section 13): 132-141.

Nemčok, A. (1977). "Geological/tectonical structures; an essential condition for genesis and evolution of slope movement." Bulletin of the International Association of Engineering Geology **16**: 127-130.

Nemčok, A. and F. Baliak (1977). "Gravitational deformations in Mesozoic rocks of the Carpathian mountain ranges." Bulletin of the International Association of Engineering Geology **16**: 109-111.

Nemčok, A., et al. (1977). "A survey of the research of slope deformations in individual regions of Czechoslovakia." Bulletin of the International Association of Engineering Geology **15**: 59-62.

Olesen, O., et al. (2003). Neotectonics in Norway - A review. EGS - AGU - EUG Joint Assembly, Abstracts from the meeting held in Nice, France, 6 - 11 April 2003.

Parise, M., et al. (1997). "Mass movements related to tectonics in the Aspromonte massif (southern Italy)." Engineering Geology **47**(1-2): 89-106.

Park, R. G. (1997). Foundations of structural geology. London ; New York, Chapman and Hall.

Pascal, C., et al. (2005). "Quantification of neotectonic stress orientations and magnitudes from field observations in Finnmark, northern Norway." Journal of Structural Geology **27**(5): 859-870.

Paterson, B. (1994). SH 73 Otira Viaduct & Approaches - Engineering geological report on design investigations, prepared for Beca Carter Hollings & Ferner Ltd. (Wellington) by Paterson & Coates Associates, Christchurch.

Paterson, B. R. (1996). "Slope instability along State Highway 73 through Arthur's Pass, South Island, New Zealand." New Zealand Journal of Geology and Geophysics **39**(3): 339-351.

Pellegrino, A. and A. Prestininzi (2007). "Impact of weathering on the geomechanical properties of rocks along thermal-metamorphic contact belts and morpho-evolutionary

processes: The deep-seated gravitational slope deformations of Mt. Granieri-Salincriti (Calabria- Italy)." Geomorphology **87**(3): 176-195.

Pere, V. (2003). Formation and Consequences of the Totangi Landslide Dam in the Ngatapa Valley, Gisborne, New Zealand. Department of Geological Sciences. Christchurch, University of Canterbury. **M.Sc. :** 180.

Persaud, M. and O. A. Pfiffner (2004). "Active deformation in the eastern Swiss Alps: post-glacial faults, seismicity and surface uplift." Tectonophysics **385**(1-4): 59-84.

Plag, H.-P., et al. (1998). "Post-glacial rebound and present-day three-dimensional deformations." Journal of Geodynamics **25**(3-4): 263-301.

Qiao, C. S. (2004). "The fracture mechanism of stratiform rocks under uniaxial compression." International Journal of Rock Mechanics and Mining Sciences **41**(Supplement 1): 99-105.

Radbruch-Hall, D. H. (1978). Gravitational creep of rock masses on slopes. Rockslides and avalanches Vol.1, Natural Phenomena. B. Voight. Amsterdam, Elsevier. **1:** 365-392.

Radbruch-Hall, D. H., et al. (1976). "Gravitational spreading of steep-sided ridges ("sackung") in western United States." Bulletin of the International Association of Engineering Geology **14**: 23-35.

Ranjith, P. G., et al. (2004). "Characterisation of fractured rocks under uniaxial loading states." International Journal of Rock Mechanics and Mining Sciences **41**(Supplement 1): 43-48.

Ringrose, P. S., et al. (1991). Quaternary tectonic activity in Scotland. Quaternary Engineering Geology, Engineering Geology Special Publications. A. Forster, M. G. Culshaw, J. C. Cripps, J. A. Little and C. F. Moon. London, Geological Society. **7:** 679-686.

Ringrose, P. S. and P. Migon (1997). "Analysis of digital elevation data for the Scottish Highlands and recognition of pre-Quaternary elevated surfaces." Geological Society, London, Special Publications **120**(1): 25-35.

Rizzo, V. and M. Leggeri (2004). "Slope instability and sagging reactivation at Maratea (Potenza, Basilicata, Italy)." Engineering Geology **71**(3-4): 181-198.

Saroli, M., et al. (2005). "Movements detection of deep seated gravitational slope deformations by means of InSAR data and photogeological interpretation; northern Sicily case study." Terra Nova **17**(1): 35-43.

Sauber, J. M. and B. F. Molnia (2004). "Glacier ice mass fluctuations and fault instability in tectonically active Southern Alaska." Global and Planetary Change **42**(1-4): 279-293.

Savage, W. and D. Varnes (1987). "Mechanics of gravitational spreading of steep-sided ridges («sackung»)." Bulletin of Engineering Geology and the Environment **35**(1): 31-36.

Savage, W. Z. and W. K. Smith (1986). A model for the plastic flow of landslides. U.S. Geological Survey professional paper 1385. Washington**:** 32.

Schwab, J. W. and M. Kirk (2002). Sackungen on a forested slope, Kitnayakwa River, British Columbia Forest Service - Forest Sciences, Prince Rupert Forest Region, Extension Note 47, March 2002

Sepulveda, S. A., et al. (2005). "Seismically induced rock slope failures resulting from topographic amplification of strong ground motions: The case of Pacoima Canyon, California." Engineering Geology **80**(3-4): 336-348.

Shalabi, F. I., et al. (2007). "Estimation of rock engineering properties using hardness tests." Engineering Geology **90**(3-4): 138-147.

Sheng-Hong Chen, P. E. (1999). "Three dimensional elasto-viscoplastic finite element analysis of reinforced rock masses and its application." International Journal for Numerical and Analytical Methods in Geomechanics **23**(1): 61-78.

Shroder, J. F. and M. P. Bishop (1998). "Mass movement in the Himalaya: new insights and research directions." Geomorphology **26**(1-3): 13-35.

Slivovský, M. (1977). "Gravitational deformations of valley slopes in tectonically fractured rock masses." Bulletin of the International Association of Engineering Geology **16**: 114-118.

Sjöberg, J., 1997, Estimating rock mass strength using the Hoek-Brown failure criterion and rock mass classification - A review and application to the Aznalcollar open pit, Internal Report BM 1997:02, Luleå University of Technology, Sweden.

Smith, L. N. (2001). "Columbia Mountain landslide: late-glacial emplacement and indications of future failure, Northwestern Montana, USA." Geomorphology **41**(4): 309-322.

Sorriso-Valvo, M., et al. (1999). "Mass-movement, geologic structure and morphologic evolution of the Pizzotto-Greci slope (Calabria, Italy)." Geomorphology **30**(1-2): 147-163.

Stead, D., et al. (2004). "Realistic simulation of rock slope failure mechanisms: the need to incorporate principles of fracture mechanics." International Journal of Rock Mechanics and Mining Sciences **41**(Supplement 1): 563-568.

Stead, D., et al. (2006). "Developments in the characterization of complex rock slope deformation and failure using numerical modelling techniques." Engineering Geology **83**(1-3): 217-235.

Stewart, I. S., et al. (2000). "Glacio-seismotectonics: ice sheets, crustal deformation and seismicity." Quaternary Science Reviews **19**(14-15): 1367-1389.

Stirling, M. W. and R. Anooshehpoor (2006). "Constraints on Probabilistic Seismic-Hazard Models from Unstable Landform Features in New Zealand." BULLETIN OF THE SEISMOLOGICAL SOCIETY OF AMERICA **96**(2): 404-414.

Stirling, M. W., et al. (2002). "A New Seismic Hazard Model for New Zealand." BULLETIN OF THE SEISMOLOGICAL SOCIETY OF AMERICA **92**(5): 1878-1903.

Stramondo, S., et al. (2005). Monitoring long-term ground movements and Deep Seated Gravitational Slope Deformations by InSAR time series: Case studies in Italy. Fringe ATSR Workshop 2005, Frascati, Italy.

Strom, A. L. and K. E. Abdrakhmatov (2007). Guidebook - ICL Summer school on rockslides and related phenomena. Rockslides and rock avalanches of the Kokomeren River Basin (Central Tien Shan), Moscow - Bishek.

Sturgul, J. R., et al. (1976). "Finite-element model of a mountain massif." Geology **4**(7): 439-442.

Suggate, R. P. and P. C. Almond (2005). "The Last Glacial Maximum (LGM) in western South Island, New Zealand: implications for the global LGM and MIS 2." Quaternary Science Reviews **24**(16-17): 1923-1940.

Tabor, R. W. (1971). "Origin of ridge-top depressions by large scale creep in the Olympic Mountains, Washington." Geological Society of America Bulletin **82**: 1811 - 1822.

Ter-Stepanian, G. I. (1977). "Deep-reaching gravitational deformation of mountain slopes." Bulletin of the International Association of Engineering Geology **16**: 87-94.

Terzaghi, K. and F. E. Richart Jr. (1952). "Stresses in rock about cavities." Geotechnique **3**(2): 57-90.

Turner, A. K. and R. L. Schuster (1996). Landslides : Investigation and mitigation. Special report 247.(National Research Council (U.S.). Transport Research Board) Washington, D.C., National Academy Press**:** 673.

van Vliet-Lanoe, B., et al. (2004). "Distinguishing between tectonic and periglacial deformations of quaternary continental deposits in Europe." Global and Planetary Change **43**(1-2): 103-127.

Varnes, D. J. (1978). Slope movement types and processes. Special Report - Transportation Research Board, National Research Council. R. L. Schuster and R. J. Krizek**:** pp.11-33.

Varnes, D. J., et al. (2000). Measurement of ridge-spreading movements (sackungen) at Bald Eagle Mountain, Lake County, Colorado; II, Continuation of the 1975-1989 measurements using a Global Positioning System in 1997 and 1999**:** 23.

Varnes, D. J., et al. (1989). Topographic and structural conditions in areas of gravitational spreading of ridges in the western United States. U.S. Geological Survey professional paper 1496. Washington**:** 28.

Vilimek, V., et al. (2005). "Influence of glacial retreat on natural hazards of the Palcacocha Lake area, Peru." Landslides **2**: 107-115.

Voight, B. (1978). Rockslides and avalanches. Amsterdam, Elsevier Scientific.

Wells, A. and J. Goff (2007). "Coastal dunes in Westland, New Zealand, provide a record of paleoseismic activity on the Alpine fault." Geology **35**(8): 731-734.

Whiteside, P. (1986). "Discussion on 'Large-scale toppling within a sackung type deformation at Ben Attow, Scotland' by G. Holmes & J. J. Jarvis." Quarterly Journal of Engineering Geology and Hydrogeology **19**(4): 439-a-.

Willett, S. D., et al. (2001). "Uplift, shortening, and steady state topography in active mountain belts." American Journal of Science **301**(4-5): 455-485.

Wilson, P. (2005). "Paraglacial rock-slope failures in Wasdale, western Lake District, England: morphology, styles and significance." Proceedings of the Geologists' Association **116**: 349-361.

Wilson, P. and A. Smith (2006). "Geomorphological characteristics and significance of Late Quaternary paraglacial rock-slope failures on Skiddaw Group terrain, Lake District, Northwest England." Geografiska Annaler, Series A: Physical Geography **88**(3): 237-252.

Wood, P. R., et al. (1990). 10 February 1990 earthquake, Lake Tennyson. NZGS/EDS Immediate Report 90/01**:** 6 + Illustrations.

Wu, P. (2004). "Using commercial finite element packages for the study of earth deformations, sea levels and the state of stress." Geophysical Journal International **158**(2): 401-408.

Yeung, M. R. (1999). Sliding and toppling of rigid blocks under base friction. Proceedings - Symposium on Rock Mechanics. B. Amadei, R. L. Kranz, G. A. Scott and P. H. Smeallie. **37:** 559-566.

Yielding, G., et al. (1981). "Relations between surface deformation, fault geometry, seismicity, and rupture characteristics during the El Asnam (Algeria) earthquake of 10 October 1980." Earth and Planetary Science Letters **56**: 287-304.

Zhang, W. J., et al. (2006). "Loading/Unloading response ratio theory applied in predicting deep-seated landslides triggering." Engineering Geology **82**(4): 234-240.

Zischinsky, U. (1966). On the deformation of high slopes. 1st International Society of Rock Mechanics Congress, Lisbon.

Appendix A: Base friction modelling

A.1 Steel M4 hexagonal nut 10mm shift confined base. 30º + vertical on the left with 60º + horizontal on the right.


120mm


130mm


140mm


150mm


160mm


170mm


180mm


190mm


200mm


210mm


220mm


230mm


240mm


250mm


260mm


270mm


280mm


290mm


300mm


310mm


320mm


330mm


340mm


350mm


360mm


370mm


380mm


390mm


400mm

A.2 Round 5c coins 50mm shift confined 30º + vert.

A.3 Round 5c coins 10mm shift confined 30º + vert.

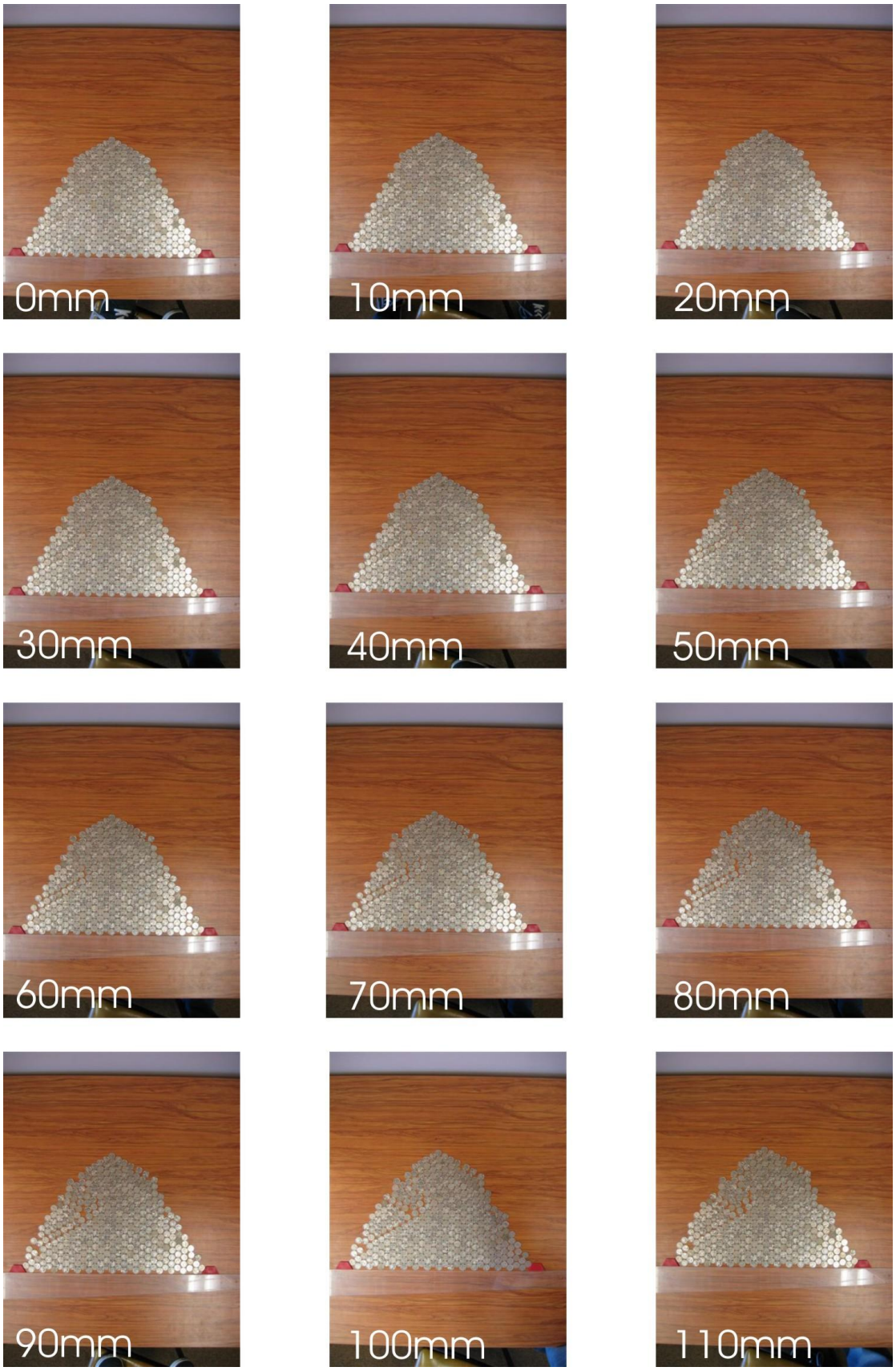


120mm


130mm


140mm


150mm


160mm

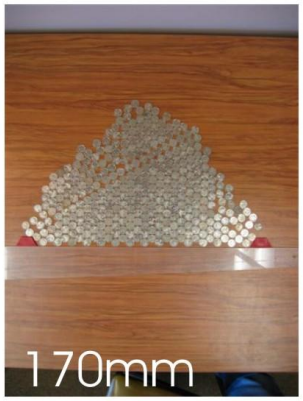
170mm


180mm


190mm


200mm


210mm


220mm


230mm


240mm


250mm


260mm


270mm


280mm


290mm


300mm

A.4 Round 5c coins 10mm shift semi-confined 30º + vert.

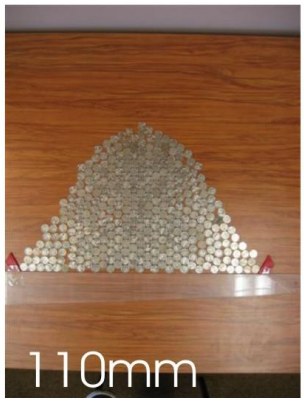


120mm

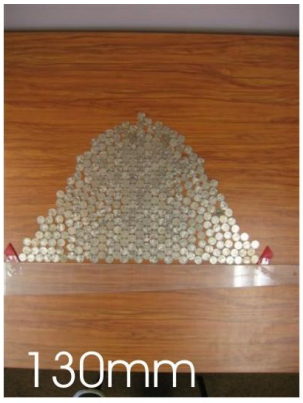
130mm

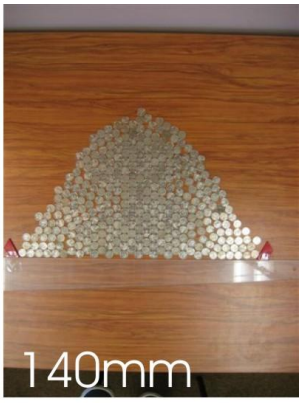
140mm


150mm


160mm


170mm


180mm


190mm


200mm

A.5 Round 5c coins 10mm shift unconfined 30º + vert.


120mm


130mm


140mm


150mm


160mm


170mm


180mm


190mm


200mm

A.6 Round 5c coins 10mm shift confined 60º + horz.

A.7 Round 5c coins 10mm shift semi-confined 60º + horz.


120mm


130mm

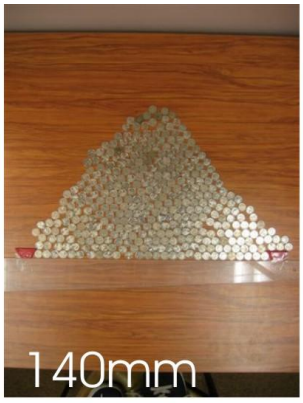
140mm


150mm

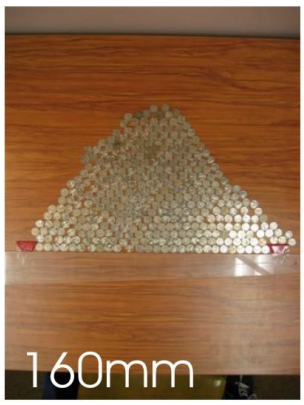
160mm


170mm


180mm


190mm

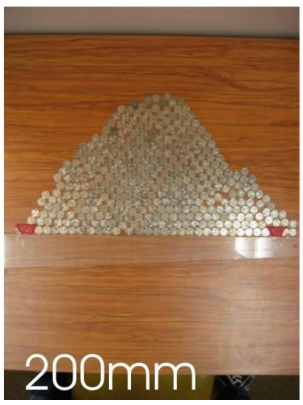
200mm

A.8 Round 5c coins 10mm shift unconfined 60º + horz.


120mm


130mm


140mm


150mm

A.9 Pattern blocks 10mm shift confined 60º

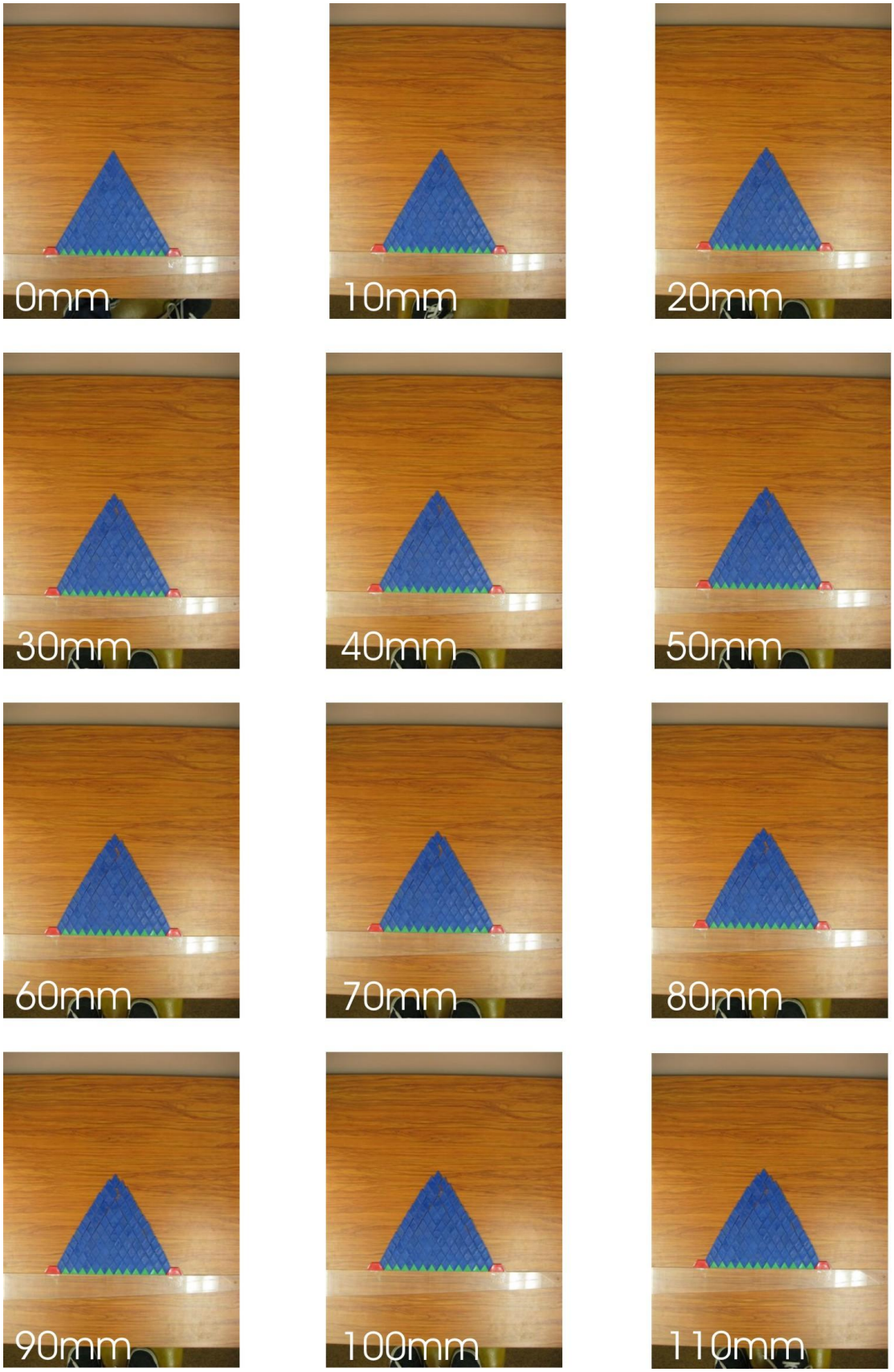

A.10 Pattern blocks 10mm shift confined 30º

Year	Author	Mechanism	Feature name	Location	Deformation style	Deformation rate	Massif rock type	Seismicity	Glaciation	Locality of feature on slope	Relationship of antiscarps to strike of slope	Ridge shape	Slope bulging	Associated slope features	Massif/slope height (m)	Slope angle	Feature length (m)	Scarp amplitude (m)
1966	**Zischinsky**	Gravity	Sackung	Matrei, Tyrolean Alps, Austria	Plastic to possible translational failure	Creep	Heterogenous - phyllites / paragneiss / mica shist	?	Yes	Upper slope	Subparallel	Asymmetrical	Lower slope inferred	?	1200m	24°	1000m	10m
1968	**Beck**	Gravity	Gravity faulting	Kelly Range, Otira, New Zealand	Brittle - along existing defects	Single event / possibly creep	Relatively homogenous -Well indurated sandstone, with argillite interbeds and minor low grade schists	Suggested association	Glacial oversteepening inferred	Upper slope, possibly to lower slope Antiscarps on both sides of the ridge	Subparallel	Symmetrical	?	?	1000m	Ridge 32° Flank 40°	1000m	?
1971	**Tabor**	Gravity	Ridge-top depressions	Olympic Mountains, Washington, U.S.A.	Creep	Creep	Isoclinally folded interbedded sandstone, slate and phyllite partially encircled by volcanic rocks	?	Glacial oversteepening	Ridge and upper slope	subparallel	?	?	Cracks in glacially scoured basins subparallel to troughs	Multiple slopes	Variable	20m -1000m	10m
1972	**Nemčok**	Gravity	Fan like	Carpathian Range, Slovakia	Brittle - along existing defects	Creep	Isotropic - granitic	?	Yes	Upper and lower slope	Subparallel	Asymmetrical/ dome	?	Rock glaciers	600m	25°	1000m	?
			Individual blocks	Carpathian Range, Slovakia	Plastic	Creep	Competent unit overlying an incompetent unit	?	Yes	Ridge and upper slope	Subparallel	Asymmetrical	?	Rockfall	800m	25°	1000m	?
			Gravity folds, (sackung)	Carpathian Range, Slovakia	Plastic to possible rotational failure	Creep to possible dynamic	Anisotrpoic, metamorphic	?	Yes	Upper slope	Subparallel	Asymmetrical	Lower slope inferred	Debris flows	900m	30°	>3500m	?
1976	**Radbruch-Hall et al.**	Gravity	Ridge splitting / spreading	Dolores Peak area, Colorado, USA	Plastic	Creep	Heterogenous -shale overlain by granogabbro	?	Yes	Ridge	Subparallel	Symmetrical	?	?	800m	Upper 50° Lower 15°	1000m	60m deep trench 120m wide
				Stillwater complex, Montana, USA	Tensional spreading on brittle, disconnected planes	Creep	Homogenous, e.g. granite	?	Glacial debuttressing inferred	Upper and lower slope	Subparallel	Asymmetrical	Lower slope	?	1250m	40°	?	?
1977	**Kamenov et al.**	Gravity	Block landslide	Bulgaria	Brittle in competent unit, and plastic in incompetent unit	Creep < 1mm/yr	Competent unit overlying an incompetent unit	?	?	Upper to mid slope, possibly lower	Subparallel	?	?	?	?	?	?	?
1977	**Mahr and Nemčok**	Gravity	Deep-seated creep deformation	Carpathian Range, Slovakia	Plastic to possible rotational failure	Creep with possible dynamic	Metamorphic - paragneiss	?	Yes	Ridge and upper slope	Subparallel	Asymmetrical	?	?	900m	30°	?	?
1977	**Slivovský**	Gravity	Release joints	Slovakia	Brittle - along stress relief fractures	Dynamic to possible ongoing creep	Variable - multiple types / non-specific	?	Yes	Valley flanks and floor	Subparallel	?	?	?	?	Variable	?	?
				Slovakia	Plastic - slow deformation exploits existing joints	Creep	Variable - multiple types Requires a lower incompetent unit	?	Yes		Subparallel	?	?	?	?	Variable	?	?
1982	**Bovis**	Gravity	Antislope scarps	Affliction Creek, B. C., Canada	Flexural toppling on existing joints\defects	Creep inferred to possible dynamic	Quartz monzonite with overlying basalt	?	Yes	Upper to mid slope	Subparallel	?	?	Tension cracks Glacier on other side of ridge	>400m	60°	900m	1-3m
1985	**Beget**	Gravity	Sackung / linear grabens, half-grabens, trenches and uphill-facing scarps	Glacier Peak, Washington, U.S.A.	Spreading	Episodic rock mass creep	Silicic tuffs and lavas overlain by andesites	No correlation with volcano-seismic events	Glacial debuttressing inferred	Ridge and upper slope	Subparallel	Asymmetrical	?	?	500m	Lower slope 30° Upper slope 40°	200m	1m - 5m
1985	**Holmes and Jarvis**	Gravity	Obsequent scarplets	Ben Attow, Kintail, Scotland (aka Beinn Fhada)	Flexural toppling	Creep inferred	Psammitic schists	?	Yes	Whole slope	Subparallel	Asymmetrical	?	?	1000m	40°	1000m >2000m discontinuous	3.5m
1987	**Savage and Varnes**	Gravity	Sackung	?	Plastic	Creep inferred	Variable - Numerical models	?	N/A	Upper and lower slope	Subparallel inferred	Variable	Inferred	?	?	Variable	?	?
1989	**Varnes et al.**	Gravity	Sackung - characterised by uphill facing scarps, trenches, graben, double crested ridges.	Mt. Nast, Colorado, U.S.A.	Topographically controlled spreading on joints	?	Jointed gneissic granite	?	Yes	Ridge and upper slope	Subparallel	Asymmetrical	Lower slope	Cirques on other side of ridge	800m	32°	800m	?
				Surprise Ridge, Colorado, U.S.A	Topographically controlled spreading on joints	?	Jointed gneissic granite	?	Yes		Subparallel	Asymmetrical	Lower slope	Cirques on other side of ridge	800m	32°	800m	?
				Sangre de Cristo, New Mexico, U.S.A	Topographically controlled spreading	?	Jointed granite	?	Yes	Ridge	Subparallel	?	Lower slope	?	?	?	?	?
				Williams Fork, Colorado, U.S.A.	Topographically controlled spreading on secondary joints	?	Jointed gneissic granite	?	Yes	Ridge and upper slope	Subparallel	Asymmetrical	Lower slope	Cirques on other side of ridge	800m	34°	1000m	9m
1992	**Chigira**	Gravity	Mass rock creep	Multiple localities, Japan	Plastic to possible rotational failure	Creep to possible dynamic	Foliated metamorphic to massive jointed sandstones	?	?	Upper slope	Subparallel	Typically asymmetrical	Bending/ buckling fold in lower slope	?		Multiple between 30° - 50°	Multiple between 200m - 1000m	?
1996	**Bovis and Evans**	Gravity	Linears / antislope scarps	Upper Ryan River, B.C., Canada	Sliding to toppling	Creep to possible dynamic	Hard, crystalline, fractured, granite and diorite	?	Yes	Mid slope	Oblique 15° to subparallel	Asymmetrical	?	Tension cracks	1800m	Mean 33° Max. 50°	<500m	?
				Handcar Creek, B.C., Canada	Sliding to toppling to toppling induced sliding	Creep inferred to possible dynamic	Metavolcanics with quartz-diorite intrusions	?	Yes	Upper to mid slope	Oblique 45° + subparallel	Asymmetrical	?	Rockslide Debris flows Tension cracks Cirques on other side of ridge	2000m	Mean 32° Max. 50°	>7000m discontinuous	Upper slope 3m Lower slope 5m
				Devastation Creek, B.C., Canada	Sliding	Creep	Jointed quartz-diorite	?	Yes	Mid slope	Subparallel	Asymmetrical	Lower slope	Rockslide Debris flows	1300m	Mean 33° Upper slope max. 40° Lower slope max. 45°	2600m discontinuous	?
1996	**Chamberlain**	Gravity	Ridge rents	Stag Hill, Cass, New Zealand	Glacially induced defect rock mass creep	Creep	Well indurated sandstone, with argillite interbeds	No indication of reactivation by proximal M6.7 event, June 1994	Yes	Ridge and upper slope	Subparallel	Asymmetrical	?	?	600m	35°	?	?
1997	**Brown**	Gravity	Ridge rents	Kelly Range, Otira, New Zealand	Toppling and wedging	?	Weakly metamorphosed, strong, interbedded sandstones and mudstones	Seismic triggering inferred	Glacial debuttressing inferred	Ridge and upper slope	?	Asymmetrical	?	?	?	?	800m - 1000m	15m - 20m
1999	**Sorriso-Valvo et al.**	Gravity	DSGSD, sackung	Pizzotto-Greci slope, Calabria, Italy	Plastic to possible translational failure	Surface 15.6 mm/yr 25-35m depth 13 mm/yr > 80m depth 0 mm/yr	Dolostones and limestones overthrust by low to intermediate grade metamorphic rocks	Dendrochronology links mass movements with seismic events	?	Upper to mid slope	Oblique 45° + subparallel Based on mapped trenches	?	Lower slope	Debris flows Adjacent amphitheatre shaped landslide Extensive lower slope landsliding	500m	20° Upper slope 40°	150m Based on mapped trenches	?

Year	Author	Mechanism	Feature name	Location	Deformation style	Deformation rate	Massif rock type	Seismicity	Glaciation	Locality of feature on slope	Relationship of antiscarps to strike of slope	Ridge shape	Slope bulging	Associated slope features	Massif/slope height (m)	Slope angle	Feature length (m)	Scarp amplitude (m)
1999	**Mokudai**	Gravity	Ridge top linear depressions	Akaishi Mountains, Japan	Plastic	Creep	Steeply dipping slate (70-90°)	?	?	Ridge	Oblique 25° + subparallel	?	?	?	?	?	?	?
2000	**Ferrucci et al.**	Gravity	DSGSD, sackung	Lago Sackung, Calabria, Italy	Sliding on existing high-angle fault surfaces	?	Phyllites overlain by gneiss	Local thrust faulting. No correlation inferred	?	Whole slope	Subparallel	?	?	Debris flows Arcuate scarps	500m	Average 25.5° Range 24.4° - 37.1°	800m	?
2000	**Varnes et al.**	Gravity	Sackung	Bald Eagle Mountain, Colorado, USA	Spreading	Creep 3.8 mm/yr	Jointed gneissic granite	?	?	Upper to mid slope	Subparallel	Asymmetrical	?	?	2400m	?	600 - 1000m	1m - 5m
2001	**Agliardi et al.**	Gravity	Sackung type DSGSD Counterscarps	Valfurva, Rhaetian Alps, Italy	Reactivation of pre-existing fractures in an isotropic elasto-plastic rock mass, triggered by post glacial unloading / debuttressing	Creep	Nappe of metapelites, metabasites, and marbles	Seismic triggering considered unfeasible relative to unloading	Glacial unloading /debuttressing	Upper to mid slope	Oblique 15° + Oblique 70° + subparallel	Asymmetrical	Lower slope	Rock glaciers Landslides	1600m	30°	750m	4m
2001	**Kellogg**	Gravity	Sackung / trenches, small-scale grabens, and upslope-facing scarps	Williams Fork, Colorado, U.S.A.	Gravitational spreading and oversteepening of the valley flanks. Fluvial incision driven debuttressing	Episodic / extremely slow	Shale and sandstone thrust footwall with jointed gneissic granite hanging wall	Fault-flexure model suggests thrust related hanging wall deformation leads to fracturing	Landsliding associated with pore water pressure increase during deglaciation	Ridge and upper slope	Subparallel	?	?	Rockslides Tension cracks Hummocky topography	1700m	?	?	10m
2002	**Jarman and Ballantyne**	Gravity	Rock slope deformation	Beinn Fhada, Kintail, Scotland (aka Ben Attow)	Possibilities considered: Debris infilled block topple Sliding induced topple Block flexural toppling Deep failure related faulting	Creep inferred	Psammitic schists	?	Glacial debuttressing inferred	Whole slope Higher concentration with elevation	Subparallel	Asymmetrical	Mid to lower slope	Cirques on other side of ridge	1000m	30° - 35°	1500m >3000m discontinuous	Maximum 10m Typically < 5m
2002	**Schwab and Kirk**	Gravity	Sackung, uphill-facing / antislope scarps	Kitnayakwa River, B.C., Canada	Topple or deep rotational sliding induced topple	Episodic with ongoing creep	Red tuff overlain by andesite	No	Yes	Upper to mid slope	Subparallel	?	Lower slope	Rockslides Tension cracks Hummocky topography	?	?	400m	10m
2004	**Di Luzio et al.**	Gravity	DSGSD / uphill-facing scarps, crossing trenches, double crest lines	Maiella anticline, Central Apennines, Italy	Gravitational spreading within a fault ridden massif	Creep inferred/possibly some episodic events	Carbonate platform with minor overlying marine sediments	History of thrust and normal faults	Yes	Ridges / whole slope	Primarily subparallel with some oblique	Asymmetrical	Lower slope	Rock avalanches	?	?	?	?
2004	**Rizzo and Leggeri**	Gravity	DSGSD, sackung	Maratea, Basilicata, Italy	Lateral spreading / sliding	Creep	Clayey flysch overlain by carbonates	No correlation with recent seismic activity	?	Whole slope	Subparallel	Asymmetrical	?	Earth flow	600m	?	900m	?
2006	**Hippolyte et al.**	Gravity	Sackung	Aiguilles Grive massif, France	Flexural toppling on subvertical bedding planes	Creep 1 mm/yr	Subvertical silts and sandstones, overthrust by gneiss and quartzites, overthrust by dolomites, gypsum and micaschist	Seismic trigger inferred	Glacial debuttressing and rebound inferred	Ridge and upper slope	Subparallel	Asymmetrical	Yes	Tension cracks Rock glaciers	1600m	20°	<2100m	3m - 5.5m
		Gravity	Sackung	Belledone Outer Crystalline Massif, France	Reactivation of conjugate tectonic faults	Rapid > 4m/event	Granite adjacent to micaschists and gneisses	Seismic trigger inferred	Glacial debuttressing and rebound inferred	Ridge and upper slope Antiscarps on both sides of the ridge	Subparallel	Asymmetrical	Inferred	?	1900m	30°	870m max. within a 7000m scarp swarm	5.3m
2008	**Gutierrez et al.**	Seismic	Sackung, DGSD, uphill-facing scarp	Whole slope	Central Spanish Pyrenees, Spain	Reactivation/formation of antiscarps by seismic events within a 600 hm^3 DSGSD	Episodic with minimum vertical slip rate of 0.19mm/yr	Paleozoic sediments and metasedimentary rocks withLimestones and slates	Yes	Yes	Subparallel	Asymmetrical	Mid to lower slope	Antiscarps inundated by solifluction lobes to form benches.	700m	17°	60m - 720m	1.3m
2009	**Agliardi et al.**	Gravity	Sackung, DSGSD counterscarps, uphill-facing scarps	Major lineaments in the upper slope with smaller antiscarps in the middle to lower slope	Mt Watles, Upper Venosta Valley, Italy	Gravitational sliding developed over a shear zone up to 500m deep	Initiation of movement soon after glaciation with peat deposition in some areas suggesting no significant displacements during the Holocene	Isoclinally folded paragneiss with orthogneiss and amphibolite intercalations against Triassic carbonates in the footwall	No	Yes	Subparallel	Asymmetrical	?	Antiscarps/scarps/half-graben infilled with colluvial deposits, and host small lakes, peat bogs, ephemeral drainage and sag ponds	1455m	25° - 30°	100m - 1500m	Upper slope 50m+ Lower slope 10m - 35m
2009	**Hippolyte et al.**	Gravity	Sackung, ridge-top troughs, double-crested ridges, uphill-facing fault scarps, open cracks, and antislope scarps	Ridge and upper slope	The Arcs, French Alps, France	Flexural toppling of vertical layers. Deformation initiated in the lower slope and propagated upslope	Inactive since rapid formation between 12.6ka to 8.5ka	Triassic quartzite, gneiss and carboniferous sandstone	Seismicity deemed to not be a factor	Glacial debuttressing and rebound inferred	Subparallel	Asymmetrical	Mid to lower slope	Tension cracks, rock glaciers	1400m	?	100m - 1500m	2m - 5m
1990	**Wood et al.**	Seismic	Ridge rents	Lake Tennyson, South Island, New Zealand	Renting along ridges to form a narrow (20m wide) series of discontinuous graben	Instantaneous	Greywacke (very well indurated sandstone with argillite interbeds)	Yes Feb. 1990 M6.0 No reactivation on observed known fault traces	?	Ridge and upper slope	Subparallel	Asymmetrical	?	Tension cracks Rockfal	?	?	1200m discontinuous series of 20m rents	0.6m deep rents
1996	**McCalpin**	Seismic	Ridge rents	Molesworth, Marlborough, New Zealand	Normal component of oblique movement on a prediominantly dextral strike-slip fault	Episodic with mean slip rate of 8 mm/yr	Greywacke (very well indurated sandstone with argillite interbeds)	Yes M7.5-7.8 predicted	Yes	Lower slope	?	?	?	?	?	?	>9000m	2.4m
2000	**McCalpin and Hart**	Seismic	Ridgetop splitting, spreading	Southern California, U.S.A.	Repeated ground rupture during large earthquakes. (not deemed conclusive)	Episodic / rapid	Jointed mica schist	Yes Multiple events	?	Ridge	Subparallel	?	?	?	?	?	?	?
2004	**Jibson et al.**	Seismic	Sackung	Black Rapids Glacier, Alaska, U.S.A.	Spreading / renting, and surface rupture	Single event	Granite inferred from proximal rockfall debris	Yes 2002 Denali M7.9	Yes	Ridge and upper slope.	Subparallel	?	?	Large rock avalanches	?	?	1500m	3m
				Gillett Pass, Alaska, U.S.A.	Surface rupture	Single event	?	Yes 2002 Denali M7.9	Yes	Mid slope	Subparallel	?	?	?	600m	?	6000m	5m extending to great depth